DISSERTATION

OF MICROBES AND MOTHERS: EVALUATING THE COMPLEX MATERNAL-NEONATAL INTERACTION AND MICROBIOME-IMMUNITY DEVELOPMENT WITH NOVEL LACTOBACILLUS VACCINATION

Submitted by

Kayl E. Ecton

Graduate Degree Program in Cell and Molecular Biology

In partial fulfillment of the requirements

For the Degree of Doctor in Philosophy

Colorado State University

Fort Collins, Colorado

Summer 2024

Doctoral Committee:

Advisor: Zaid Abdo
Co-Advisor: Gregg Dean

Kelly Wrighton
Allison Vilander
Lucas Argueso

ABSTRACT

OF MICROBES AND MOTHERS: EVALUATING THE COMPLEX MATERNAL-NEONATAL INTERACTION AND MICROBIOME-IMMUNITY DEVELOPMENT WITH NOVEL LACTOBACILLUS VACCINATION

The task of identifying an optimal vaccination strategy for neonates has been challenging scientists and physicians alike. Multiple factors contribute to the difficulty in establishing an optimal platform including the complexity of the maternal-fetal dyad, a neonatal Th2 skewed profile and the role of the parallel development of the immune system and the gut microbiome (8). Disease remains a main cause of infant morbidity and mortality, encouraging the discovery of novel infant vaccinations to be delivered during the first 28 days of life to provide protection (41). Passive protection from the maternal transfer of transplacental IgG and both IgG and IgA in breastmilk has a limited window of operation, leaving the maturing neonate at risk (128). Although exact mechanisms remain to be elucidated, here we examine the complex crosstalk between mother-fetus and maternal-neonate dyads, neonatal microbiome-immunity development, and optimal delivery strategies for neonatal vaccine development.

In this dissertation we investigated the role of maternal infection prior to gestation, neonatal challenge after vaccination, and vaccine effectiveness after exposure to virus. We evaluated the use of a novel vaccine platform developed previously in the lab as an orally delivered mucosal targeting subunit vaccine in *Lactobacillus acidophilus.* We investigated the effectiveness of the recombinant vaccine with and without adjuvants in a neonatal experimental design model and discovered increased virus specific responses in neonates vaccinated with

adjuvants when challenged with rotavirus. We show a significant impact of maternal influence on neonatal outcomes.

Beyond the immunogenic strength of the novel *Lactobacillus acidophilus* vaccine platform in neonates, we identified induced shifts to the gut microbial communities that occurred with vaccination or infection. We saw a shift in the gut microbiome over the course of a 7-day rotavirus challenge in neonates that did not return to baseline during the observation period, even after no virus shedding was detected in fecal samples. We also evaluated the impact of different doses, $1x10^6$ CFU/dose and $1x10^9$ CFU/dose, on the immune response and the gut microbiome. We confirmed the role of fecal microbiome transplants in breeding does to normalize for the maternal microbiome prior to gestation. Our results indicate that there are modifications to the gut microbiome and changes in immune antibodies during vaccination and infection. While we did not pursue a specific mechanism crosslinking the maternal-neonatal interaction and the gut-immunity relationship, we do consider the presence of such a connection.

ACKNOWLEDGEMENTS

I would like to thank Dr. Mark Brown for being a critical mentor in encouraging me to pursue research as an undergraduate and beginning my trajectory in science. I would like to thank Dr. Jeff Wilusz for teaching me passion in science at the early stage of my graduate career, igniting the joy in thinking outside the box. Thank you, Dr. Carol Wilusz for being instrumental in my transition into a PhD program, and an essential mentor during my pursuit of the National Science Foundation GRFP fellowship.

The work in this dissertation would not have been possible without the guidance and inquisition of Drs. Tiffany Weir and Christopher Gentile. Thank you for allowing me to start my journey in research as a first-year undergraduate in your lab, and for 6.5 years of valuable lessons. Thank you, Dr. Zaid Abdo, Dr. Gregg Dean, and Dr. Allison Vilander, for offering me the computational wisdom and new benchtop techniques that led me to flourish as a scientist. You gave me freedom to develop methodologies for the lab and guided me through pitfalls, you gave me a chance to pursue science at a novel frontier and uncovered inspiration that I hadn't known to exist. I would like to thank Dr. Kelly Wrighton for being a tireless committee member and mentor, and Dr. Lucas Argueso for offering invaluable questions to strengthen my scientific skillset. I would like to recognize lab members for the work presented, specifically: Gabby Brown, Gracie Stark, Dr. Micah Battson, Dr. Dustin Lee, Alora LaVoy, Callie Lang, Dr. Darby Gilfillan, Dr. Benjamin Swartzwelter, and Dr. Benjamin Curtis.

I would like to recognize the steadfast support of my wonderful parents, my incredible sisters, and my inspiring grandparents. Finally, I would like to extend thanks to my best friend, CJ, and our beloved Augie, Dixie and Ferguson for unwavering love, joy and support toujours.

TABLE OF CONTENTS

LIST OF TABLES

LIST OF FIGURES

CHAPTER 1 EVALUATION OF MATERNAL-NEONATAL INTERACTIONS FOR OPTIMAL VACCINATION.

1.1: Introduction

During its time in utero the fetus undergoes extensive development all while in direct communication with the maternal environment. It has been well documented that maternal health and exposures during gestation have an influence on offspring development of illness and disease later in life (22, 41). Critical exposures and events that affect infant health include maternal stress, exposure to toxins, and infections, in addition to maternal lifestyle choices such as diet and smoking. These parameters have been also noted to influence shifts in the maternal microbiome (22, 127, 128).

In what follows I will discuss the interwoven relationships between maternal-fetus and maternal-neonate microbiome-immunity development and interaction, then also consider what that means for current and future strategies to address neonatal vaccination. Maternal factors that influence neonatal immunity and neonatal microbiome will be discussed before considering the neonatal microbiome-immunity interaction and the neonatal microbiome-vaccination paradigm.

1.2: Maternal factors that influence neonatal immunity

A variety of factors influence the maturation and function of a neonatal immune system, including maternal immunity and infections. Immunological factors that increase maternal protection of the neonate include bioactive molecules in breastmilk, transplacental IgG, and passive transfer of maternal antibodies (Figure 1.1). Strategies to increase maternal immunity

and the degree of passive immunity provided to the neonate are important in reducing the gap in vulnerability to pathogens the neonate experiences early in life. It has been documented that transplacental IgG transfer starts early in gestation, peaking during the last four weeks of gestation (129). Antibody concentrations vary between mothers, therefore also varying between neonates. One suggested method to increase passive immunity to neonates is to deliver the vaccine to the mother during the third trimester to increase maternal antibodies (130, 131, 132). In one study maternal vaccination with the combined tetanus, diphtheria, and acellular pertussis vaccine (Tdap) increased neonatal anti-pertactin (PRN) and anti-pertussis toxin (PT) titers at birth when born to a vaccinated mother compared to a placebo mother but these titers quickly decreased until two months of age (67). At the two-month routine infant vaccination, infants born to placebo (non-vaccinated) mothers had a greater increase in anti-PT antibodies compared to infants born to vaccinated mothers suggesting a role of maternal antibody interference in infant seroconversion (67). Navigating maternal health and vaccination to increase the neonatal immune system is a limited option given that live attenuated vaccines are contraindicated for pregnant women due to the potential risk of transplacental transmission of the virus and subsequent infection of the fetus (133).

Breastmilk is a dominant factor that influences neonatal immunity by providing the neonate with an array of cytokines like interleukin (IL) Il-6, IL-8 and IL-10, active leukocytes including macrophages, and other immune stimulating factors including soluble CD14 and glycosylated proteins. Leukocytes are highest in colostrum and gradually decrease during the postnatal timeframe (134). Soluble CD14 is a component of the lipopolysaccharide (LPS)-recognition complex that binds bacterial LPS and participates in Toll Like Receptor (TLR) 4

activation in turn increasing IL-12, a pro-inflammatory cytokine, secretion (135). Several proteins found in breastmilk mediate nutrient absorption, have antimicrobial properties, and promote growth which plays a role in preventing infections while the neonatal immune system is immature (41). Many studies have shown that exclusively nursing during the first months of life reduce the onset of gastrointestinal illnesses for the first year (136). Antibodies that target enteric pathogens are abundant in breastmilk and are found in the stool of breastfed but not formula fed infants (137). This breastmilk induced protection has been associated with IgA-mediated immune mechanisms (138). Neonatal protection can also be mediated by maternal IgG in breastmilk (139). Understanding the mechanisms of the maternal-fetus communication is essential for neonatal immune development and longterm protection. Evidence suggests that passive protection from maternal antibodies can limit the effectiveness of vaccine responses in the neonate when maternal antibodies capture the vaccine antigens and dampen the vaccine response (140, 141). Often this interference references transplacental antibodies, but recently the role of maternal breastmilk transferred antibodies and neonatal vaccine effectiveness has surfaced. Maternal breastmilk and transplacental antibody interference on neonatal vaccination has been explored for rotavirus. A differing prevalence of rotavirus and success of rotavirus vaccines exists between low- and middle-income countries compared to high income countries (142). Higher titers of anti-rotavirus IgA in breastmilk have been documented in women living in low- income countries compared to women in high income countries (143, 144). One study found blunted immune responsiveness to a live attenuated rotavirus vaccine in cross-fostered mice suggesting that both transplacental and breastmilk maternal antibodies can influence vaccine immunogenicity in the early life of the neonate (145). While this is not exhaustive

evidence of maternal interference, it does encourage the consideration of antibody interference on neonatal vaccine strategies.

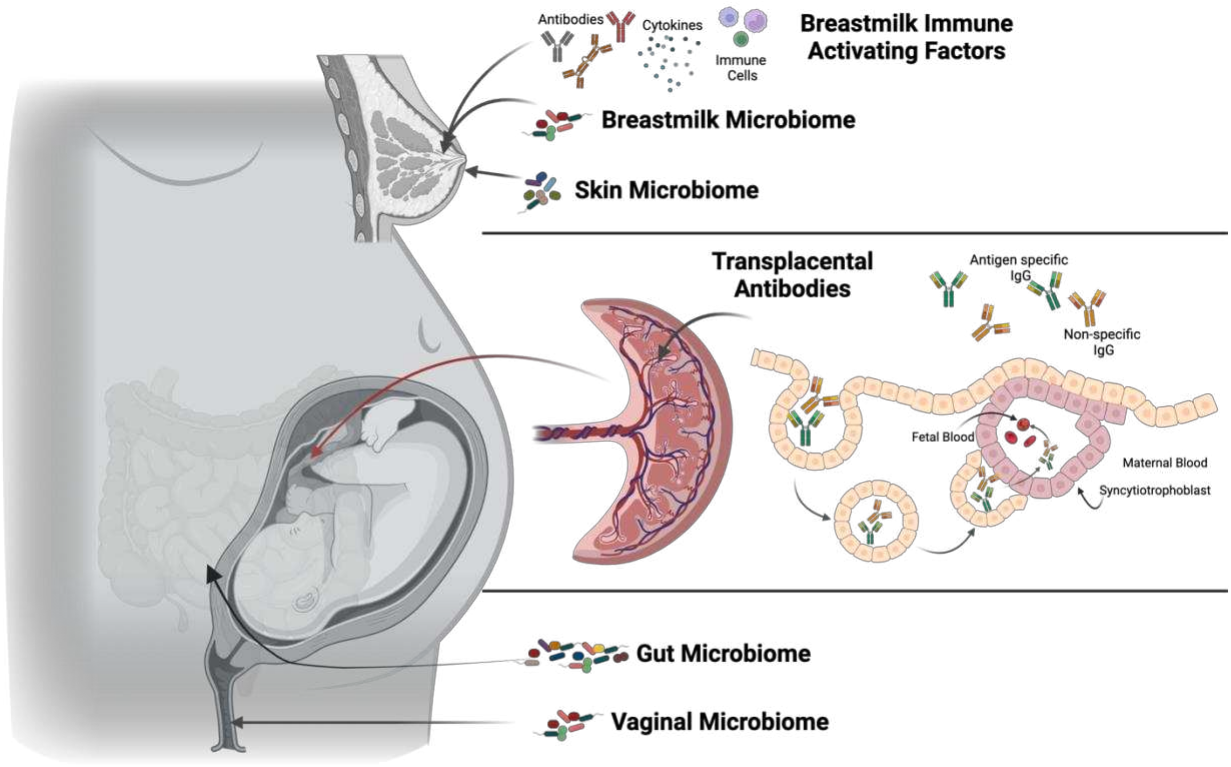

Figure 1.1 Overview of the maternal-fetal interaction between breastmilk, placenta, and the gut, skin and breastmilk microbiomes.

1.3: Maternal factors that influence the neonatal microbiome

Although the exact mechanism remains to be elucidated, it is also thought that the microbiome during pregnancy plays a role in the initiation of early programming of the offspring immune system (22). Post pregnancy, the neonatal gut microbiome is remarkably lacking in diversity and is predominantly colonized by a handful of bacterial species. This low diversity is

in part due to the hypoxic intestinal environment of neonates which allows facultative anaerobes to dominate. The neonate's initial exposure and intestinal colonization is largely dependent on mode of delivery with colonization patterns differing if the infant is born vaginally or via cesarean section. While this first microbiome may change with the subsequent dietary selection of formula or breastfeeding, the bacterial populations inhabiting the infant gut most mirror the bacterial populations the infant is exposed to at birth (2, 7, 3). In fact, Knight et al. has shown the infant gut representation mirrors the maternal vagina or skin microbiome depending on mode of delivery (146). Although this is the first perinatal influence on the infant microbiome development, it is worth mentioning that the mode of delivery has been shown to play a lesser role in preterm infants. It is expected that this is in part due to preterm infants increased likelihood of exposure to antibiotics and additional treatments during time in neonatal intensive care units (NICU) (147, 1, 6). Additionally, heath interventions like antibiotics treatment delivered to the mother during pregnancy influence neonatal immunity. For example, oral antibiotic treatment with vancomycin during gestation resulted in a shift in maternal gut microbiome and perturbations to breastmilk and vaginal microbiomes (148). These altered maternal microbiomes influenced pup immunity 14 days postpartum, with pups born to treated does having significantly higher $CD4^+$ T and B cells compared to the control pups. The maternal microbiome and necessary health interventions begin during the perinatal timeframe but continue throughout the offspring's infancy.

After delivery, the continuation of the maternal-fetal dyad communication phases into nutritional requirements for the infant. Breastfed infant gut microbiomes are colonized rather uniformly by *Lactobacillus* and *Bifidobacterium* whereas formula fed infant gut microbiomes

harbor higher abundances of *Bacteroides, Clostridium, Streptococcus, Enterobacteria,* and *Veillonella spp* (128, 149). Human milk satisfies the nutritional qualifications for neonates but differs from formula in that it offers additional immune protection through transmission of maternal breastmilk microbes and antimicrobial factors.

In addition to the microbial communities within breast milk that can impact the neonatal microbiome composition, human milk oligosaccharides (HMOs) promote neonatal gut microbial growth as digestion of HMOs requires specific bacterial species. These species, like *Bifidobacterium spp,* possess genes that are responsible for metabolism of HMO substrates and in turn flourish in the neonatal gut with a consistent and unique nutrient intake (150, 151). Metabolism of HMOs results in production of short chain fatty acids (SCFA) increasing the acidity of the gut environment which reduces the affinity for pathogen invasion (152). HMOs also play a role in recovery from pathogenic exposure. Li et al. conducted a study in which piglets were infected with rotavirus and fed either a formula with HMO supplementation or control formula. Piglets fed the supplemented formula recovered from rotavirus-induced diarrhea quicker and had increased abundance of the SCFA butyrate compared to the control formula fed group (153). Metabolites and byproducts of fermentation are only one aspect of the gut microbiome that relate to neonatal health outcomes. Fecal-oral pathogen exposure has been shown to influence the infant gut microbiome leading to anatomical deficits such as malabsorption, chronic inflammation and villous blunting (154, 155, 156). The microbiome is dynamic and responsive to the gut environment, playing a critical role in neonatal protection from early life into adulthood.

Daily consumption of breastmilk provides the infant with $1x10^5$-$1x10^7$ commensal bacteria (157). Infant suckling unavoidably explains some commensal exposure given contact to maternal skin and the skin microbiome. However, many in the field also consider the role of the entero-mammary pathway by which maternal gut microbes navigate to the mammary tissue via macrophages and dendritic cells to play an important role (158). Various gut associated bacterial genera were represented in neonatal feces, maternal feces, and maternal breastmilk (158), further pyrosequencing of breastmilk from seven mothers resulted in presence of dominant gut microbe DNA (159), and microbial signatures in neonatal feces align with maternal breastmilk microbiome signatures in infant-maternal pairs (160). These studies indicate that while the mechanism of the entero-mammary pathway may remain unclear, there is evidence to support its existence and influence.

1.4: Microbiome factors that influence neonatal immunity

It has been suggested that the phases of the gut microbiome development occur in parallel to the infant's immune system development. During the years that the gut microbiome of an infant is establishing stability, the immune system is expanding toward maturation. The infant intestinal immune system has unique developmental strategies to confer protection and deter overactivation and infection. One such example is the development of microfold (M) cells in the intestine that begin to increase at 8 days postnatal in mice, reaching mature adult levels at 2-3 weeks of age. M cells are a passageway by which microbes are sampled from the lumen into immune inductive sites. This sampling pathway is accessible to both commensal microbes and enteric pathogens.

The mutualistic relationship with the host microbiome begins with 'colonization resistance' which is defined as the commensal bacteria settling on the surface of the intestines and deterring pathogen mediate gastrointestinal inflammation (161). This first microbiome has time to establish itself without activating an inflammatory cascade because the neonatal immune system is characterized by dampened pro-inflammatory responses. Certain microbes inhabit the mucus layer and maintain the health of the mucosal lining which serves as a first defense to the invasion of pathogens. The microbiome also supports neonatal immunity with short chain fatty acids (SCFAs) which are produced as a metabolic byproduct from certain microbes and serve downstream as a source of energy for epithelial cells in the colon. The intestinal epithelial cells are a physical barrier to prevent pathogen invasion but also provide chemical signaling to maintain homeostasis in the intestines. Cytokines derived from intestinal epithelial cells play a significant role in priming the responses of adaptive immune cells and homeostasis.

Germ free mice have underdeveloped mucosal immune systems that can be restored with the introduction of commensal bacteria. Secretory IgA, CD4+ T cells, and the organization of gut-associated lymphoid tissue are all influenced by the lack or presence of gut microbiome (5, 13). Various studies have identified that specific bacteria in the gut microbiome community possess unique roles in regulation and development of the immune system, suggesting that variance in the gut microbiome has a role in differences in immune responses to infection or orally delivered live attenuated vaccines.

1.5: Microbiome and Vaccination

There is a multifactorial affect that modifies the effectiveness of vaccination in neonates, but several studies have emerged investigating the role that the gut microbiome plays with oral rotavirus vaccine immunogenicity. Rotavirus causes severe gastroenteritis and can lead to hospitalization and dealth in lower income countries, it remains the leading cause of diarrheal disease in children globally. Majority of deaths occur in children under the age of 5 and in African and Asian countries (126). *Streptococcus bovis*, *Serratia*, and *Escherichia coli* were bacteria that were identified to vary in pre-vaccinated responders and non-responders in Ghana and Pakistan, respectively (19, 20). They further identified that the increased Bacteroides in non-responders included various phyla that possessed unique lipopolysaccharide (LPS) structure and function that in turn influenced the immunogenicity via inhibition of the inflammatory cytokine stimulation (10, 26). More broadly, high abundance of Actinobacteria, specifically *Bifidobacterium longum*, in infant stool was positively correlated with T cell responses to tetanus toxoid vaccines, Bacillus Calmette-Guérin, and oral polio (29). By contrast, poor vaccine responses are associated with high abundance of Clostridiales, Enterobacteriace, and Pseudomonadales (29). Beyond clinical studies, animal model studies also associate oral vaccine immunogenicity with the presence and relative abundance of certain gut microbes. Using a translational model, fecal content from children that had gut inflammation, permeability and impaired immune responses to rotavirus vaccination or children with low enteropathy was delivered to gnotobiotic pigs. Pigs treated with the inflamed inoculum had significantly less effector T cell immune responses to the orally delivered rotavirus vaccine compared to the healthy donor inoculated pigs (30). Another study using gnotobiotic piglets showed improved oral rotavirus vaccination effectiveness by increasing innate immune responses when orally supplementing with *Lactobacillus* and *Bifidobacterium* (14). Interestingly, a study in gnotobiotic

piglets used differing doses of probiotics prior to vaccination to determine how supplemented microbes impacted the immune response from the vaccine (31). Piglets received a daily dose of either a high dose ($1x10^9$), or a low dose ($1x10^6$), or no dose, of *Lactobacillus acidophilus* to provide a controlled initial colonization. At days 5 and 15 the piglets were vaccinated orally with the attenuated human rotavirus vaccine. Low dose piglets had higher CD4+ and C D8+ T cells in the intestine and systemically where high dose piglets had enhanced mucosal and system Tregs. Probiotics have been used in human studies and increased IgA seroconversion with *Lactobacillus casei* (21). However, to attempt to match the gnotobiotic piglet model the infants would need rounds of antibiotics to deplete their microbiome prior to probiotic supplementation with the vaccine which has a separate set of complications for neonates. To effectively vaccinate the infant population there must be consideration of the developing gut microbiome and immune system. Future models for neonatal vaccination could benefit from including specific immunomodulatory probiotics with the vaccine to assist in stabilizing the neonatal gut microbiome for those who lack essential immunostimulatory bacteria.

1.6: Taken Together

In summary, as described above, there are various tactics to navigate and improve neonatal vaccination effectiveness and infection prevention when considering maternal factors and neonatal factors influencing neonatal development and immunity. The work outlined in this dissertation addresses maternal factors that influence neonatal immunity and neonatal microbiome development by broadly examining the interrelationships between maternal-neonatal microbiomes and the impact and association of microbiome-immunity development. Further, we include contributions of the neonatal microbiome factors that influence neonatal immunity and

neonatal vaccination with a temporal intervention strategy considering before, during, and after maternal rotavirus infection, neonatal vaccination, and neonatal rotavirus challenge. More specifically the challenges addressed are: 1) the specific role that maternal rotavirus infection prior to gestation had on neonatal vaccination; 2) neonatal vaccination success with a recombinant bacterium; 3) neonatal vaccination effectiveness and protection after a rotavirus challenge; and 4) neonatal microbiome communities after vaccination and during recovery from rotavirus challenge.

CHAPTER 2 MATERIALS AND METHODS FOR NOVEL VACCINATION OF NEONATES

2.1: Introduction

This chapter serves to provide the methodology used throughout the studies in subsequent chapters that aim to investigate neonatal vaccination and its impact on the immune system and the gut microbiome. The format within this chapter mirrors the larger chapter format for this dissertation. The first section of methods pertains to the neonatal experimental design including all immunology associated methods for analysis of the neonatal immunological response to vaccination, maternal infection, and neonatal rotavirus challenge. Subsequent sections include microbiome associated methods including experimental sampling and downstream processing for sequencing of the gut microbiome. Results and discussions of the immunological dataset and the microbiome dataset are presented in chapters three and four, respectively.

2.2: Materials & Methods

2.2.1: Animal IACUC/Ethics

BALB/c male and female mice were ordered from Jackson Labs (Bar Harbor, Maine) and acclimated in the CSU Lab Animal Resources (LAR) facility for two weeks prior to breeding. All mice had ad libitum access to standard chow (Teklad Global, Envigo, Indianapolis, IN, USA) and autoclaved water. All procedures were approved by the Colorado State University Institutional Animal Care and Use Committee (IACUC, protocol #4463). Mice were monitored

daily for signs of illness and euthanized with carbon dioxide overdose prior to a cardiac puncture and thoracotomy.

2.2.2: Breeding

One male and two to three female mice were housed together for two weeks to breed. All does received a fecal microbiome transplant that included donor material from all breeders involved in the study after the two weeks of breeding. After the fecal microbiome transplant, males were removed from the cages and females were separated and housed individually. Pregnant does underwent daily checks and the first day neonates were observed was considered date of birth. Does and their respective litters were housed together for the remainder of the 21-day pre-weaning timeframe.

2.2.3: Fecal microbiome transplant

Fresh murine fecal samples were collected from all adult donors involved in breeding for the fecal microbiome transplant. Feces were individually weighed then pooled and added to phosphate buffered saline (1:10; w/w). After homogenization, content was passed through a 40μm filter (Millipore Sigma) and each breeding female mouse was gavaged with 200μL. Remaining fecal microbiome transplant gavage content was stored at -80°C for later microbiome analyses.

2.2.4: Maternal rotavirus infection

To determine the role of maternal rotavirus antibody influence, does were infected with 100μL $1x10^5$ ID_{50} of EDIM rotavirus stock (38). Fecal samples were collected prior to rotavirus

infection and for the following seven days after rotavirus infection to evaluate rotavirus fecal shedding (2.1.8). After seven days, does were moved into new clean cages and remained individually housed. After an additional three days in independent clean cages, the does were moved into a new clean cage with the sire to breed (2.1.4). Serum was collected prior to rotavirus infection, 14 days after rotavirus infection, and 28 days after rotavirus infection for confirmation of rotavirus seroconversion presence prior to breeding with sires (2.1.10).

2.2.5: Neonatal vaccination timeline and experimental design

Neonatal mice received a 50 μL oral gavage of recombinant *Lactobacillus acidophilus* GAD85 which contains adjuvants FliC and FimH or GAD84 which does not (Table 2.1). Control groups included 7-day old neonatal mice receiving 50 μL oral gavage of wild type *Lactobacillus acidophilus* (NCK56) or 50 μL of soybean trypsin inhibitor (Sigma-Aldrich) buffer via oral gavage at 7 days of age. A double negative, no dose control group did not receive any treatment or handling outside of fecal collection. Neonatal mice received a booster dose of 50 μL of their respective treatment group at 14 days of age. At 21 days of age half of the neonatal mice were euthanized and the others were challenged with murine rotavirus.

GAD85, GAD84 and NCK56 were delivered to neonatal mice at 7 and 14 days of age at $1x10^9$ CFU (Table 2.1). To further complete the analysis of our vaccine effectiveness, additional mouse groups were subject to maternal rotavirus infection and/or neonatal rotavirus infection (Figure 2.1). Nomenclature for neonatal groups is provided in Table 2.1 and Table 2.2.

Table 2.1 Lactobacillus acidophilus strains

Strain Name	Strain contents	Reference

NCK56	Wild type *Lactobacillus acidophilus*	38
GAD85	VP8-1, VP8Pep, FliC, FimH	38
GAD84	VP8-1, VP8Pep	38

Table 2.2 Subset of Neonatal Experimental Design Treatment Groups

Group	N	Treatment	Rotavirus Infection	Dose delivered (per 50μL)
STI		Delivery buffer only	None	None
NCK56		NCK56	None	$1x10^9$ CFU
GAD84		GAD84	None	$1x10^9$ CFU
GAD85		GAD85	None	$1x10^9$ CFU
STI_NR		Delivery buffer only	Neonatal	None
NCK56_NR		NCK56	Neonatal	$1x10^9$ CFU
GAD84_NR		GAD84	Neonatal	$1x10^9$ CFU
GAD85_NR		GAD85	Neonatal	$1x10^9$ CFU
None_MR		None	Maternal	None
NCK56_MR		NCK56	Maternal	$1x10^9$ CFU
GAD84_MR		GAD84	Maternal	$1x10^9$ CFU
GAD85_MR		GAD85	Maternal	$1x10^9$ CFU
STI_MNR		Delivery buffer only	Maternal & Neonatal	None
NCK56_MNR		NCK56	Maternal & Neonatal	$1x10^9$ CFU
GAD84_MNR		GAD84	Maternal & Neonatal	$1x10^9$ CFU
GAD85_MNR		GAD85	Maternal & Neonatal	$1x10^9$ CFU

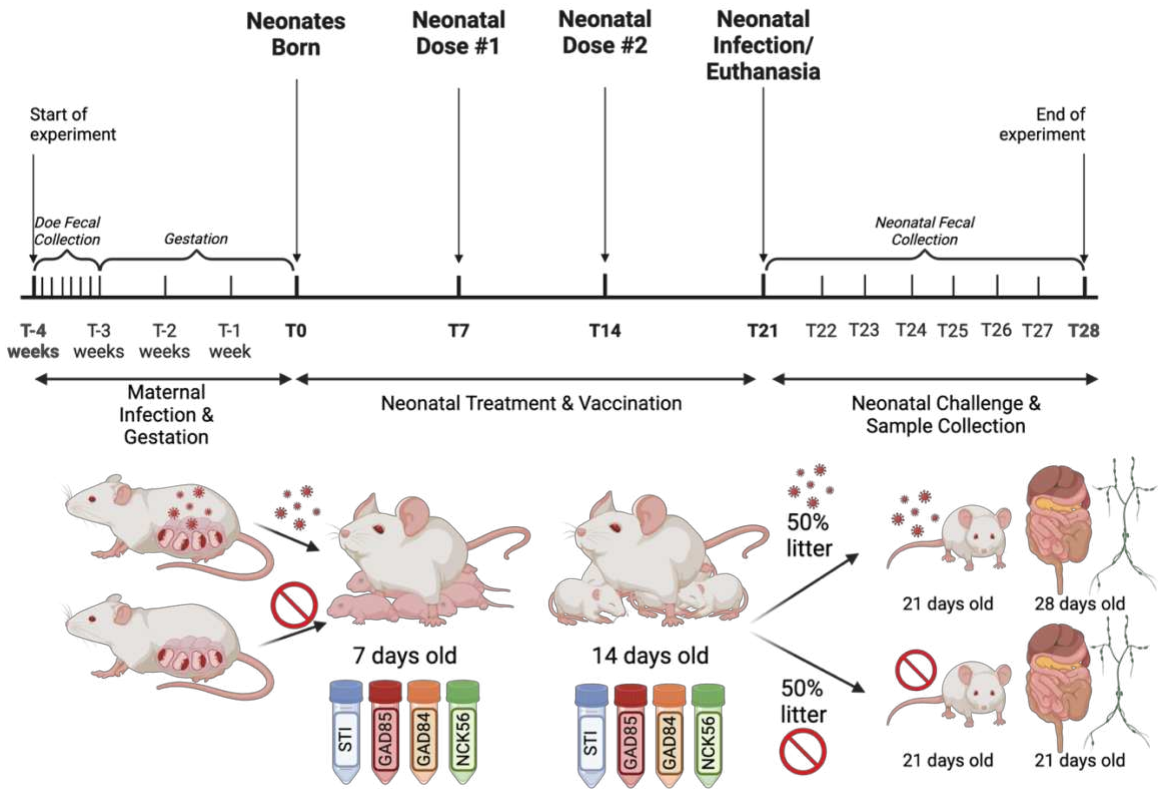

Figure 2.1 **Experimental Design Graphic.** Neonatal experimental design included maternal rotavirus infection prior to gestation, neonatal treatment intervention at 7 and 24 days of age, and neonatal rotavirus challenge at 21 days of age.

2.2.6: Neonatal Vaccine preparation and dosage

Stocks of GAD85, GAD84, and NCK56, were placed on ice after removal from the -80°C freezer. Bacterial stocks were diluted 1:10 in MRS broth (BD DIFCO) with 5µg/mL erythromycin (Teknova) and grown overnight at 37°C. GAD84 bacterial stocks diluted 1:10 in MRS broth (BD DIFCO) and grown overnight at 37°C. GAD85 and GAD84 overnight cultures were placed into prewarmed MRS media for exponential growth for 2 hours at 37°C. After 2 hours, bacteria were pelleted and washed twice in 1x PBS and the OD at 600nm was used to calculate CFU/mL. Bacteria were then resuspended in soybean trypsin inhibitor (Supplemental

1.1) for gavage at a concentration of $1x10^9$ CFU/50μL. Bacterial constructs were validated for antigen and adjuvant expression after culture for each stock (38).

2.2.7: Neonatal rotavirus infection

At 21 days of age, neonates were infected with $1x10^5$ ID_{50} of EDIM rotavirus stock diluted in 100μL gavage of the rotavirus stock delivered in soybean trypsin inhibitor before being placed in individual cages (38). Fecal samples were collected prior to the infection and each day following for seven days until euthanasia at 28 days of age for analysis of rotavirus fecal shedding (2.1.9).

2.2.8: Fecal Antigen ELISA

Rotavirus antigen ELISA was performed on fecal samples from the does and neonates dosed with rotavirus before virus delivery for the following seven days. Immediately after collection, fecal samples were weighed and diluted to 1:10 (w/v) in ProteaseArrest protease inhibitor (G-biosciences) and vortexed. After homogenization, samples were centrifuged at 13,500xg for 10 minutes at 4°C. Supernatants were collected and frozen at -80°C until ELISAs were performed. Greiner (Greiner Bio-One) plates were coated with 100μL/well of rotavirus polyclonal antibody (ThermoFisher PA1-7241) 1μg/mL in carbonate buffer overnight at 4°C. After a 3-hour block with 5% Blotto at room temperature, duplicate samples were incubated for two hours at room temperature at a 1:10 dilution in sample buffer (1% Blotto) 50μL/well followed by a PBST wash. 50μL/well anti-rotavirus NCDV HRP antibody (ThermoFisher PA1-73015) diluted 1:500 in 1% Blotto was added and plates were incubated at room temperature for one hour. After PBST washes, 100μL/well TMB was added to each well for 15 minutes at room

temperature before adding 50µL/well HCL to stop the reaction. The plate was read at 450-570nm. VP8 fecal shedding was calculated using the standard curve of positive control EDIM homogenized intestinal tissue (propagated in lab) run on each plate. For neonatal fecal antigen shedding evaluation a threshold was set based on the baseline maximum of neonatal samples at 0dpi, before rotavirus challenge.

2.2.9: Rotavirus Antibody & Cell Supernatant ELISAs

Rotavirus antibody ELISA was performed on sera samples from all does that were involved in the study before rotavirus infection, 14 days after infection, and 28 days after infection. Greiner plates were coated with 100µL/well of VP8-1 rotavirus protein (Colorado State University Protein Core, Fort Collins, CO) at 1µg/mL in 1xPBS overnight at 4°C. After a 1-hour block with 1% BSA at room temperature, duplicate samples were incubated for 2-hours at room temperature at a 1:80 dilution (1% BSA/PBST sample diluent) at 100µL/well followed by a PBST wash. 100µL/well HRP anti-mouse IgG antibody (Cell Signaling #7076) diluted 1:10,000 was added and plates were incubated for 1-hour at room temperature protected from light. After PBST washes, 100µL/well TMB was added to each well for 15 minutes at room temperature before adding 100µL/well 1M HCL to stop the reaction. The plate was read at 450-570nM. Positive titer was determined using the positive control doe sera (propagated in lab) run on each plate.

Rotavirus specific and total antibody cell supernatant ELISAs were performed on cell supernatant samples from all neonates that were involved in the study. Cell supernatants were collected after the B cell stimulation and culturing was complete (2.2.11). Greiner plates were

coated with 100μL/well of VP8-1 rotavirus protein (Colorado State University Protein Core, Fort Collins, CO) at 1μg/mL in 1xPBS overnight at 4°C. After a 1-hour block with 1% BSA at room temperature, duplicate samples were incubated for 2-hours at room temperature followed by overnight at 4°C at a 1:10 dilution for IgM and a 1:2 dilution for IgA and IgG for spleen and mesenteric lymph node isolated cells (1% BSA/PBST sample diluent) at 100μL/well followed by a PBST wash. 100μL/well HRP goat anti-mouse IgG Fc antibody (Southern Biotech #1033-05) and HRP anti-mouse IgM (Southern Biotech #1020-05) diluted 1:4,000, and HRP rat anti-mouse IgA (Southern Biotech #1165-05) diluted 1:5,000 was added and plates were incubated for 1-hour at room temperature. After PBST washes, 100μL/well TMB was added to each well for 15 minutes at room temperature before adding 100μL/well 1M HCL to stop the reaction. The plate was read at 450-570nM.

For total antibody IgG, IgM, IgA ELISAs on cell supernatants, Greiner plates were coated with 100μL/well of anti-IgG goat anti-mouse IgG Human ads-UNLB (Southern BioTech #1030-01), anti-IgM goat anti-mouse IgM-UNLB (Southern BioTech #1021-01), anti-IgA goat anti-mouse UNLB (Southern BioTech #1040-01) at 1μg/mL in 1xPBS overnight at 4°C. After a 1-hour block with 1% BSA at room temperature, duplicate samples were incubated for 2-hours at room temperature followed by overnight at 4°C at a 1:300 dilution for IgM,1:100 dilution for IgG, and 1:5 dilution for IgA for spleen isolated cells and 1:100 dilution for IgM and IgG, and 1:2 dilution for IgA for mesenteric lymph node isolated cells (1% BSA/PBST sample diluent) at 100μL/well followed by a PBST wash. 100μL/well HRP goat anti-mouse IgG antibody (Pierce #31430) diluted 1:800, HRP anti-mouse IgM (Tonbo Biosciences #72-8064-M001) diluted 1:1,000, and HRP rat anti-mouse IgA (Southern Biotech #1165-05) diluted 1:500 was added and

plates were incubated for 1-hour at room temperature. After PBST washes, 100µL/well TMB was added to each well for 15 minutes at room temperature before adding 100µL/well 1M HCL to stop the reaction. The plate was read at 450-570nM.

2.2.10: Sample Collection & Processing

Mice were euthanized using CO_2 overdose. Blood was collected by cardiac puncture and tissues were harvested and placed into processing buffer (Supplemental 1.1). The blood was centrifuged at 2348xg for 10 minutes for serum collection and frozen at -80°C. Spleens were homogenized in GentleMacs tubes using gentleMACS Tissue Dissociator (Miltenyi Biotec) with culture media (CTL media; Supplemental 1.1) followed by centrifugation at 13,000xg for 10 minutes. Red blood cells were then lysed in cold ACK lysis buffer (Supplemental 1.1). Following lysis, remaining cells were filtered through a 40µm filter tube and cell counted using a Cellometer Auto2000 (Nexcelom Bioscience). Cells from mesenteric lymph node tissue were isolated via manual disruption through a 70µm filter and following washing with CTL media, were passed through a 40µm filter tube. Cell counts were obtained as described above. Peyer's patches were removed from the small intestine with scissors and the tissue was dissociated in 5 mL culture media using the gentleMACS Tissue Dissociator. Cells were collected by centrifugation at 13,500xgfor 5 minutes and resuspended cells were passed through a 40µm filter tube before counting.

2.2.11: B Cell Stimulation & Culturing to single cell suspensions

Live B cells in the spleen, MLN, and Peyer's patches were measured using CTL Immunospot analysis. Cells were counted following 2.2.9 then cultured in round bottom Falcon plates (Corning) following CTL B-poly stim (ImmunoSpot, Cellular Technology) based on the manufacturers recommended protocol at $2.5x10^5$ cells/well. Plates were incubated at 37°C and 5% CO_2 for 72 hours of culture. Cells were collected and cell count and viability was determined using a Nexcelom Cellometer.

2.2.12: ELISpot Assays

VP8-1 and VP8-10aa specific IgM, IgG, and IgA in addition to total IgM, IgG, and IgA were measured using the enzyme linked immunosorbent spot (ELISpot) assay. The low autofluorescence PVDF plate was activated with 70% ethanol before adding the capture antibodies for an overnight incubation at 4°C. Igκ/λ anti-mouse capture antibody was used for total IgG, IgA, and IgM. Recombinant VP8-1protein (Colorado State University) and VP8-10aa peptide (Genscript MASLIYRQLLC) were used to coat the plates at 1μg/mL for rotavirus specific anti-mouse capture for IgG, IgA, and IgM. The plate was washed with 1x PBS and incubated for 1 hour at room temperature with assay medium (Supplemental 1.1). VP8-1 protein and VP810aa peptide virus specific wells were plated at $5x10^5$ cells/well while total IgA, IgM, or IgG wells were plated at $5x10^4$ cells/well in assay medium and plates were incubated without movement for 16-18 hours at 37°C and 5% CO_2. The wells were washed with 1x PBS followed by 1x PBST and the respective anti-mouse IgA, IgG, or IgM detection solution based on the manufacturers recommendations was added at 80μL/well. Plates were incubated at room temperature in the dark for two hours. After incubation, plates were washed with PBST before adding 80μL/well of the CTL Red or Alexa Fluor 488 detection antibody per manufacturers

recommendations (https://immunospot.com/b-cell-mouse). Plates were incubated at room temperature for one hour before washing the plate twice with 150µL/well of distilled water. The plates were allowed to dry overnight in the dark before scanning and counting.

Plates were imaged using ImmunoSpot Professional Analyzer DC (Cellular Technology). Cells were counted using the Basic Count function of CTL ImmunoSpot 7.0.30.4 software and wells individually underwent quality control. The VP8 specific data were measured via maximum intensity fluorescence of spots within the well. Total data output for ELISpot assays were raw spots per well.

2.2.13: Fecal sample collection

In the following section we describe the culmination of various pilot studies that were conducted with the intention of establishing a neonatal model to investigate the interaction of the maternal-neonatal dyad including the roles of the gut microbiome, the immune system, and the novel recombinant *Lactobacillus acidophilus* vaccine. The studies listed below include: 1) Pilot Neonate Vaccination Study where experimental design was established after which a follow up 2) Expanded Dose Neonate Vaccination Study was conducted with expanded group and neonatal sizes including two different doses of the recombinant *Lactobacillus acidophilus* (GAD85) at either $1x10^6$ CFU/50µL (6GAD85) or $1x10^9$CFU/50µL (9GAD85). Given the prevalence of rotavirus fatalities, we considered it essential to also determine how well GAD85 performed when neonates were challenged with rotavirus after vaccination in 3) Pilot Neonate Vaccination & Challenge Study. Additionally of interest was how well GAD85 performed when neonates were born to infected does in 4) Pilot Maternal Antibody Influence Neonate Vaccination Study.

Neonatal treatment groups described in the follow studies are explained briefly below and more in depth in 2.2.5, 2.2.6, and 2.2.7.

Table 2.3 Comprehensive list of treatments involved in experiments to optimize neonatal experimental design including vaccination, challenge, and maternal infection.

Strain Name	Strain contents	Dose delivered (per 50µL)
Strain Name	Strain contents	Dose delivered (per 50µL)
Strain Name	Strain contents	Dose delivered (per 50µL)
None	No delivery	None
STI	Buffer delivery only	50µL buffer
6NCK56	Wild type *Lactobacillus acidophilus*	$1x10^6$ CFU
9NCK56	Wild type *Lactobacillus acidophilus*	$1x10^9$ CFU
6GAD85	VP8-1, VP8Pep, FliC, FimH	$1x10^6$ CFU
9GAD85	VP8-1, VP8Pep, FliC, FimH	$1x10^9$ CFU
None	No delivery	None
STI	Buffer delivery only	50µL buffer
6NCK56	Wild type *Lactobacillus acidophilus*	$1x10^6$ CFU
9NCK56	Wild type *Lactobacillus acidophilus*	$1x10^9$ CFU
6GAD85	VP8-1, VP8Pep, FliC, FimH	$1x10^6$ CFU
9GAD85	VP8-1, VP8Pep, FliC, FimH	$1x10^9$ CFU
None	No delivery	None
STI	Buffer delivery only	50µL buffer
6NCK56	Wild type *Lactobacillus acidophilus*	$1x10^6$ CFU
9NCK56	Wild type *Lactobacillus acidophilus*	$1x10^9$ CFU
6GAD85	VP8-1, VP8Pep, FliC, FimH	$1x10^6$ CFU
9GAD85	VP8-1, VP8Pep, FliC, FimH	$1x10^9$ CFU

2.2.13.1: Pilot Neonate Vaccination Study

To determine effectiveness of the novel recombinant *Lactobacillus acidophilus* (GAD85) vaccine, we sought to use it in a neonatal model given that most rotavirus fatalities occur in the first year of life. To establish a neonatal model, we began with this pilot study including four treatment groups and treatment interventions at 7 and 14 days of age. To establish what occurs to the neonatal gut during the treatment intervention process, fecal samples were collected from

neonates at seven days of age prior to any treatment intervention and were used for microbiome analysis. After this initial collection, the neonates received a 50μL oral gavage of their respective treatment (6GAD85, 6NCK56, STI, no dose, Table 2.3). We sought to study the neonatal gut microbiome throughout the experimental design, so fecal samples were collected each day thereafter until 17 days of age, including at 14 days of age before the booster dose of 50μL of their respective treatments was administered. Terminal fecal samples were collected at 21 days of age prior to euthanasia. All samples from 7-17 days of age, and at 21 days of age were stored at -80°C until processed for microbiome sequencing. Total sample collection is listed in Table 2.4.

To understand the maternal-neonatal dyad we included maternal fecal sampling from does. Samples were collected each day that the neonatal samples were collected in addition to prior to a fecal microbiome transplant (FMT, 2.2.3) and 24 hours after to validate the FMT as a normalization factor for the neonatal experimental design. These samples were stored for future work.

Table 2.4 Fecal sample collection from neonates in pilot study optimizing neonatal experimental design platform for neonatal rotavirus vaccination study where *do=days old.*

Timepoint	Treatment	# Fecal Samples Collected	# Fecal Samples included in Analysis
7do	None	3	0
	STI	3	
	6NCK56	4	
	6GAD85	3	
8do	None	3	0
	STI	2	
	6NCK56	2	
	6GAD85	5	
9do	None	1	0

	STI	2	
	6NCK56	4	
	6GAD85	6	
10do	None	5	3
	STI	1	
	6NCK56	10	
	6GAD85	4	
11do	None	0	0
	STI	2	
	6NCK56	8	
	6GAD85	3	
12do	None	3	0
	STI	0	
	6NCK56	6	
	6GAD85	8	
13do	None	3	4
	STI	2	
	6NCK56	3	
	6GAD85	5	
14do	None	4	11
	STI	4	
	6NCK56	9	
	6GAD85	9	
15do	None	3	11
	STI	1	
	6NCK56	2	
	6GAD85	6	
16do	None	1	16
	STI	3	
	6NCK56	3	
	6GAD85	4	
17do	None	3	5
	STI	4	
	6NCK56	4	
	6GAD85	6	
21do	None	5	0
	STI	5	
	6NCK56	14	
	6GAD85	11	
NA	Doe FMT gavage content	12	8

2.2.13.2: Expanded Dose Neonate Vaccination Study

To confirm the dose for neonatal treatments, we next expanded the study participants to include more litters than in 2.2.13.1. We included additional treatment groups with bacterial loads in the 50µL neonatal dosage (9NCK56, 9GAD85, representative of $1x10^9$ CFU/dose instead of $1x10^6$CFU/dose (Supplemental 1.1., Table 2.4)). Frequent neonatal fecal sampling prior to 16 days of age was difficult to sustain since the murine ear does not fully develop until after 16 days of age, so during 2.2.13.1 pilot study, neonatal tails were marked with a sharpie to identify neonates within a litter. However, the doe regularly nurtures her young and nearly removed the sharpie marks from each neonate within each 24-hour timeframe between sampling. Additionally, neonatal handling before 7 days resulted in a marked increase in maternal cannibalization of the young. Thus, for this and following studies, no fecal samples were collected prior to 16 days of age. For this study, terminal neonatal fecal samples were collected at 21 days of age and frozen at -80°C until processed for microbiome sequencing (Table 2.5). Does received a fecal microbiome transplant (2.2.3) to normalize and make their microbiomes comparable and fecal samples from does were collected prior to the FMT and 24 hours after the FMT before breeding (Supplemental 1.1, Table S2.4).

Table 2.5 Terminal fecal sample collection from expanded dose neonatal vaccination study where *do = days old.* Neonatal mice received respective treatments at 7 and 14 days of age, including two different doses ($1x10^9$ CFU/dose, $1x10^6$ CFU/dose) of GAD85 and NCK56.

Timepoint	Treatment Group	# Litters Included	# Fecal Samples Collected	# Samples included in Analysis
21do	None	1	4	
21do	STI	2	8	
21do	6NCK56	2	12	
21do	9NCK56	2	14	

21do	6GAD85	2	15	
21do	9GAD85	2	12	
NA	Doe FMT gavage content	11 Does + 3 Sire	14	1
NA	Doe	11	11	

2.2.13.3: Pilot Neonate Vaccination & Challenge Study

To determine if the vaccine (GAD85) offers protection to the neonates after two dose treatments at 7 and 14 days of age, the neonate was challenged with rotavirus at 21 days of age. Fecal samples were collected from neonates after the two-dose treatment at 7 and 14 days of age, and prior to rotavirus infection at 21 days old, this sample was taken for a pre-infection baseline. Two fecal samples were collected from each neonate each day following infection for 7 days (Table 2.6). One fecal sample was processed and stored for 16S sequencing for the microbiome to investigate how rotavirus challenge after treatment intervention modified the gut microbiome. The second fecal sample collected from each neonate after rotavirus infection was processed for the fecal antigen ELISA to determine how much the neonate was shedding rotavirus in feces (2.2.9).

Table 2.6 Fecal sample collection throughout neonatal rotavirus challenge post treatment intervention from pilot neonate vaccination & challenge study where *do = days old, dpi = days post infection.* Neonatal mice were challenged with rotavirus after treatment interventions at 7 and 14 days of age to identify the immune and microbial response to direct rotavirus challenge.

Timepoint	Days Post Rotavirus Infection (dpi)	Treatment Group	# Litters Included	# Microbiome Fecal Samples Collected over 6-day Infection Period
21do	0	STI	1	4
21do	0	9NCK56	2	5
21do	0	9GAD85	2	10

22do	1	STI	1	4
22do	1	9NCK56	2	4
22do	1	9GAD85	2	10
23do	2	STI	1	3
23do	2	9NCK56	2	6
23do	2	9GAD85	2	8
24do	3	STI	1	5
24do	3	9NCK56	2	2
24do	3	9GAD85	2	7
25do	4	STI	1	4
25do	4	9NCK56	2	4
25do	4	9GAD85	2	11
26do	5	STI	1	4
26do	5	9NCK56	2	5
26do	5	9GAD85	2	5
27do	6	STI	1	3
27do	6	9NCK56	2	4
27do	6	9GAD85	2	4

2.2.13.4: Pilot Maternal Antibody Influence Neonate Vaccination Study

Given the presence of maternal antibodies from passive transfer to the fetus in utero and after birth in breastmilk we sought to determine the role of maternal rotavirus infection and maternal antibody influence on neonatal GAD85 vaccination. With the complex maternal-neonatal connection, we aimed to investigate maternal infection status relation to neonatal microbiome and neonatal vaccination. As such, neonates were born to rotavirus infected does (2.2.4). A fecal microbiome transplant occurred before the infection (2.2.3). Neonates received their respective treatment at 7 and 14 days of age (2.2.13.1) and terminal fecal samples were collected at 21 days of age to identify if maternal rotavirus infection manipulated the neonatal gut microbiome (Table 2.7).

Table 2.7 Terminal neonatal fecal sample collection from pilot maternal antibody influence study where *do = days old.* Neonates were born to rotavirus infected does to understand the potential role of maternal antibody influence on vaccine effectiveness and neonatal gut microbiome composition.

Timepoint	Treatment Group	# Litters Included	# Fecal Samples Collected
21do	None	1	3
21do	6NCK56	2	2
21do	6GAD85	2	3

2.2.13.5: Maternal Antibody Influence Neonate Vaccination & Challenge Study

To reproduce the aforementioned pilot studies, we repeated the combined experimental design of maternal rotavirus infection, neonatal vaccination, and neonatal challenge within one study. Breeding does were split into two cohorts (Supplemental 1.1, Table S2.5), a rotavirus infected group and an uninfected group. Fecal samples were collected from all does prior to infection for later microbiome analysis, during infection for fecal antigen ELISA (2.2.9), and during FMT (2.2.3). Fifty percent of neonates from all litters were infected with rotavirus, while the remaining 50% was not. Neonates that were not infected with rotavirus were euthanized at 21 days of age and fecal samples were collected prior to euthanasia (Table 2.8). For the neonates infected with rotavirus, fecal samples were also collected each day after infection for the following seven days. Neonatal fecal samples collected prior to infection, 3 days post infection, and six days post infection were used for a fecal antigen shedding assay to evaluate rotavirus infection (2.2.9). Seven days post infection and at 28 days of age, fecal samples were collected from all weaned and challenged neonates prior to euthanasia. All samples were frozen at -80°C for future ELISA and microbiome analysis.

Table 2.8 Fecal sample collection for maternal antibody influence neonatal vaccination and challenge study where *do = days old.* Neonates were born to uninfected or infected does,

received treatment intervention at 7 and 14 days of age, then at 21 days of age 50% of every litter was euthanized and the remaining 50% received a rotavirus challenge.

Timepoint	Group	# Fecal Samples	# Litters Included	Treatment	Rotavirus Infection
21do	STI	10	4	Delivery buffer only	None
21do	NCK56	9	3	NCK56	None
21do	GAD84	8	3	GAD84	None
21do	GAD85	11	3	GAD85	None
28do	STI_NR	8	4	Delivery buffer only	Neonatal
28do	NCK56_NR	8	3	NCK56	Neonatal
28do	GAD84_NR	5	3	GAD84	Neonatal
28do	GAD85_NR	12	3	GAD85	Neonatal
21do	STI_MR	11	3	Delivery buffer only	Maternal
21do	NCK56_MR	7	2	NCK56	Maternal
21do	GAD84_MR	5	2	GAD84	Maternal
21do	GAD85_MR	13	4	GAD85	Maternal
28do	STI_MNR	10	3	Delivery buffer only	Maternal & Neonatal
28do	NCK56_MNR	7	2	NCK56	Maternal & Neonatal
28do	GAD84_MNR	5	2	GAD84	Maternal & Neonatal
28do	GAD85_MNR	15	4	GAD85	Maternal & Neonatal

2.2.14: Microbiome Sample DNA Extraction and Quantification

Fecal samples were extracted using the ZymoBIOMICS 96 DNA Kit and ZymoBIOMICS lysis tubes (Zymo Research Cat. D4303, D4307, D4309). Samples were extracted following the kit protocol. The silicon-A-HRC plate was loaded onto the collection plate and after piercing the cover foil, 150µL ZymoBIOMICS HRC prep solution was added and incubated for 5 minutes before centrifugation at 3500xg. Samples were added to the ZymoBIOMICS BashingBead lysis tubes with 750µL/well ZymoBIOMICS lysis solution.

Samples were homogenized using BeadBeater at maximum speed for 3 minutes. Homogenized material was added to the BashingBead Lysis rack and centrifuged at 4000xg for 5 minutes. Four hundred μL/well of each supernatant were transferred to the kit 96-well block and 1200μL ZymoBIOMICS DNA binding buffer was added and vortexed for 2 minutes. 800μL/well of the mixture were transferred to a Zymo-Spin I-96-Z plate in a collection plate and spun at 3500xg for 5 minutes. Flow through was discarded and repeated with remaining 800μL/well of supernatant:binding buffer mixture. Four hundred μL/well ZymoBIOMICS DNA wash buffer 1 was added and discarded, followed by 900μL ZymoBIOMICS DNA wash buffer 2. The I-96-Z plate was transferred to an elution plate and 50μL DNase/RNase free water was added to the column matrix. After 1 minute incubation, the plate was spun at 3500xg for 5 minutes to elute the DNA. Eluted DNA was transferred to a prepared Silicon-A-HRC plate and centrifuged at 3500xg for 3 minutes. Filtered DNA was stored at -80°C for downstream applications.

For DNA quantification samples were plated on Greiner polypropylene plates (Greiner Bio-One) at a 1:100 dilution and analyzed following the Quant-iT 1x dsDNA HS Assay kit protocol (Thermo Scientific).

2.2.15: Microbiome Library Preparation

To prepare a pooled library for 16S sequencing on an Illumina platform, we amplified DNA via PCR using 515F and 806R fusion primers following the Earth Microbiome Project protocol (IDT, Table 2.1, https://earthmicrobiome.org/protocols-and-standards/16s/). The PCR program ran 25 cycles including a denature step at 98°C for 40 seconds, followed by annealing at 50°C for 60 seconds, and extension at 72°C for 90 seconds. We found this protocol to be optimal for the low concentration sample and the Phusion polymerase (ThermoFisher) selected for

microbiome sequencing with low concentration samples. To confirm amplification, samples were run on a 1% agarose gel at a 1:5 dilution of DNA with VisiOne (Amresco). Bead (KAPA/Roche) clean up purified the samples prior to PCR amplification with barcodes (IDT, Table 2.1). Beads and DNA were allowed to come to room temperature before beginning the protocol. Fresh 80% ethanol was made using molecular grade ethanol and DNase free water. Beads were mixed thoroughly before adding 0.8% of beads to the total DNA volume from the first PCR amplification with Phusion. Tubes were incubated at room temperature for two minutes. The tubes were then placed on a magnetic rack for two minutes until the beads were removed and produced a pellet. While on the magnetic rack, the supernatant was removed and discarded. The bead pellets were washed twice with 200μL 80% ethanol, then left to dry for two minutes after the second ethanol wash was removed. The tubes were removed from the magnetic rack and 52μL IDTE buffer (IDT) was added and mixed with repeat pipetting, then incubate at room temperature off the rack for five minutes. Tubes were then returned to the magnetic rack for two minutes or until beads were removed from solution and produced a pellet. Fifty μL of supernatant was collected without perturbation of the beads and placed into a new tube. The purified product was quantified right away using the ds DNA high sensitivity Quant-iT (Thermo Fisher) then stored at -20°C long term and prior to library pooling.

Paired-end 2 x 250 reads and index reads for multiplexing were generated by loading a standard kit (Illumina) onto a MiSeq analyzer (Illumina Inc). Before preparing the library for sequencing, the reagent cartridge was placed in a water bath at room temperature to thaw and the Hyb buffer was placed on ice to thaw. Prior to denaturing the library, a fresh aliquot of 0.2N NaOH was prepared. The library was diluted to 4nM then was denatured via brief vortex of 5μL

4nM library and 5μL 0.2N NaOH then centrifuge at 280xg for 1 minute. After a five-minute incubation at room temperature, the 4nM denatured library was mixed with 990μL prechilled Hyb to produce a 20pM denatured library. To produce the desired 8pM library for sequencing, 240μL of 20pM library was mixed with 360μL prechilled Hyb buffer by inverting the tube then pulse centrifuge before adding PhiX. Per Illumina protocol, 10% 12.5pM denatured PhiX was spiked into the 8pM library. The prepared 8pM library was left on ice until the reagent cartridge thawed. To add the library to the reagent cartridge, the foil seal covering the library load reservoir was pierced and 600μL prepared library was loaded without touching the foil seal. The sample sheet was loaded to the MiSeq analyzer, and the flow cell was loaded after rinsed with laboratory-grade water and an alcohol wipe. The incorporation buffer and waste bottles were loaded and checked then the reagent cartridge was loaded. Run parameters were reviewed and the kit was left to run overnight (MiSeq Reagent Kit v2 – 500 cycles MS-102-2003).

2.2.16: Microbiome Data Processing

The softwares Fastqc (version 0.12.0, 116) and Multiqc (123) were used to assess the quality of reads before using the software Trimmomatic (version 0.39, 116) with sliding window size of 3 base pair (bp) with PHRED quality cutoff of 25; minimum length MINLEN 150bp; and an average post trimming quality of 25 to ensure the highest quality samples were used in following analyses. The ILLUMINACLILP command with parameters NexteraPE-PE.fa:2:30:10:2:true was utilized, prior to trimming, to remove the used Nextera adapters presented in Table 2.9 below. The minimum length of 150 bp was used to ensure overlap between the forward and reverse reads. DADA2 (version 1.16, 124) and the SILVA database (version 138.1, 117) were used to identify Amplicon Sequence Variants (ASVs) and for bacterial

taxonomic classification, respectively. Rarefaction curves were generated to examine diversity and depth of coverage in the sequencing run utilizing the 'vegan' package (version 2.4-6, 118) in R (version 4.3.3, 119). Samples and taxa were dropped from analysis if there were no reads detected or if the rarefaction curves indicated that the sequencing depth was not sufficient for a satisfactory representation of the diversity within a sample. The resulting ASV table and taxonomy table were used in later data analysis with 175 of the initial samples sequenced.

Table 2.9 Nextera paired end adaptor sequences.

Nextera paired end adaptor	Nucleotide Sequence
Prefix NX/1	AGATGTGTATAAGAGACAG
Prefix NX/2	AGATGTGTATAAGAGACAG
Trans1	TCGTCGGCAGCGTCAGATGTGTATAAGAGACAG
Trans 1_rc	CTGTCTCTTATACACATCTGACGCTGCCGACGA
Trans2	GTCTCGTGGGCTCGGAGATGTGTATAAGAGACAG
Trans2_rc	CTGTCTCTTATACACATCTCCGAGCCCACGAGAC

2.2.17: Statistical Analyses

In the following two sections statistical analysis is explored for the immunology related data and the microbiome data respectively.

2.2.17.1: Immunology datasets

Analysis of Variance (ANOVA) was used to examine differences in responses associated with the different experimental components (neonatal treatment, neonatal challenge, maternal infection, timepoint, etc.) and to examine the role of interactions between maternal-neonate microbiome and immunology. The emmeans package (version 1.10.1, 120) in R was used to determine the estimated marginal means for the multifactor combinations in this maternal-

neonatal model and to conduct pairwise comparisons correcting for multiple testing utilizing Tukey's HSD (Honest Significant Difference). Pairwise comparisons were reflected and produced on the figures produced by ggplot2 package (version 3.5.0, 121) using compact letter displays to show potential significant differences based on these multiple comparisons.

2.2.17.2: Microbiome datasets

We used Alpha diversity, Beta diversity and pairwise, pair taxon comparisons to investigate differences between treatment groups, timepoints, does and neonates.

For Alpha diversity we evaluated rarefied richness (referred to as Richness hereafter) which was calculated using the 'vegan' package (version 2.6-4, 118) in R (version 4.3.3, 119) and the Shannon and Inverse Simpson diversity indexes that were computed using the 'phyloseq' (version 1.46.0, 122) in R (version 4.3.3, 119). ANOVA tests were used to assess significance within each study's treatment groups and levels of analysis (including neonatal age, timepoint post rotavirus challenge, etc.).

Beta diversity was evaluated using with Nonmetric Multidimensional Scaling (NMDS) that utilized Bray-Curtis similarity at the Genus level as implemented in 'phyloseq' (version 1.46.0, 122). The aim was to identify how the microbial communities clustered within studies, treatment groups and timepoints. Data for analysis was normalized using cumulative sum scaling prior to analysis of the Beta diversity utilizing package 'MetagenomeSeq' (version 1.43.0, 125). Three dimensional NMDS ordination was also produced in R using the 'vegan' (version 2.4-6, 118) package. When possible, the 95% confidence ellipsoids were plotted for each treatment group

and by each separate study dataset. To determine significant differences between the microbial communities, permutation based multivariate analysis of variance (PerMANOVA) was used.

Bar graphs were produced using the relative abundance data produced from the OTU table and the taxonomy table with the 'ggplot2' (version 3.5.0, 121) package in R. Samples included in the bar graphs had a relative abundance greater than 1. The 'MetagenomeSeq' (version 1.43.0, 125) package in R was used utilizing a zero inflated lognormal model to determine which Genera differed between treatment groups and timepoints within respective studies.

CHAPTER 3 MATERNAL-NEONATAL IMMUNITY AND ROTAVIRUS EXPOSURE

3.1: Introduction

Rotavirus is an enteric virus that causes severe gastroenteritis, predominantly afflicting children under the age of 5 years old. The World Health Organization has approved four vaccines for the prevention of rotavirus, but it remains a major cause of disease particularly in low- and middle-income countries (126). All the approved vaccines currently in use are attenuated live vaccines. Varying levels of vaccine effectiveness have been reported across the globe with respect to the four currently approved vaccine platforms (115). While the decreased vaccine effectiveness is multifaceted, one proposition is the role of maternal antibodies interfering with the neonatal immune recognition of the vaccine (54).

Passive immunity is critical for early life survival. The neonate acquires transplacental IgG while in utero and later receives antibodies through breastmilk. These antibodies serve as part of the neonatal immune system while the Th2 skewed, anti-inflammatory immune profile begins to mature and evolve (48). This anti-inflammatory profile is critical to prevent an overpowering immune response to the influx of bacteria that arrive as the first colonizers of the neonatal gut. While tactical, this dampened immune awareness leaves the neonate susceptible to infection and more dependent on vertically transferred immunity from their mother. Neonatal anti-inflammatory response also affects how vaccines induce the neonatal immune system to produce memory cells for protection from future exposures which leaves the neonate vulnerable to these preventable diseases. Maternal virus specific antibodies are another contributing factor that can

decrease vaccine effectiveness (60). Immune blunting can occur when the presence of maternal virus specific antibodies in the neonate recognizes viral components of the vaccine. The maternal antibodies respond, interpreting the vaccine as infection resulting in clearing of the viral recognized complexes. Next generation neonatal vaccines need to consider the effect of maternal antibody interference in neonatal vaccine performance. Here we evaluate a novel probiotic based oral vaccine platform that can target neonatal immune inducing sites in the intestines. This platform has been shown to induce virus specific antibodies in adult mice (38) but it has not been evaluated in neonates. Additionally, it is unknown how its performance will be affected by the presence of maternal antibody.

Lactic acid bacteria (LAB) are generally regarded as safe (GRAS) and have been considered for vaccine delivery (66). Not only does using LAB for a vaccine platform negate the necessity for cold chain storage, but they are naturally resistant to stomach acid and are commensal microbes widely present in the gut microbiome (65.). We have developed a recombinant *Lactobacillus acidophilus* to deliver rotavirus surface proteins and immune stimulating adjuvants. Both strains of our vaccine, GAD85 and GAD84, express the rotavirus capsid protein VP8 intracellularly and a broadly conserved neutralizing peptide (VP8Pep) on the cell surface. In addition to the rotavirus epitopes, GAD85 also includes surface expressed adjuvants, FliC and FimH, to increase immunogenicity of the vaccine. FliC is a component of bacterial flagella on *Salmonella enterica* serovar Typhimurium that serves as a ligand to Toll like receptor (TLR) 5 and stimulates mucosal immunity. TLRs are on many cell surfaces and play a significant role in activation of the innate immune response. FimH is a type I pilus protein from *E. coli* that serves as a second adjuvant in GAD85. FimH is an adhesion protein on certain pathogenic strains of E.

coli and Salmonella spp., it has an essential role in virulence as it has been found to increase uptake into Peyer's patches, one of the intestinal immune inductive sites. It is also a TLR4 ligand.

Here we examined the neonatal immune response to the recombinant *Lactobacillus acidophilus* vaccines. We hypothesized that GAD85 would induce an immune response in neonatal mice even in the presence of maternal influence, and that the vaccine would offer protection during a rotavirus challenge.

3.2: Results

The experimental design is as follows. Neonates were born to uninfected does (STI, NCK56, GAD84, GAD85) or does that were infected with rotavirus prior to gestation (STI_MR, NCK56_MR, GAD84_MR, GAD85_MR) (2.2.4). All does received a fecal microbiome transplant (2.2.3) to attempt to normalize for maternal variation before half were infected with rotavirus. Neonates received their respective treatment (STI, NCK56, GAD84, GAD85) at 7 and 14 days of age (2.2.5). Half of each litter was challenged with rotavirus at 21 days of age (STI_NR, NCK56_NR, GAD84_NR, GAD85_NR) while the other half of the litter remained a nonchallenged control (2.2.7). Enzyme linked immunosorbent assays (ELISAs) were performed on cell supernatants (2.2.9) collected from the media that was used to culture cells. The cultured cells (2.2.11) were used for enzyme linked immunosorbent spot (ELISpot) analyses (2.2.12) to determine antibody levels and antibody affinity.

To better investigate the maternal-neonatal relationship with this novel neonatal vaccination we evaluated 1) maternal rotavirus infection, 2) neonatal vaccination, 3) neonatal rotavirus challenge and how these three variables interacted with one another (Table 3.1).

Table 3.1 Neonatal experimental groups included in the study results in this chapter. Where NR is representative of neonatal rotavirus challenge, MR is representative of maternal rotavirus infection, and MNR is representative of maternal rotavirus infection and neonatal rotavirus challenge.

Group	# Litters Included	Total number of neonates	Treatment	Rotavirus Infection
STI	4	10	Delivery buffer only	None
9NCK56	3	9	NCK56	None
9GAD84	3	8	GAD84	None
9GAD85	3	11	GAD85	None
STI_NR	4	8	Delivery buffer only	Neonatal
9NCK56_NR	3	8	NCK56	Neonatal
9GAD84_NR	3	5	GAD84	Neonatal
9GAD85_NR	3	11	GAD85	Neonatal
STI_MR	3	9	Delivery buffer only	Maternal
9NCK56_MR	2	8	NCK56	Maternal
9GAD84_MR	2	8	GAD84	Maternal
9GAD85_MR	4	13	GAD85	Maternal
STI_MNR	3	7	Delivery buffer only	Maternal & Neonatal
9NCK56_MNR	2	7	NCK56	Maternal & Neonatal
9GAD84_MNR	2	9	GAD84	Maternal & Neonatal
9GAD85_MNR	4	15	GAD85	Maternal & Neonatal

3.2.1: Confirming maternal rotavirus infection

To investigate neonatal responses to our LA-VP8 vaccine platform and protection from rotavirus infection in the presence of maternal antibodies it was critical to evaluate maternal rotavirus infection and immune response to infection. Anti-rotavirus IgG serum titer 28 days post infection in combination with fecal shedding of rotavirus 7 days post infection were used to

confirm infection and recovery prior to breeding. Our results showed that rotavirus infected does had an increased anti-rotavirus IgG serum titer compared to the uninfected does. These antibodies were detected 14 days after infection but were significantly greater than the uninfected does at 28 days post infection at which point the breeding began (Figure 3.1A). Rotavirus infected does were confirmed to shed virus starting one day after infection and return to pre-rotavirus infection levels beginning two days after infection (Figure 3.1B). Table S3.1 describes the associated ANOVA tables.

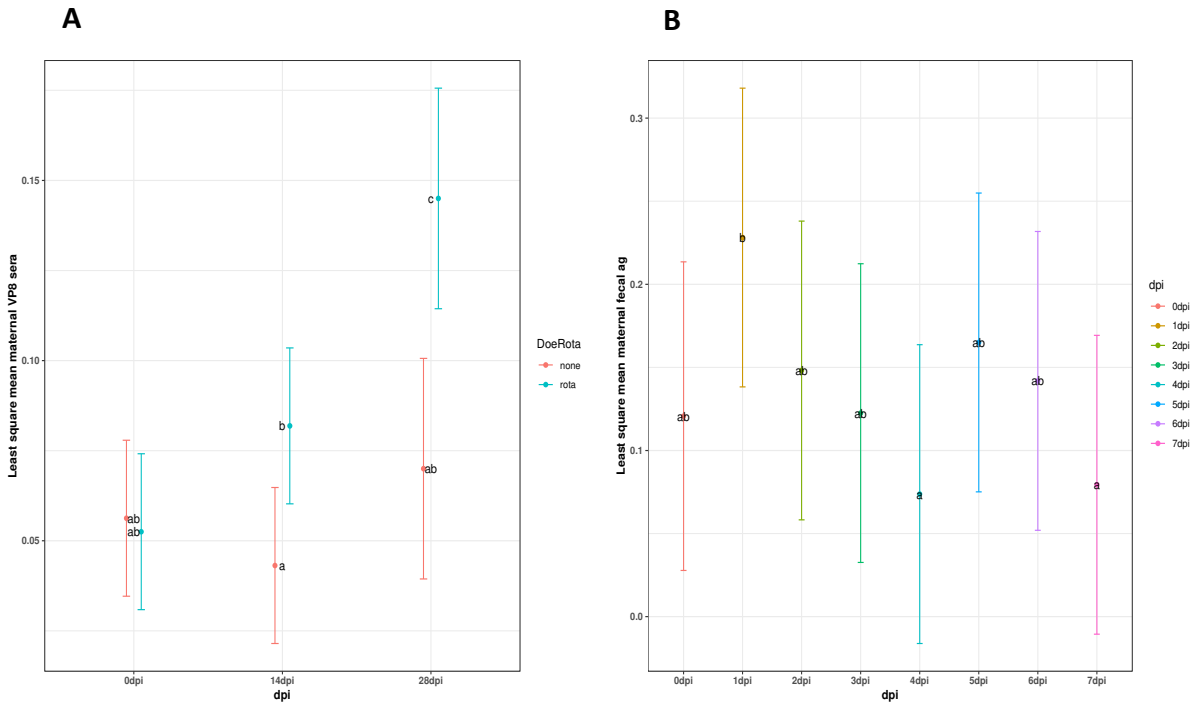

Figure 3.1 **Maternal serum antibody and fecal antigen shedding ELISA.** (A) Rotavirus IgG serum titer on does before infection (0dpi), 14 days after infection (14dpi) and 28 days after infection (28dpi), (B) rotavirus fecal shedding for does during the seven days following the rotavirus infection prior to breeding where dpi = days post infection. Significant differences are denoted on the figure (a, b) at the 0.05 level of significance.

3.2.2: Doe significantly impacts neonatal outcome for rotavirus specific and total antibodies.

There was a significant impact of doe on the neonatal outcomes in total IgM, IgG, and IgA secreting cells in the spleen and MLN. In all tissues and for all antibodies there was an interaction between the doe and the treatment group (Figure 3.2).

VP8-1 specific IgM in the spleen also had a significant interaction between the doe and treatment group, however for VP8-1 specific IgA fluorescence intensity in the spleen there was a significant effect only of the doe (Figure 3.3A, Figure 3.3E). In the MLN, there was a significant interaction effect of doe and treatment on VP8-1 specific IgM fluorescence intensity, and a significant effect of treatment for VP8-1 specific IgG fluorescence intensity (Figure 3.3B, Figure 3.3D). This suggests that the doe to which the neonate was born within a given treatment group needs to be included for analyses of total spleen and MLN IgM, IgA, and IgG secreting cells in addition to VP8-1 specific IgM fluorescence intensity in the spleen and MLN. Where the doe did not have a significant interaction effect with neonatal treatment group but was significant independent of neonatal treatment, we evaluated the doe specific influence on neonatal outcomes including VP8-1 specific IgA fluorescence intensity in the spleen (Figure 3.3E). Interestingly, there was no effect of doe on the VP8-1 IgA MLN data (Figure 3.3F). Taken together, this result suggests that maternal influence goes beyond passive antibody transfer and requires more dramatic control or fostering of pups to properly navigate the maternal impact on immunological datasets included in this study.

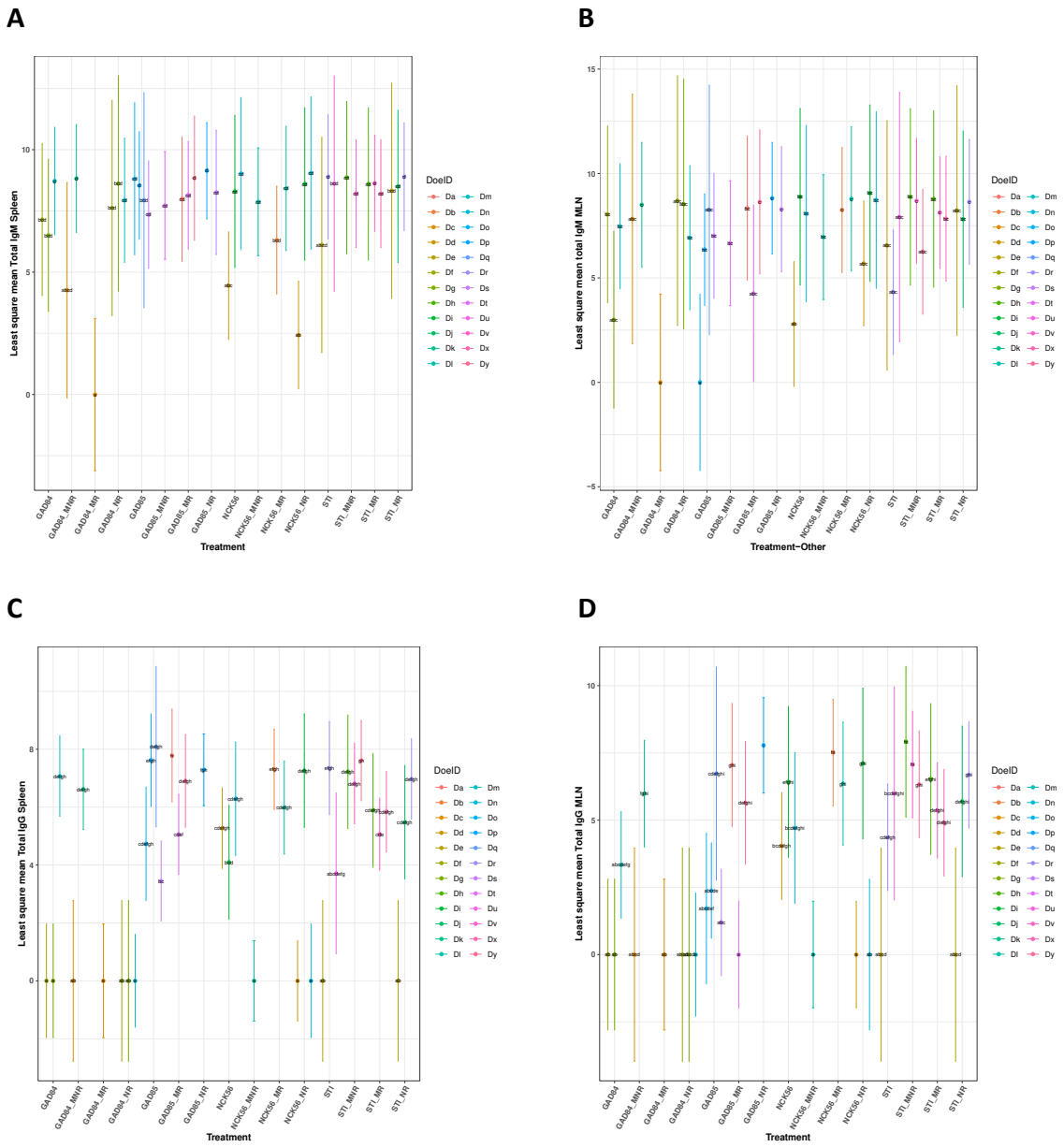

Figure 3.2 **Doe specific influence on litter treatment response in total IgM and IgG secreting cells in the spleen and MLN.** There is a significant effect of doe on neonatal treatment outcomes for total IgM secreting cells in the spleen (A), and MLN (B), in addition to total IgG secreting cells in the spleen (C), and MLN (D). Where each doe is represented by a unique color and plotted by neonatal treatment group. Significant differences are denoted on the figure (a, b) at the 0.05 level of significance.

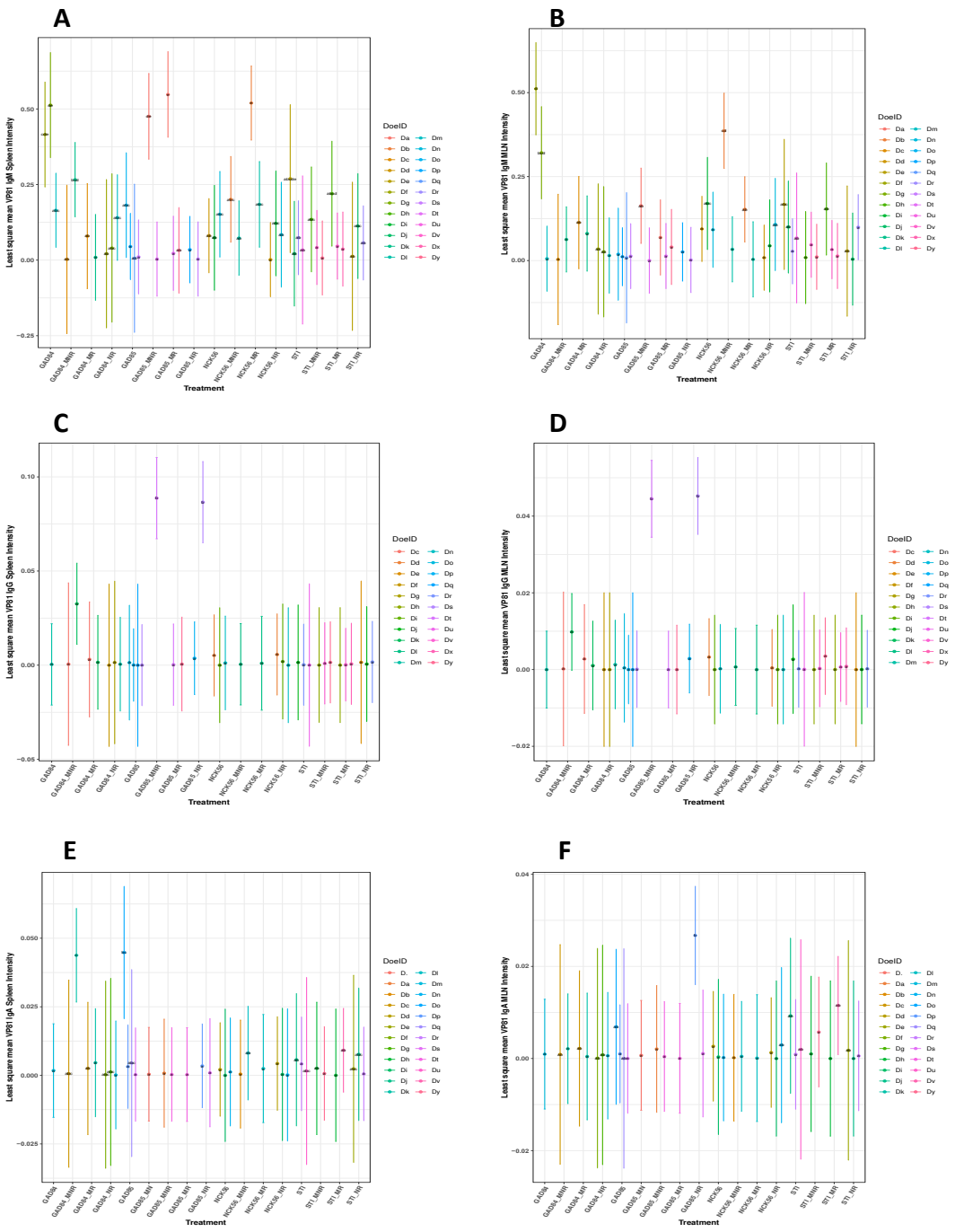

Figure 3.3 **Doe specific influence on litter treatment response in VP8-1 specific IgM, IgG and IgA fluorescence intensity in the spleen and MLN.** There is a significant effect of doe on neonatal treatment outcomes for VP8-1 specific IgM fluorescence intensity in the spleen (A), and MLN (B), in addition to VP8-1 specific IgG fluorescence intensity in the spleen (C), and MLN (D), and VP8-1 specific IgA fluorescence intensity in the spleen (E), and MLN (F). Where each doe is represented by a unique color and plotted by neonatal treatment group. Significant differences are denoted on the figure (a, b) at the 0.05 level of significance.

In the cell supernatants there was a significant impact of doe on the neonatal outcomes in total IgM and IgG in the spleen and MLN (Figure 3.4A-D).

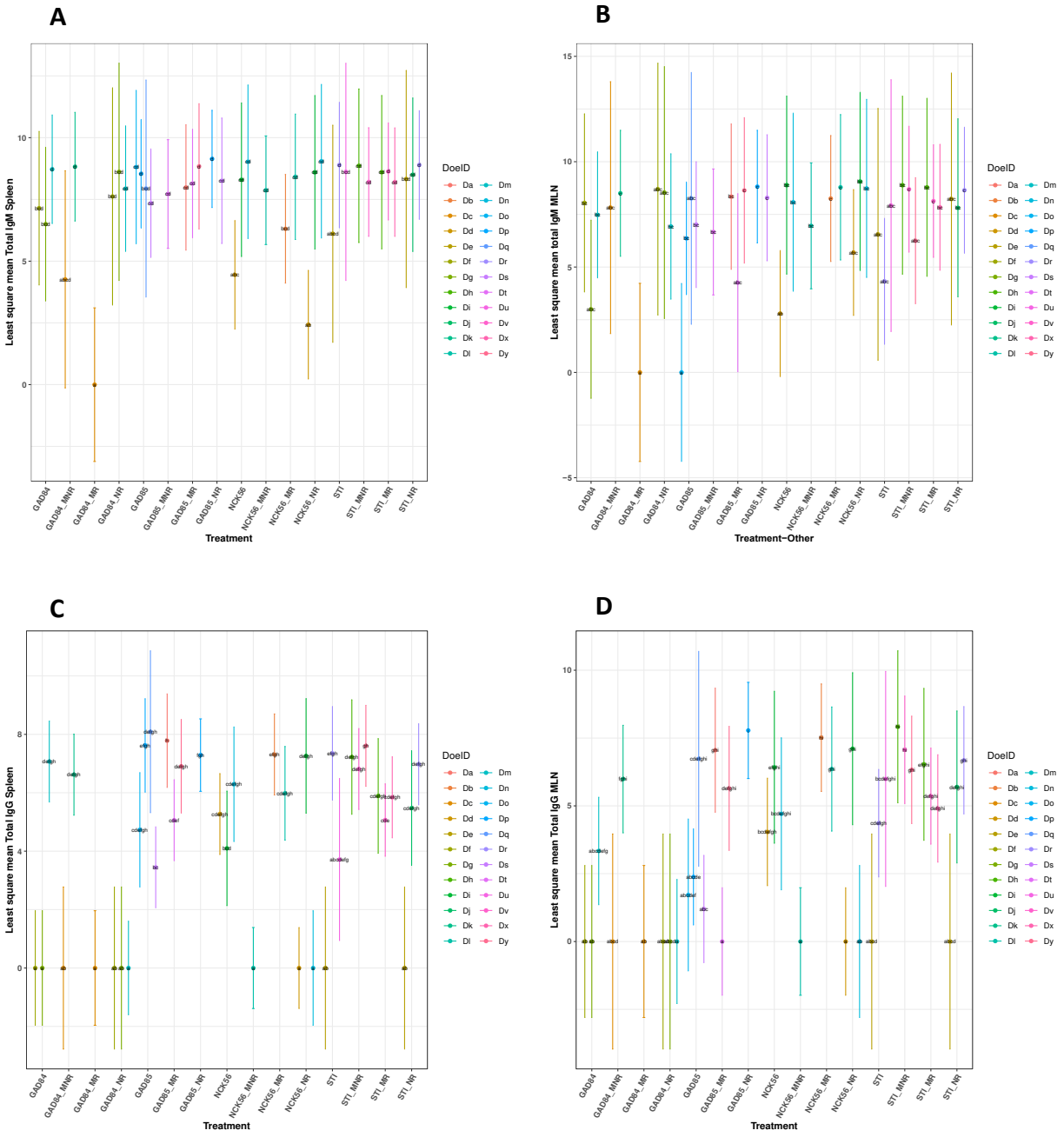

Figure 3.4 A-D **Doe specific influence on litter treatment response in total IgM and IgG in the spleen and MLN.** There is a significant effect of doe on neonatal treatment outcomes for total IgM in the spleen (A), and MLN (B), in addition to total IgG in the spleen (C), and MLN (D). Each doe is represented by a unique color and plotted by neonatal treatment group. Significant differences are denoted on the figure (a, b) at the 0.05 level of significance.

VP8-1 specific IgM in the spleen also had a significant interaction between the doe and treatment group, however for VP8-1 specific IgA and IgM in the spleen there was a significant effect only of the doe. In the MLN, there was a significant effect of doe on VP8-1 IgM, IgG, and a significant effect of treatment for VP8-1 IgA and IgM (Figure 3.5). This suggests that the doe to which the neonate was born to within a given treatment group needs to be included for analyses of total spleen and MLN IgM, IgA, and IgG in addition to VP8-1 specific IgM in the spleen. Where the doe did not have a significant interaction effect with neonatal treatment group but was significant independent of neonatal treatment, we evaluated the doe specific influence on neonatal outcomes including VP8-1 specific IgM, IgG in MLN and VP8-1 specific IgG and IgA in the spleen. Taken together, this result suggests that maternal influence goes beyond passive antibody transfer and requires more dramatic control or fostering of pups to properly navigate the maternal impact on immunological datasets included in this study.

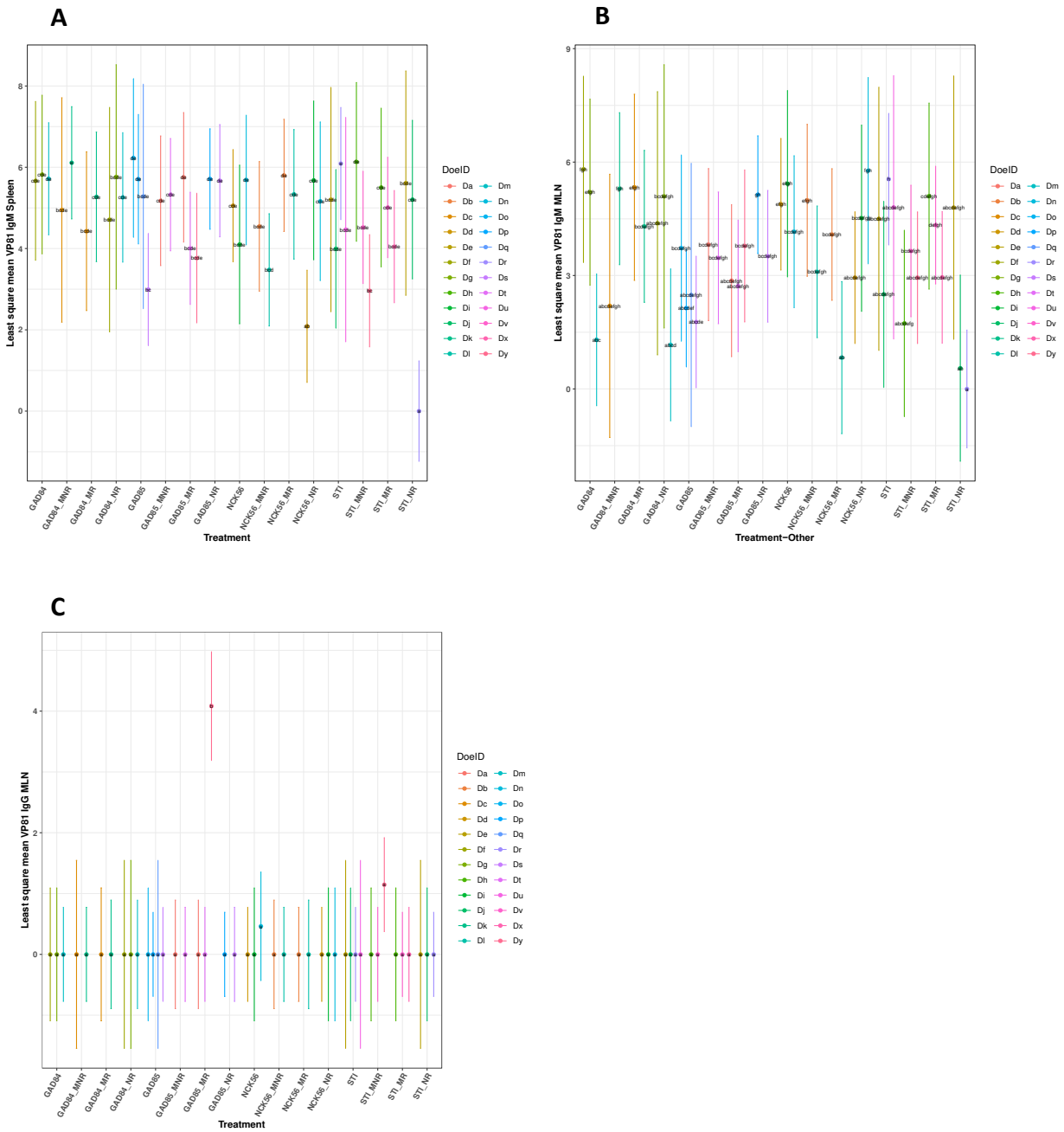

Figure 3.5 A-C **Doe specific influence on litter treatment response in VP8-1 specific IgM in the spleen and MLN, VP8-1 specific IgG in the MLN.** There is a significant effect of doe on neonatal treatment outcomes for VP8-1 specific IgM in the spleen (A), and MLN (B), in addition to VP8-1 specific IgG in the spleen (C). Each doe is represented by a unique color and plotted by neonatal treatment group. Significant differences are denoted on the figure (a, b) at the 0.05 level of significance.

These results indicate the maternal influence on neonatal experimental design and methodological analyses of neonatal outcomes is essential to evaluate before developing further conclusions on independent neonatal results and treatments.

3.2.3: Neonatal rotavirus antigen shedding peaks one day after challenge and is dependent on maternal infection.

There was no interaction effect between neonatal treatment group and timepoint, nor was there a significant difference between treatment groups for neonatal fecal shedding therefore we conclude that we did not successfully infect all neonates with rotavirus (Table S3.2). However, there was a significant effect of timepoint, ($p=8.969e-7$, Table S3.3) with a significant increase in fecal shedding one day after rotavirus infection and a return to pre-rotavirus challenge fecal shedding levels beginning at two days post challenge (Figure 3.6A). When all mice are combined, neonatal fecal antigen shedding significantly increased and peaked one day after rotavirus challenge in neonates born to rotavirus infected does, but not in neonates born to uninfected does (Figure 3.6B). Given this significant difference in maternal rotavirus infection and neonatal fecal shedding (Figure 3.6B) we then graphed the individual neonatal datapoints per treatment group and found that neonates born to uninfected does had a greater number of days of fecal shedding, 47 days of total 128 days compared to 13 days of total 138, across all treatment groups (Figure 3.7 A-B, Table 3.3) compared to neonates born to rotavirus infected does (Figure 3.7 C-D, Table 3.3). This result shows that the maternal rotavirus infection protected neonates that were challenged with rotavirus from infection regardless of treatment type (Table 3.2, Figure 3.5B).

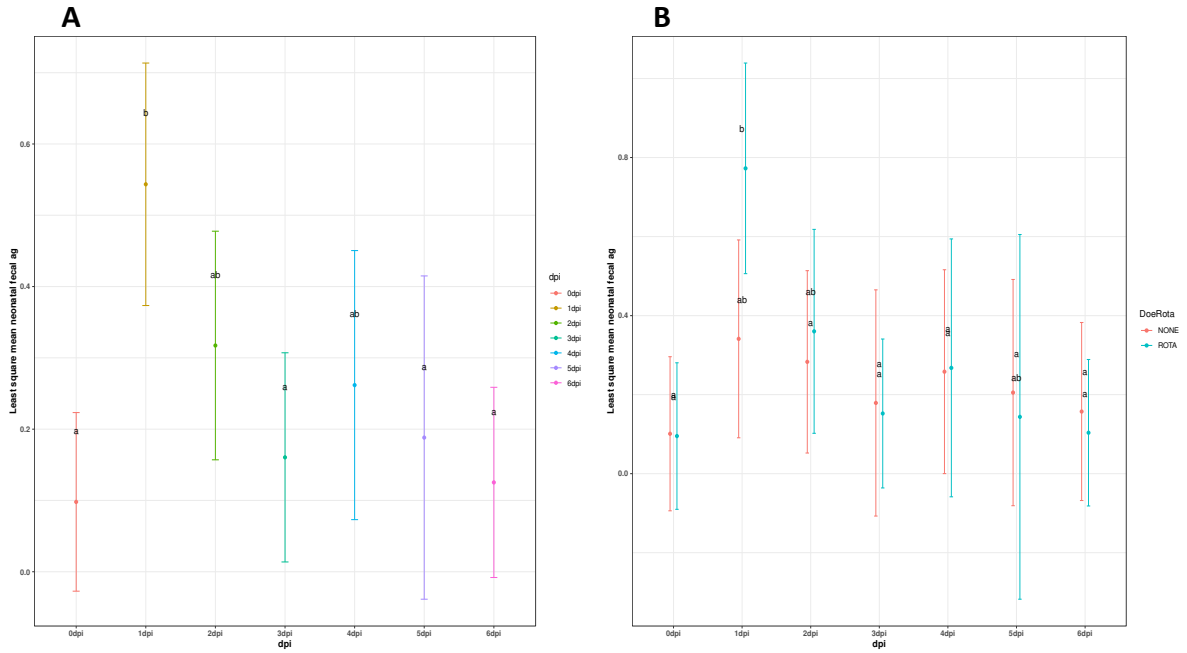

Figure 3.6 A-B **Neonatal fecal shedding ELISA.** Neonatal fecal antigen shedding significantly increases one day after rotavirus challenge and returns to pre-challenge levels beginning three days after challenge (A), neonatal fecal antigen shedding significantly increases one day post challenge in neonates born to rotavirus infected does compared to 0dpi, however there is no significant different between 0dpi and 1dpi in neonates born to uninfected does (B). Significant differences are denoted on the figure (a, b) at the 0.05 level of significance.

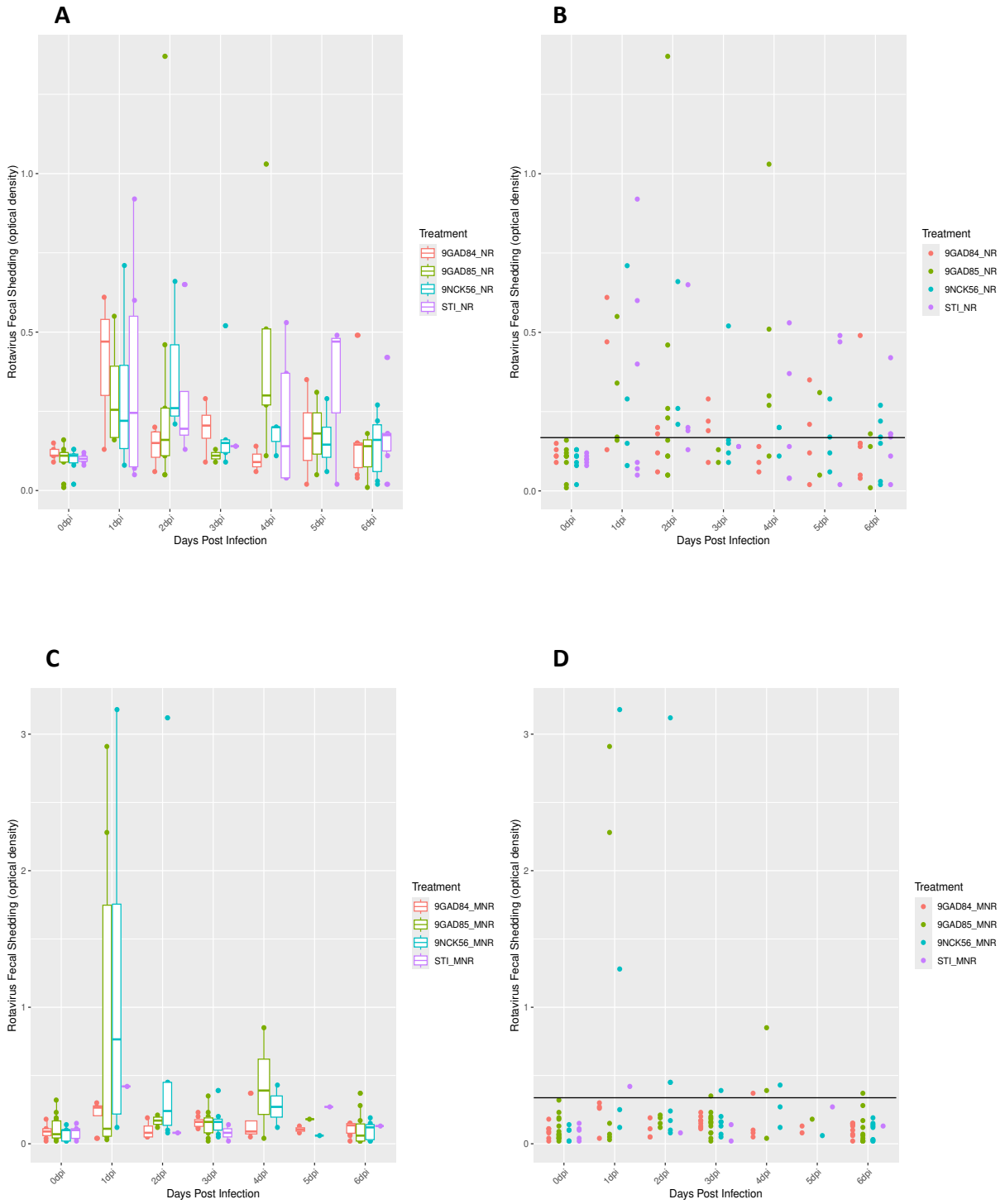

Figure 3.7 **Neonatal fecal antigen shedding by neonatal treatment group and maternal infection.** Neonatal mice born to uninfected does have increased number of fecal shedding days (A-B) compared to neonates born to uninfected does (C-D).

Table 3.2 Neonatal fecal shedding days represented by number of neonates shedding more than baseline in each treatment group over six-day neonatal rotavirus challenge born to uninfected does, or rotavirus infected does.

Uninfected Does				Rotavirus Infected Does			
Days post infection	Total neonates shedding	Number of neonates shedding	Neonatal Treatment Group	Days post infection	Total neonates shedding	Number of neonates shedding	Neonatal Treatment Group
1	10	3	STI_NR	1	5	1	STI_MNR
		2	NCK56_NR			2	NCK56_MNR
		2	GAD84_NR			0	GAD84_MNR
		3	GAD85_NR			2	GAD85_MNR
2	11	3	STI_NR	2	1	0	STI_MNR
		3	NCK56_NR			1	NCK56_MNR
		2	GAD84_NR			0	GAD84_MNR
		3	GAD85_NR			0	GAD85_MNR
3	4	0	STI_NR	3	2	0	STI_MNR
		1	NCK56_NR			1	NCK56_MNR
		3	GAD84_NR			0	GAD84_MNR
		0	GAD85_NR			1	GAD85_MNR
4	7	2	STI_NR	4	4	NA	STI_MNR
		1	NCK56_NR			1	NCK56_MNR
		0	GAD84_NR			1	GAD84_MNR
		4	GAD85_NR			2	GAD85_MNR
5	7	2	STI_NR	5	0	0	STI_MNR
		2	NCK56_NR			0	NCK56_MNR
		2	GAD84_NR			0	GAD84_MNR
		1	GAD85_NR			0	GAD85_MNR

6	8	3	STI_NR	6	1	0	STI_MNR
		3	NCK56_ NR			0	NCK56_ MNR
		1	GAD84_ NR			0	GAD84_ MNR
		1	GAD85_ NR			1	GAD85_ MNR

Table 3.3 Summary table of the total number of fecal shedding days for all neonates born to uninfected does and rotavirus infected does.

	Neonates born to Uninfected Does	Neonates born to Infected Does
Total days fecal shedding	47	13
Total number of samples	128	138

3.2.4: Maternal rotavirus infection significantly influences neonatal total and VP8-1 specific antibodies more than neonatal treatment alone.

There was a significant increase in GAD85_MR and NCK56_MR compared to GAD85 in VP8-1 specific IgM in the spleen (Figure 3.8A). There was no interaction effect of maternal rotavirus infection and neonatal rotavirus challenge at 21 days of age, but maternal infection was independently significant for VP8-1 IgM in the spleen ($p=0.0183$) ELISA indicating the significance of maternal rotavirus infection influence on neonatal outcomes (Figure 3.8B, Table S3.3). There was a significant interaction effect for maternal infection and neonatal treatment ($p=0.019641$) for total spleen IgM where nonchallenged neonates born to rotavirus infected does had significantly higher total IgM than nonchallenged neonates born to uninfected does (Figure 3.8C, Table S3.3). Neonates born to rotavirus infected does had increased IgM VP8-1 specific responses suggesting that the maternal infection influenced neonatal VP8-1 specific antibodies, however the only treatment group that was significantly different between rotavirus infected does

and uninfected does was GAD85 which suggests that the vaccine including adjuvants was able to perform better in the presence of maternal antibodies than GAD84.

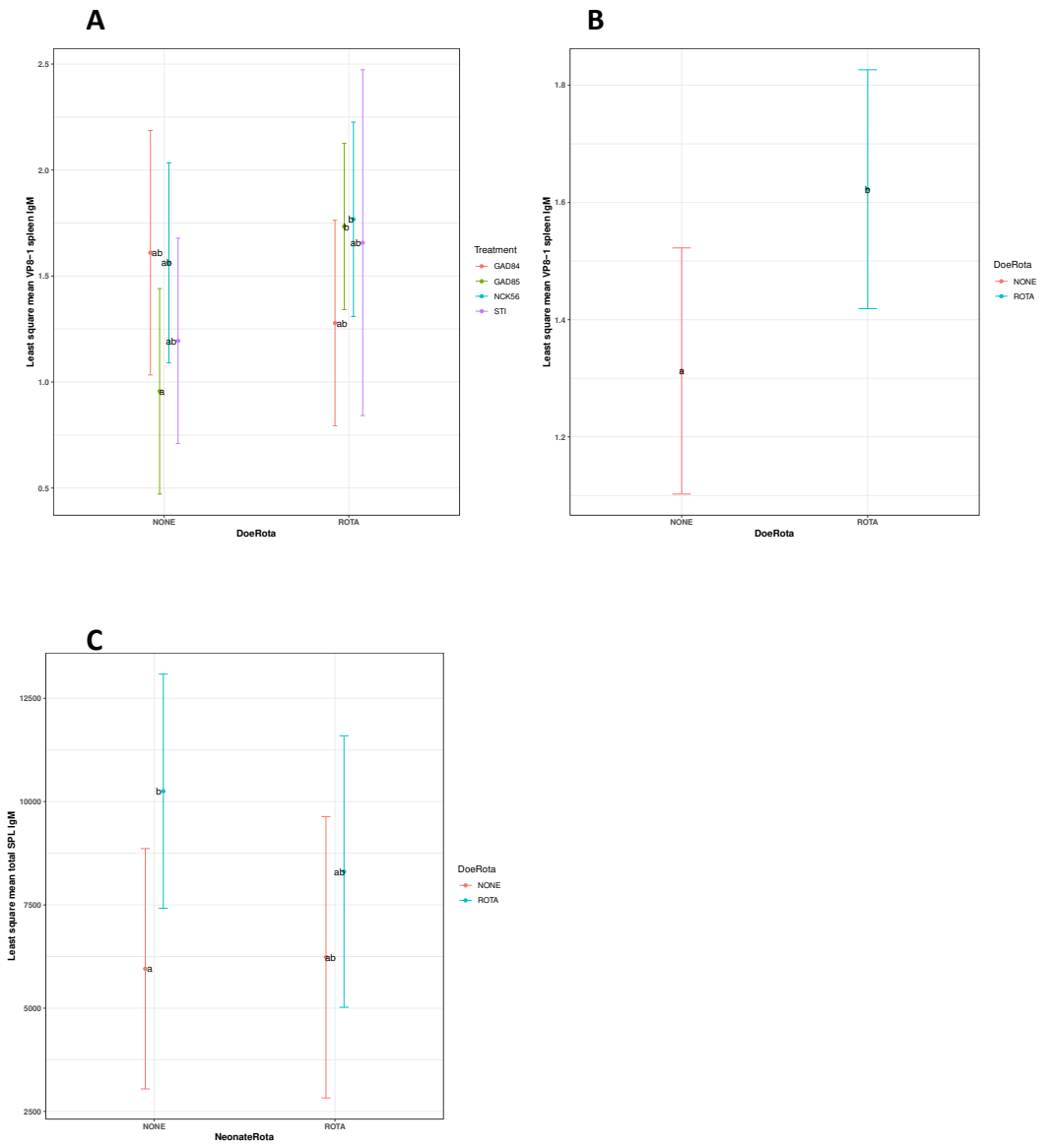

Figure 3.8 **Rotavirus significant total and VP8-1 specific IgM in the spleen cell supernatants of neonates.** VP8-1 specific IgM in the spleen by maternal infection and treatment (A), by maternal infection and neonatal challenge (B), all neonatal VP8-1 specific IgM in MLN by maternal infection (C), and the significant interaction between maternal infection and neonatal challenge in total IgM in the spleen (D). Significant differences are denoted on the figure (a, b) at the 0.05 level of significance.

The role of maternal infection continued in the IgG dataset where VP8-1 IgG in the spleen was significantly different between rotavirus infected and uninfected does (Figure 3.9A, Table S3.4). There was a significant interaction effect between maternal infection and treatment that resulted in a significant increase in total IgG for GAD85_MR compared to GAD85 (Figure 3.9B). There were no significant differences for total IgG, or total IgM in the MLN ELISA nor was there an effect of maternal infection on VP8-1 IgA (Table S3.5, Table S3.6). VP8-1 IgG in the MLN was significantly different between rotavirus infected does and uninfected does and total IgA had a significant interaction effect of maternal infection and neonatal treatment (Table S3.7).

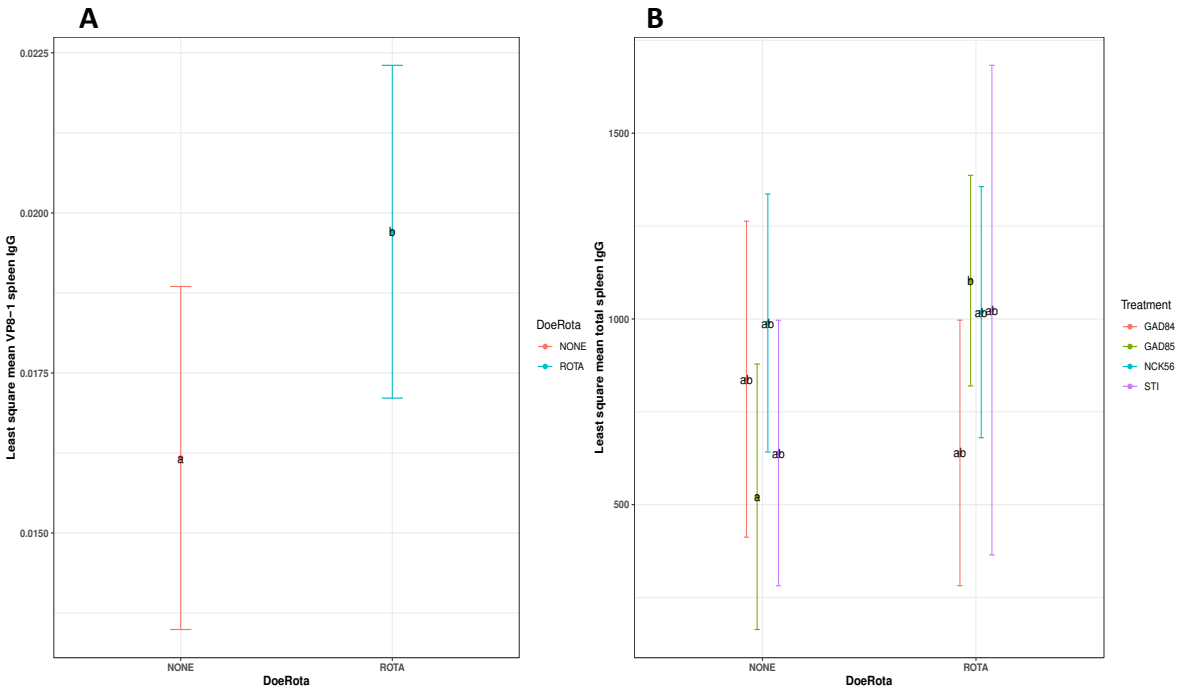

Figure 3.9 A-B **Cell supernatant ELISA has a significant effect of maternal rotavirus and an interaction effect of maternal rotavirus infection and neonatal treatment in IgG.** VP8-1 specific IgG in the spleen significantly increased in rotavirus infected does (A) and total IgG in the spleen had a significant interaction between maternal infection and neonatal treatment (B). Significant differences are denoted on the figure (a, b) at the 0.05 level of significance.

Taken together these results suggest that the maternal infection plays a dynamic role in the rotavirus specific and total antibody production in neonates. However, the GAD85 vaccinated neonates were the only neonatal treatment group that had significant increases in the presence of maternal anti-rotavirus antibody. This suggests that the GAD85 vaccine is producing a more robust immune response in rotavirus specific IgM and total IgG compared to the GAD84 vaccine, and the control groups, NCK56 and STI. We next sought to use the live B cell dataset to confirm these patterns of maternal infection influence.

While there were no significant differences for VP8-1 IgA fluorescence intensity in live B cells in the spleen or MLN, maternal rotavirus infection was significant for IgA fluorescence intensity in live B cells in the Peyer's patches ($p=0.008867$, Figure 3.10A, Table S3.8-10). There was a significant interaction effect for VP8-1 IgM fluorescence intensity in live B cells in MLN ($p=0.03882$, Figure 3.10B, Table S3.9), and in the spleen there was no interaction effect, but maternal rotavirus infection was independently significant ($p=0.04983$, Figure 3.10C, Table S3.8). VP8-1 specific IgG fluorescence intensity was not significantly different for maternal rotavirus infection at all (Table S3.8-3.10). This data suggests that maternal rotavirus infection is significantly influencing the VP8-1 antibody specific affinity of live B cells in these neonatal tissues. While maternal rotavirus infection was a significant aspect of the study design, and it is clearly associated with increased rotavirus specific and total antibody responses in the neonate, we also aimed to investigate the role of the neonatal challenge on the dataset before pursuing the specific treatment groups and their effectiveness in rotavirus protection.

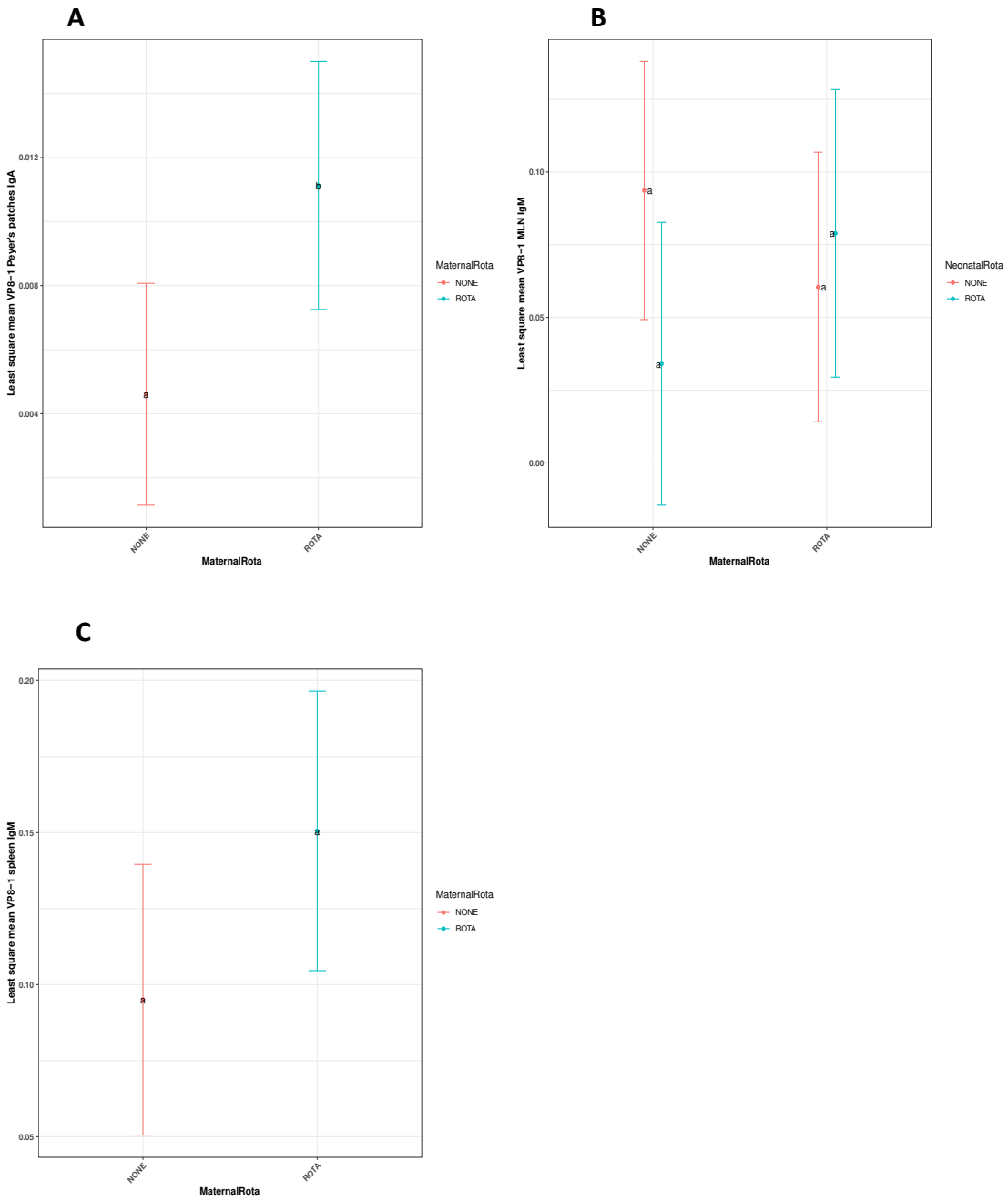

Figure 3.10 A-C **Live B cell fluorescence intensity changes with maternal rotavirus infection in VP8-1** IgA Peyer's patches (A), VP8-1 IgM in MLN (B), and VP8-1 IgM in spleen p=0.05177 (C) when all neonatal treatment groups are combined. Significant differences are denoted on the figure (a, b) at the 0.05 level of significance.

3.2.5: Neonatal rotavirus challenge significantly influences VP8-1 specific and total antibodies than neonatal treatment alone.

We saw a significant interaction effect for neonatal challenge and treatment in total IgA in the MLN cell supernatants, (Table S3.11) and total IgG in the spleen cell supernatants (Table S3.12). Regardless of maternal infection status, NCK56_NR, GAD85_NR and STI_NR had significantly increased total IgA in MLN after rotavirus challenge compared to NCK56, GAD84, and GAD85 suggesting that neonatal challenge did increase total IgA in the MLN (Figure 3.11A, Table S3.13). Similarly, there were no significant differences between treatment groups before rotavirus challenge but after rotavirus challenge GAD84_NR had significantly less total spleen IgG than NCK56_NR (Figure 3.11B).

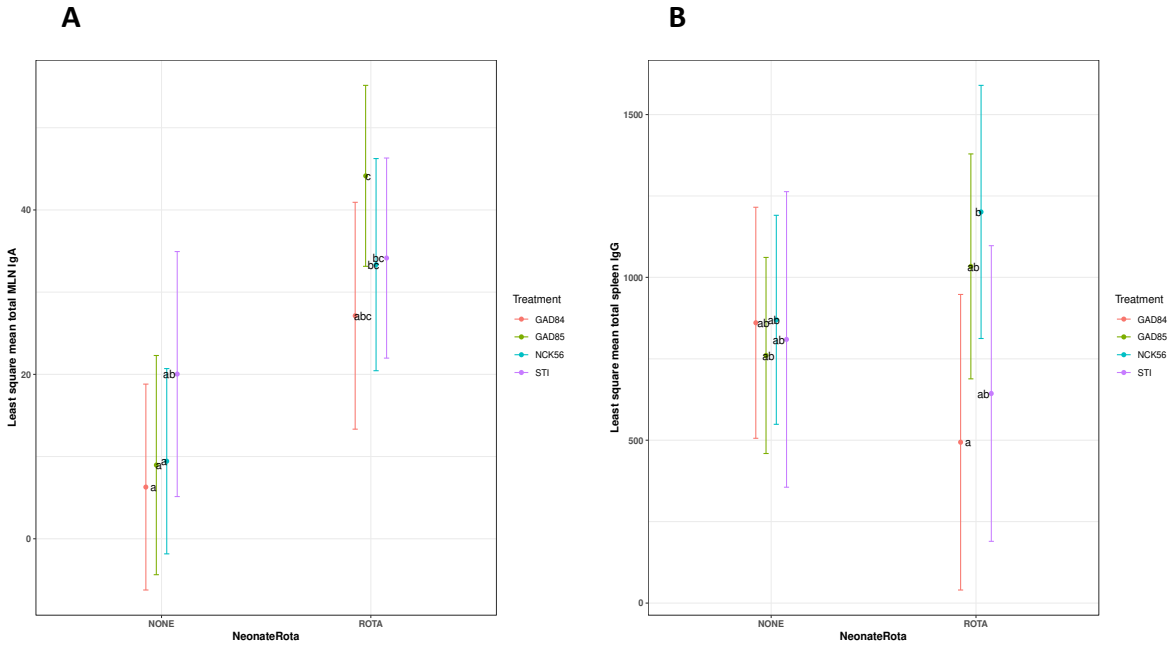

Figure 3.11 A-B **Cell supernatant ELISA shows significant role of rotavirus challenge in neonates for total IgA and total IgG.** Total IgA in MLN significantly increases in rotavirus challenged neonates compared to nonchallenged littermates (A) and IgG in the spleen significantly increases in NCK56_NR compared to STI_NR (B). Significant differences are denoted on the figure (a, b) at the 0.05 level of significance.

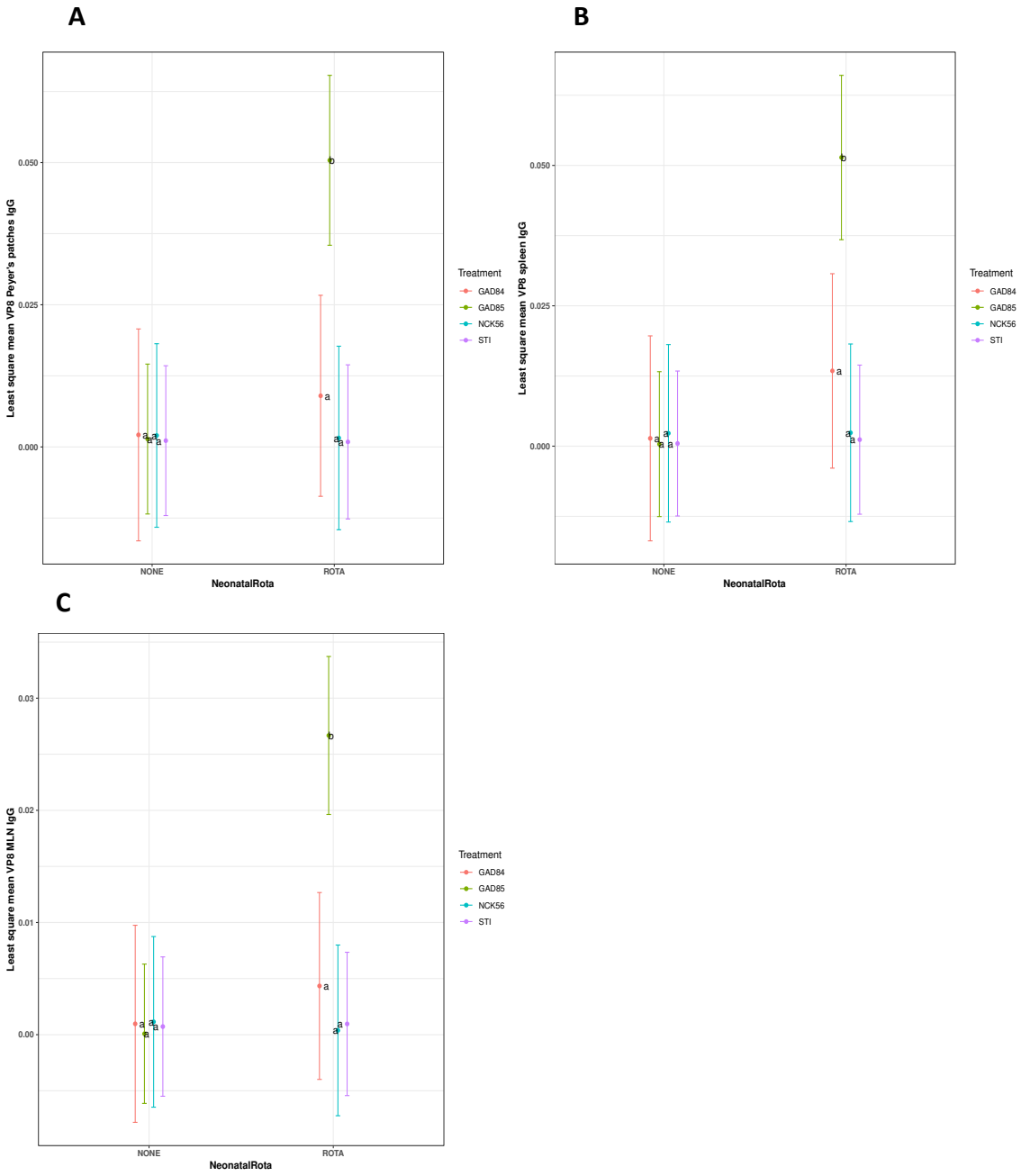

Figure 3.12 A-C **Cell supernatant ELISA indicates GAD85_NR has greatest rotavirus specific affinity in all tissue types compared to all other groups.** VP8-1 specific IgG maximum fluorescence intensity from live B cell ELISpot assays were significantly different between treatment and neonatal rotavirus challenge where GAD85_NR is significantly increased compared to all other groups in the Peyer's patches (A), spleen (B), and MLN (C). Significant differences are denoted on the figure (a, b) at the 0.05 level of significance.

By contrast, VP8-1 specific IgG fluorescence intensity in live B cells in the spleen, MLN, and Peyer's patches did not have a significant interaction effect but were significantly different

based on neonatal challenge for all three tissue types (p=0.0006989, p=0.001277, p=0.003245, Table S3.8-S3.10). VP8-1 specific IgG fluorescence intensity in live B cells significantly increased in GAD85_NR compared to all other groups in the spleen, MLN, and Peyer's patches (Figure 3.12A-C). This suggests that the adjuvant inclusive vaccine increased the VP8-1 specific IgG affinity of the B cells. There were no significant effects of neonatal challenge on VP8-1 specific IgA fluorescence intensity in live B cells in the spleen, MLN or Peyer's patches.

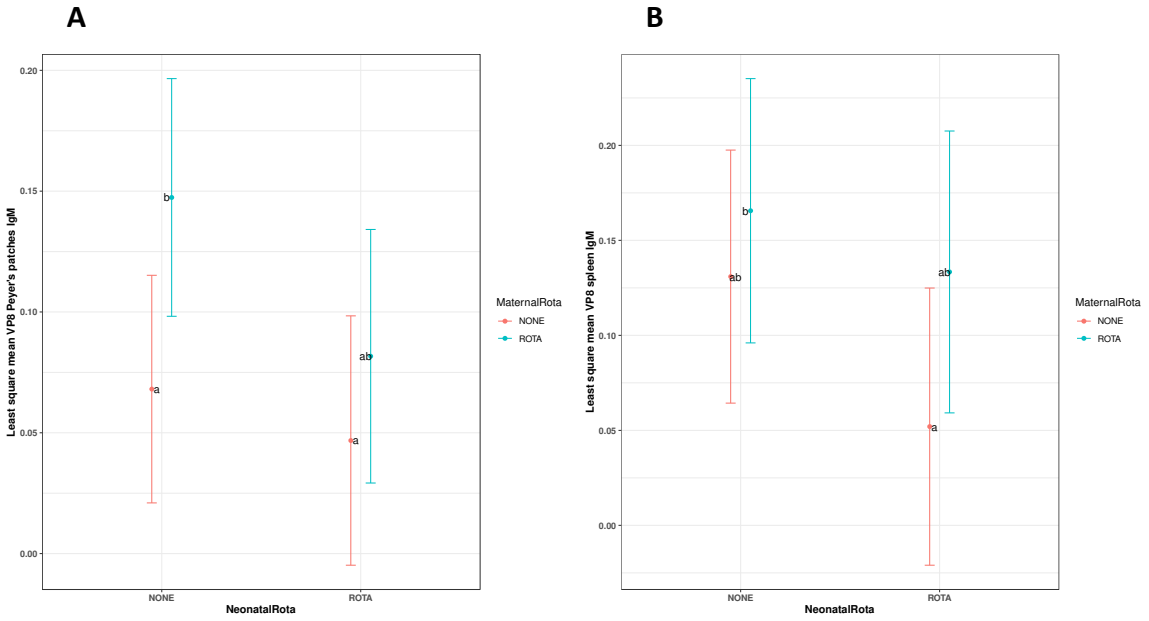

Figure 3.13 A-B **Cell supernatant ELISA has significant maternal rotavirus infection and neonatal challenge interaction effect in VP8-1 specific IgM data.** VP8-1 specific IgM is significantly different for maternal infection and neonatal rotavirus challenge in the Peyer's patches (A) and spleen (B). Significant differences are denoted on the figure (a, b) at the 0.05 level of significance.

There was a significant interaction effect of maternal infection and neonatal challenge for VP8-1 specific IgM in the spleen and Peyer's patches cell supernatants (Table S3.3). Regardless of treatment, nonchallenged neonates born to rotavirus infected does had significantly higher VP8-1 IgM in Peyer's patches compared to both nonchallenged and rotavirus challenged

neonates born to uninfected does (Figure 3.13A). In the spleen, nonchallenged neonates born to rotavirus infected does had higher VP8-1 IgM compared to rotavirus challenged neonates born to rotavirus infected does (Figure 3.13B).

In the spleen and Peyer's patches there was no significant interaction effect, but neonatal challenge was independently significant ($p=0.04689$, Figure 3.14A, $p=0.032609$, Figure 3.14B) for VP8-1 specific IgM fluorescence intensity. There was a significant decrease in VP8-1 specific IgM fluorescence intensity for both spleen and Peyer's patches in neonatal mice challenged with rotavirus compared to their control littermates that were not challenged. This indicates that neonates challenged with rotavirus at 21 days of age had decreased VP8-1 specific IgM affinity. We suggest that after the rotavirus challenge the neonates increased production of IgM and since these samples were collected only seven days after rotavirus challenge, the neonatal immune system did not have sufficient time to undergo somatic hypermutation to produce high affinity VP8-1 specific IgM. Similarly, maternal rotavirus infection was independently significant ($p=0.05177$, Figure 3.14C, $p=0.004387$, Figure 3.14D) for VP8-1 specific IgM fluorescence intensity. There was a significant increase in neonates born to rotavirus infected does compared to uninfected does but without an interaction effect we will consider these rotavirus exposures independent of one another.

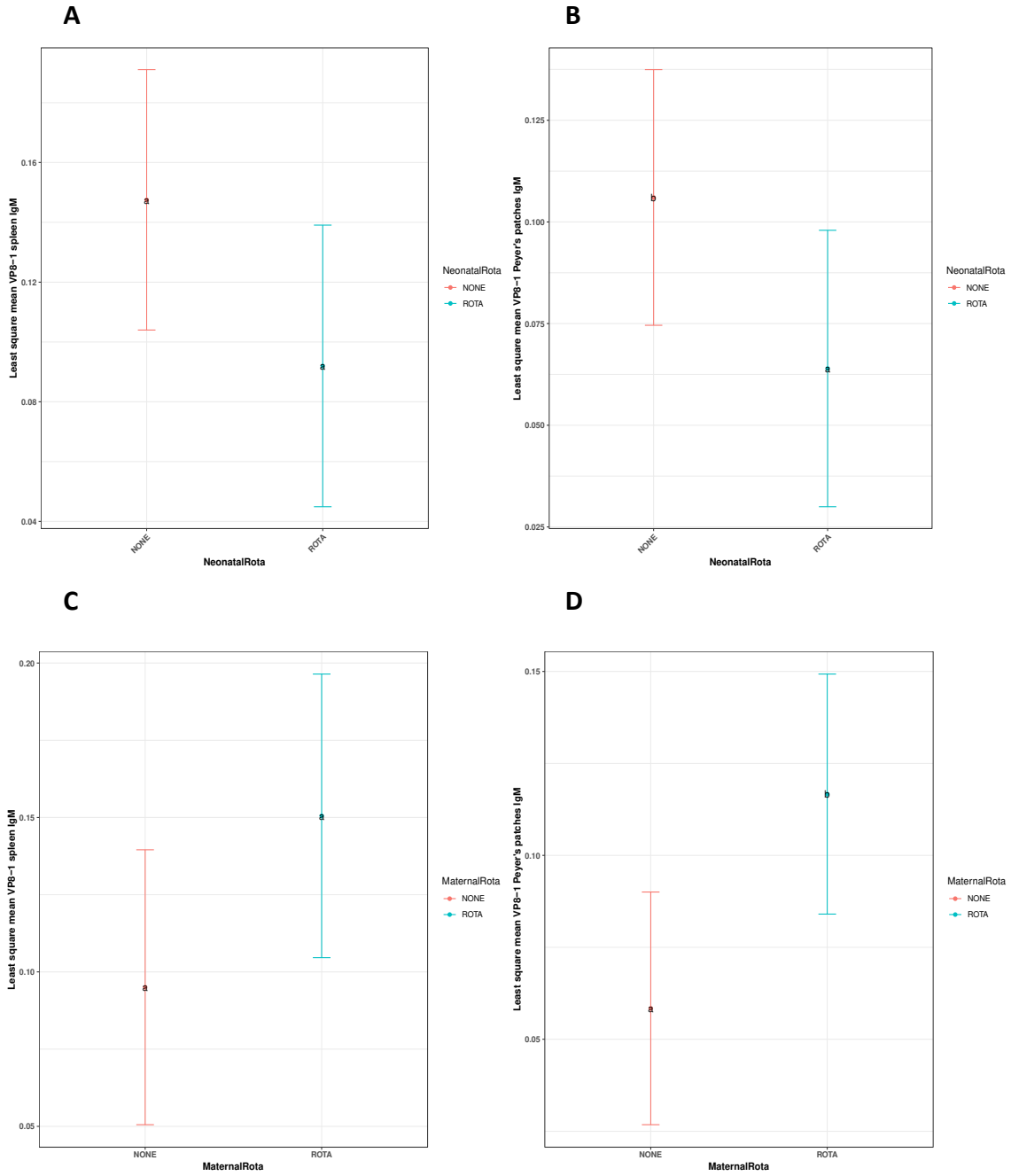

Figure 3.14 A-B **Live B cell VP8-1 IgM fluorescence intensity was significantly decreased** in the spleen (p=0.04689) (A), and Peyer's patches (B) when neonates were challenged with rotavirus compared to their control littermates. There was a significant increase in VP8-1 specific IgM affinity in neonates born to rotavirus infected does compared to uninfected does in the spleen (p=0.05177) (C) and Peyer's patches (D). Significant differences are denoted on the figure (a, b) at the 0.05 level of significance.

These data confirm that maternal rotavirus infection prior to gestation and neonatal challenge after treatment have a significant influence on neonatal immunologic outcomes. Further, the significant differences between groups when there is an interaction effect of maternal rotavirus infection and neonatal challenge correlate to differences between nonchallenged neonates born to infected does and challenged neonates born to infected does. When neonates had both maternal rotavirus infection and neonatal challenge there was a canceling effect where the VP8-1 specific levels were not significantly different from nonchallenged neonates born to uninfected does. By contrast, when there were no significant interaction effects, and only maternal infection was significant there was a consistent increase in the neonatal immune outcome. The role of repeated virus exposure is a valuable trend to consider before investigating the effectiveness of the vaccines because it broadly examines the maternal-neonatal relationship and immunity regardless of neonatal treatment. Next, we will look at changes within specific treatments to determine how each neonatal treatment interacts with the maternal infection and neonatal challenge.

3.2.6: GAD85 has an increase in VP8-1 specific and total antibodies even in the face of maternal antibodies, unlike GAD84.

Maternal rotavirus infection, neonatal rotavirus challenge and doe specific influences have been shown to impact the neonatal immune outcomes in rotavirus specific affinity of B cells and antibodies in cell supernatants (3.2.2, 3.2.4, 3.2.5). At a more detailed level, we wanted to investigate the specific differences between treatment groups when all rotavirus infection parameters (maternal infection, neonatal challenge) were included. We found that total IgG in

the spleen significantly increased in GAD85_MR and GAD85_MNR compared to GAD85 suggesting that both maternal rotavirus infection and neonatal rotavirus challenge increased total IgG (Figure 3.15A). Total IgM in the spleen significantly increased in GAD85_MR compared to GAD85 but was not significant compared to GAD85_NR or GAD85_MNR (Figure 3.15B). By contrast, there was no significant difference in total IgG or total IgM in GAD84 groups. NCK56_NR significantly increased total IgG in the spleen compared to NCK56 suggesting that neonatal challenge increased total IgG more than maternal infection or neonatal challenge and maternal infection together.

Further, GAD85_MR had a significant increase in VP8-1 specific IgM compared to GAD85 (Figure 3.15C). There were no significant differences in VP8-1 specific IgG or IgA for the spleen, and the only total IgA significant difference was in NCK56_NR and NCK56_MR compared to NCK56 (Figure 3.15D).

In the MLN GAD85_MNR and GAD85_NR had significantly higher total IgA compared to GAD85 (Figure 3.16). There were no significant differences in total IgG and IgM. NCK56_MNR was significantly higher in total IgA than NCK56 (Figure 3.16).

Taken together these results validate the effectiveness of the GAD85 vaccine operating in the presence of maternal antibodies and neonatal rotavirus challenge after vaccination given that there were significant increases in GAD85_MR, GAD85_MNR and GAD85_NR compared to GAD85. While all three rotavirus exposed groups (GAD85_NR, GAD85_MR, GAD85_MNR) do not have increased responses for all total and VP8-1 specific IgM, IgA and IgG, we suggest

this may be in part due to the maternal influence and how the neonatal system differs depending on when and how it is exposed to rotavirus. In addition, there are increases in GAD85_NR, GAD85_MR and GAD85_MNR compared to GAD85 that do not reach significant difference but do have a higher mean.

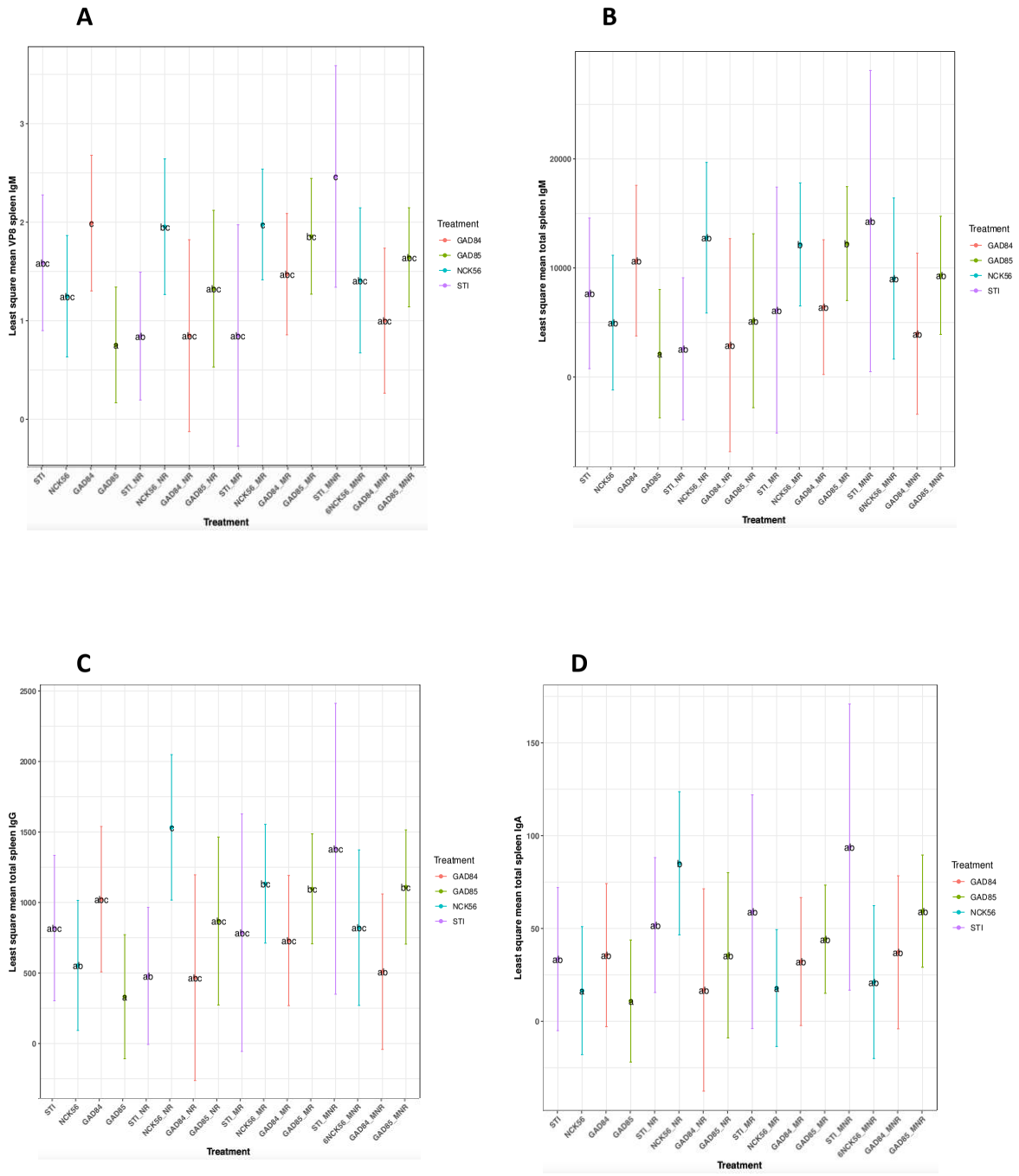

Figure 3.15 A-D **Cell supernatant ELISA investigating all significant changes between all independent treatment groups.** Total IgG in the spleen is significantly different for GAD85 and NCK56 (A), total IgM in the spleen is significantly different for GAD85 (B), VP8-1 IgM in the spleen is significantly different in GAD85 and STI (C), and total IgA in the spleen is significantly different in NCK56 (D).

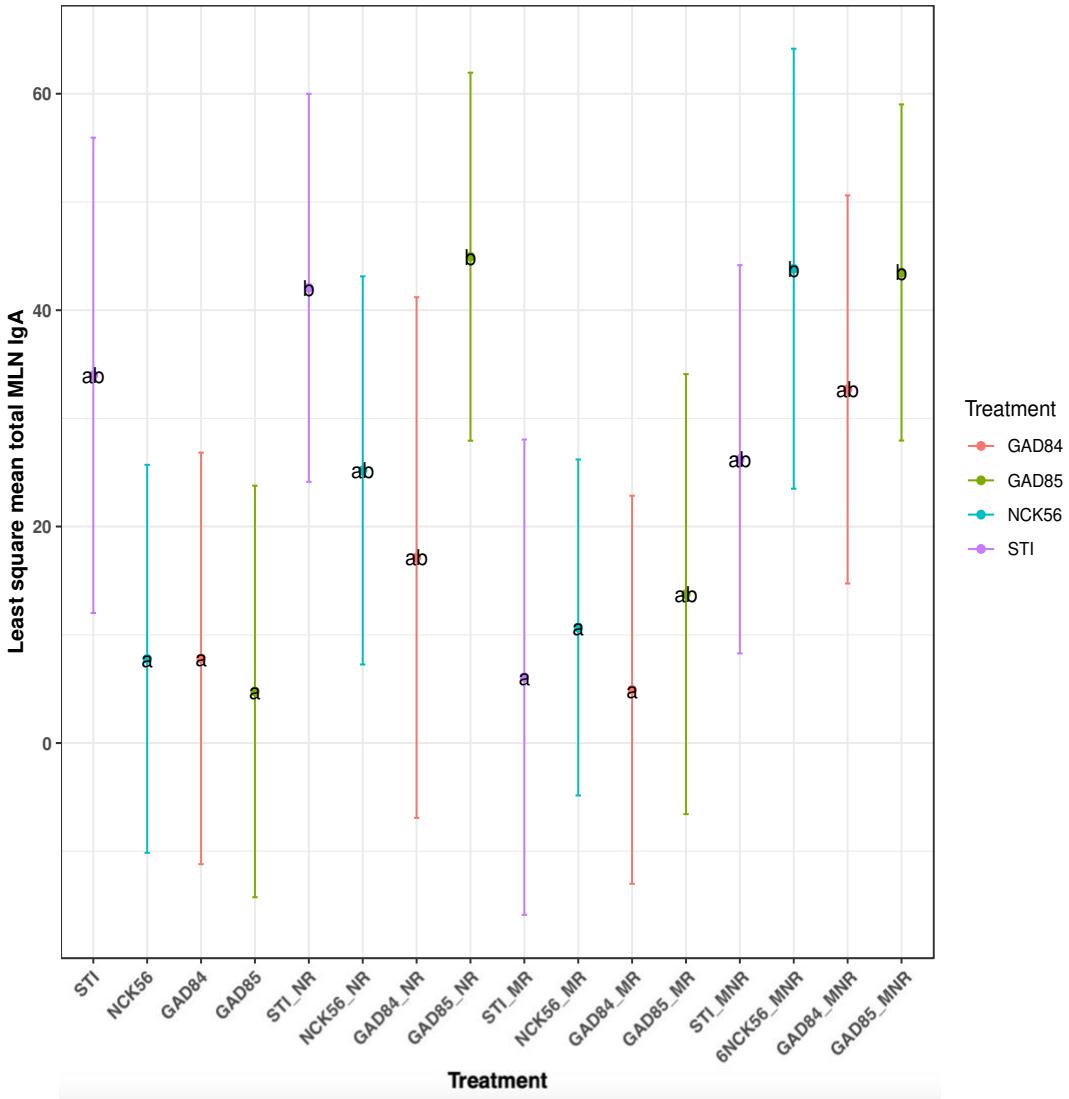

Figure 3.16 **Cell supernatant ELISA shows significant total IgA changes in the MLN within all treatment groups.** Total IgA in MLN is significantly higher in STI_NR compared to STI_MR and in NCK56_MNR compared to NCK56_MR.

3.3: Discussion/Conclusion/Future Directions

The maternal-fetal and maternal-neonatal relationship is complex and inextricably linked. To better address neonatal protection in the first months of life, it is critical to consider maternal influence on the neonatal system. Maternal influence can affect the neonatal microbiome and immune development beginning in utero with transplacental transfer of antibodies and continue

postpartum with transfer of antibodies through breastmilk. Maternal gut, skin, and vaginal microbiomes influence neonatal colonization and immune cell maturity (53, 62). Maternal immunity and microbiomes can influence the effectiveness of neonatal vaccination (52, 50). We sought to determine the effectiveness of our novel recombinant vaccine in a neonatal model in the presence of maternal antibodies, and its protection from infection to neonatal challenge. Here we show that maternal rotavirus infection prior to gestation had a significant impact on neonatal immune outcomes but more specifically which doe the neonate was born to had a far greater association with the neonatal outcomes. Additionally, neonates born to does that had been previously infected with rotavirus had increased rotavirus-specific immune responses when vaccinated with the rLA vaccine containing adjuvants (GAD85). The strong association between neonatal immune outcomes and which mother the neonate was born to, suggests that understanding the different factors driving the maternal influence and the mechanisms of communication between mother and the neonate's immune system should be assessed when evaluating next generation rotavirus vaccine platforms. Consideration of all maternal health factors that have been shown to influence neonatal immune outcomes like stress (37), infections (46), and environmental stimuli like smoking (51, 63) would be an overwhelming affair. As such, we suggest that this maternal specific evaluation begin with investigation of maternal microbiomes and maternal rotavirus antibody status.

Previous studies have shown that differences in maternal microbiomes and breastmilk compositions during periods of infection impact the neonate (36, 45). Rotavirus infection and prevalence varies around the world, with some countries experiencing as low as a 44% efficacy in vaccination (33). One hypothesis to explain the variance in neonatal vaccine effectiveness is

the influence of maternal antibodies during neonatal vaccination (55). To combat the different responses to the current attenuated live vaccines, we suggest considering different vaccines for neonates located in high rotavirus incidence areas compared to those of low rotavirus incidence. Here we showed that neonates delivered the rLA adjuvanted vaccine (GAD85) and born to infected does have increased rotavirus specific responses where there were no significant differences within neonatal treatment groups that were born to uninfected does. It is possible that different vaccine platforms will be needed for populations where rotavirus infection, maternal or neonatal, is lower than where rotavirus infection is higher.

When a neonatal vaccine is cleared by maternal virus specific antibodies, the neonate is unable to mount an immune response which leaves them unprotected when maternal antibodies wane. This lack of immune preparation due to maternal antibody interference can be fatal during the first year of life. We set out to determine if the novel recombinant *Lactobacillus acidophilus* vaccine would offer protection to vaccinated neonates compared to the controls when maternal rotavirus-specific antibodies are present. We showed that VP8-1 specific IgM increased in cell supernatants of rotavirus vaccinated neonates compared to all other treatment groups. This suggests that the GAD85 vaccine was able to induce rotavirus-specific immune responses even in the presence of maternal antibodies. Perhaps mucosal vaccines are the next frontier for neonates, particularly in countries where rotavirus infection is higher.

This data suggests that effective vaccination of neonates requires the use of adjuvants to increase immunogenicity. Neonatal immune systems are skewed toward a Th2 phenotype (). This anti-inflammatory status is intentionally implemented to provide the neonatal immune

system time to progressively adapt from a life in utero to one outside of it. Maternal passive immunity is intended to provide protection during this transition as the neonatal immune system sequentially activates and awakens. In this dataset, the non-adjuvant vaccine did not show an increased specific immune response in neonates during the neonatal rotavirus challenge or when neonates were born to an exposed mother. The FliC and FimH adjuvants included in GAD85 provided enough additional immune stimulation to result in an immune response even in the presence of material antibody. Adjuvants have been considered for use in vaccines to enhance immunogenicity for vulnerable populations (59) and results here suggest they are likely to be necessary to stimulate an immune response to probiotic based vaccines.

Previous pilot studies in the lab have shown the significant role of maternal interaction in neonatal results (4.2.3.1, 4.2.3.2) similar to results represented in this chapter. As such, we consider that normalizing for maternal variation with the fecal microbiome transplant (FMT) may be an insufficient method. Future studies should consider optimal normalization with other techniques including fostering pups between does in addition to the FMT. Further, maternal samples could be collected for VP8 specific antibodies for ELISA and ELISpot analyses and used as an additional normalization at the level of analysis. Expanding breeding to ensure treatments are equally represented would improve these data and would be more plausible by using a fostering pup system as the treatment group would not be dependent on litter size. Future directions for this study include analysis of maternal fecal microbiome samples in addition to the neonatal samples to determine the success of the FMT and how similar maternal-neonatal pairs are in the context of their gut microbiomes. Beyond that, additional analyses and samples to consider would include breastmilk collection given the remarkable influence of the mother in

this dataset, and collection of her skin and vaginal microbiomes. Consideration of gnotobiotic maternal models or antibiotic treated maternal models prior to gestation could be included for another aspect of maternal normalization.

Taken together, the mechanisms of influence between mother and neonate are far from completely understood. We set out to consider the interaction from the perspective of the microbiome, the immune system, and the interjection of vaccination. We found that maternal rotavirus infection and maternal rotavirus specific antibodies affected neonatal immune outcomes and indeed did protect the neonate from rotavirus infection at weaning age of 21 days old. The long-term effect on this "protection" in the form of maternal interference on neonates' anti-rotavirus immune response is beyond the scope of this experiment as it was not designed to evaluate adapted immunity to challenge or repeat rotavirus exposure. Perhaps more importantly, this passive protection from the mother did not interfere with antibody production of neonatal mice who received the adjuvanted vaccine followed by rotavirus challenge indicating that adjuvants a are likely to necessary in next generation mucosal vaccine platforms.

CHAPTER 4 INVESTIGATING MATERNAL-NEONATAL IMMUNITY RELATIONS WITH THE GUT MICROBIOME

4.1: Introduction

Neonatal vaccination success against rotavirus differs around the globe. We aim to combat the gap in vaccine effectiveness by using an orally delivered and mucosal targeted platform. To best comprehend the vaccine performance, we considered the maternal and neonatal gut environments by studying the gut microbiome. The gut microbiome has various health implications including its influence on the maturation of the neonatal immune system in the first two years of life. Maternal passive protection wanes as neonates age and develop their independent immune memory. Optimizing a vaccine strategy to target the neonatal immune system without being cleared by maternal antibodies is an important step for vaccine development in neonates. To study the impact of our vaccination scheme on the neonate and how it is influence by maternal factors and how it is affected by rotavirus infection we sought to 1) establish a neonatal experimental model and identify the longitudinal shift of the neonatal gut microbiome with treatment intervention, 2) determine the effects of neonatal vaccination dose, 3) determine the trajectory of change of the microbiome during neonatal vaccination and rotavirus challenge, and 4) identify the role that maternal rotavirus infection has on neonatal microbiome development and stabilization.

4.2: Results

4.2.1: Data Processing

All samples were run through software Fastqc (version 0.12.0, 116), Multiqc (123), and Trimmomatic (version 0.39, 116) to assess quality of reads and trimmed with PHRED quality cutoff of 25 and minimum length of 150 base pairs. Trimmomatic parameters removed Nextera adapters (Table 2.11, 2.2.16). DADA2 (version 1.16, 124) and SILVA database (version 138.1, 117) were used to determine amplicon sequence variants (ASVs) and bacterial taxonomic identification. Figures that follow were generated in R with various packages (2.2.16). For analyses samples within each independent study were segregated into different dataframes in R. Distribution of sequencing depth (SFigure 4.1-3) was evaluated for each study involved to determine if sufficient depth was accessed to evaluate the data.Rarefaction curves (SFigure 4.4-6) were used to examine diversity and depth of coverage for the sequencing run. Samples were dropped from each study analysis if there were no reads detected or if the depth was insufficient for adequate representation. Here we discuss the major findings of the sequencing in parallel with the immunology datasets for four studies: 1) pilot neonate vaccination study (2.2.13.1), 2) expanded dose neonatal vaccination study (2.2.13.2), 3) pilot neonate vaccination and challenge study (2.2.13.3), and 4) pilot maternal antibody influence neonate vaccination study (2.2.13.4).

4.2.2: Neonatal exposure to treatment and maternal fecal microbiome transplants changes the gut microbiome.

To investigate the effectiveness of our recombinant vaccine in neonates, we sought to establish a neonatal vaccination model (2.2.13.1). This preliminary study established the base for the experimental design used in further studies. Only 29 samples, out of the 58 that were sequenced in association with this pilot study, survived preprocessing and were included in downstream analyses. These 29 samples included neonatal samples at 10, 14, 15, and 16 days of age, in addition to doe samples before and after fecal microbiome transplant (FMT, 2.2.3) and

the FMT gavage content. Samples included had a total number of reads between 455 at the minimum and 172,893 at the maximum.

4.2.2.1: Increased *Akkermansia* and *Lactobacillus* after FMT.

There was a significant difference in timepoint for richness (p=0.008088), Shannon diversity (p=0.05128), and InvSimpson diversity (p=0.03723) (Table S4.1) when does were evaluated before and after a fecal microbiome transplant. InvSimpson diversity and Shannon diversity decreased in does after the fecal microbiome transplant (FMT) compared to before the FMT (Figures 4.1A and C). Richness also significantly decreased in does after the FMT compared to before (Figure 4.1B). On average, post FMT does had an increase in *Akkermansia* and *Lactobacillus* compared to does before the FMT (Figure 4.1D).

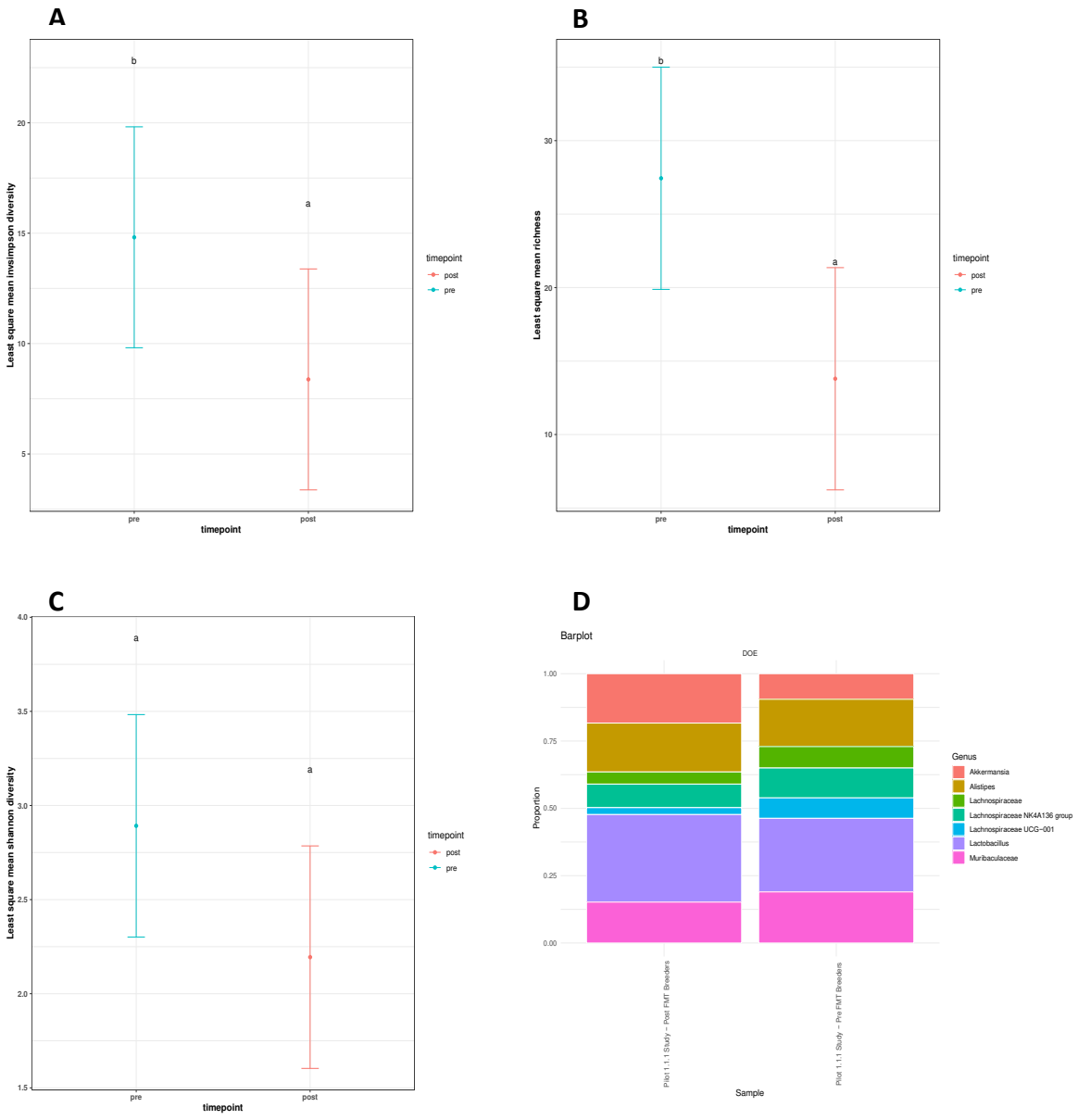

Figure 4.1 **Fecal microbiome transplant in does.** The fecal microbiome transplant delivered to breeding does significantly decreased InvSimpson diversity (A), Richness (B), and Shannon diversity (C), and had a community shift at the Genus level represented by the breeder bar plot (D). Significant differences are denoted on the figure (a, b) at the 0.05 level of significance.

4.2.3: Increased bacterial treatment dose modified the gut microbiome without shifting the immune response.

Once neonatal sampling and processing experimental design was confirmed we set out to identify the optimal dose delivery for neonates (2.2.13.2). We utilized two doses 10^6 (6GAD85 and 6NCK56) and 10^9 (9GAD85 and 9NCK56) CFU of the vaccine and the negative control to assess the potential impact on immune response and the microbiome. This study included fecal samples from 21-day old (do) neonates, breeder samples, and fecal microbiome transplant (FMT) gavage content. Of the 90 samples collected during this study, a subset of 75 samples were sequenced and 51 samples were included in analyses after preprocessing.

4.2.3.1: Dose delivery matters for neonatal gut microbiome but not secreting IgA or IgM.

There were no significant differences in rotavirus specific antibody secreting cells in GAD85 vaccinated neonates compared to their control groups although we did see a significant increase in 9GAD85 compared to 9NCK56 in VP8-1 and VP8Pep specific B cells in the spleen ($p=0.0017$, $p=0.0253$, SFigure 4.3A-C). We found a consistent trend of maternal influence in the immunology dataset. Within 6NCK56, 9NCK56 and 6GAD85, there were differences in total IgA secreting cells between treatment groups that were dependent on the breeding doe (Figure 4.2A). Total IgM secreting cells were increased in 9GAD85 compared to STI and 9NCK56 and again depended on the doe effect within each treatment group (Figure 4.2B). The extent of the maternal influence was surprising, so we elected to pursue investigation of the maternal and neonatal gut microbiomes to identify if the secreting antibody clustering was also reflected in differences between the gut microbial communities.

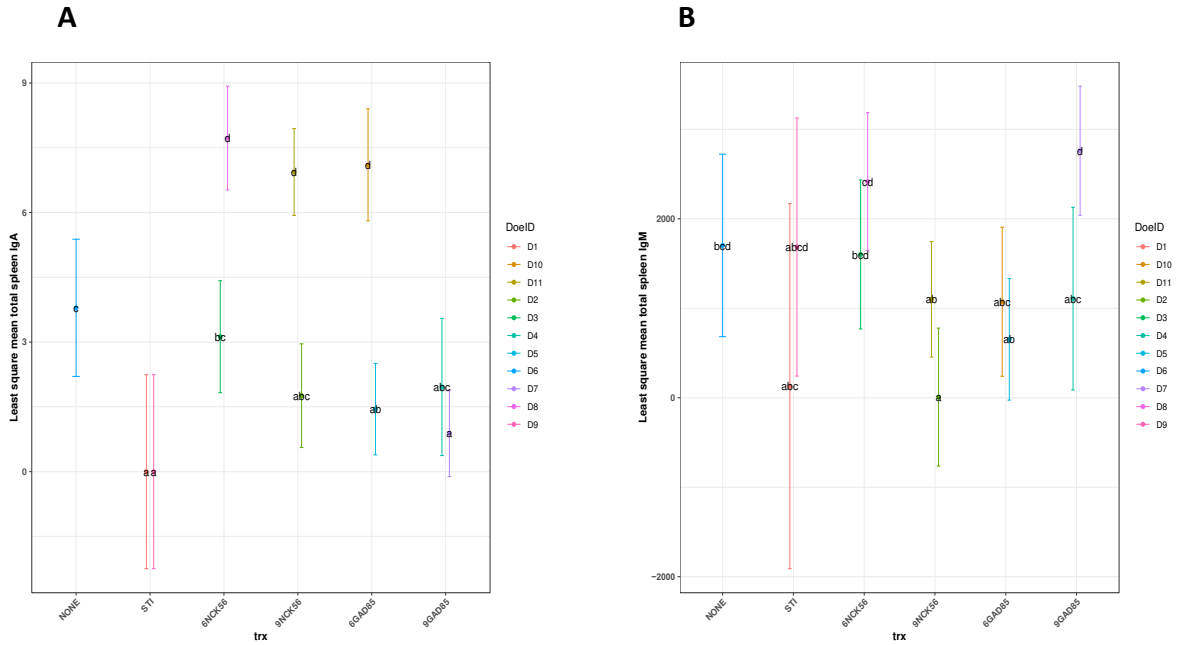

Figure 4.2 **Log of Total IgA and IgM secreting cells in the spleen.** Neonates have varying levels between and within treatment groups, but an essential pattern of breeding doe impact emerges within treatment groups (A) and consistently occurs in total IgM secreting cells in the spleen (B).

There was not a significant difference in alpha diversity between neonatal treatment groups, but we did note significant fold changes of certain bacteria (Table S4.2).

Neonates from both 6NCK56 and 9GAD85 had increased richness compared to 9NCK56 and 6GAD85 respectively. *Akkermansia* was significantly increased (5-fold) in 6NCK56 compared to 6GAD85 (Figure 4.3A). However, *Akkermansia* was significantly decreased in 6GAD85 and 9GAD85 compared to None (Figure 4.4 C-D). *Akkermansia* plays an essential role in the maintenance of the mucin layer in the intestines, these results are intriguing since the vaccine reduced *Akkermansia* abundance compared to the double negative no dose control group, None, and *Akkermansia* abundance increased in the wildtype positive control.

While *Lactobacillus* was significantly increased in 6NCK56, 9NCK56, 6GAD85, 9GAD85 compared to STI (Figure 4.4 A-D), it was not significantly different between any NCK56 or GAD85 groups (Figure 4.5 A-F). This suggests that while a higher concentration of *Lactobacillus acidophilus* was delivered to the 9NCK56 and 9GAD85 groups, the neonatal gut microbiome modulated this increase and within the seven days following the booster dose, we did not measure a significant increase in Lactobacillus *acidophilus* in the high dose groups (9GAD85, 9NCK56) compared to the low dose groups (6GAD85, 6NCK56). Further, *Lactobacillus* was significantly increased in the 9GAD85 vaccinated neonates compared to the no dose, double negative control group (None) (Figure 4.6 D), but not any of the other *Lactobacillus acidophilus* exposed groups (6NCK56 (Figure 4.7A), 9NCK56 (Figure 4.6 B), and 6GAD85 (Figure 4.6 C). Given that *Lactobacillus* increased in NCK56 and GAD85 groups compared to STI controls, but only 9GAD85 increased compared to the no dose double negative control, we suspect that delivery of the vaccine or wild-type *Lactobacillus acidophilus* supplemented the neonatal gut microbiome but did not outcompete other microbes present since we did not see a significant difference in *Lactobacillus* between STI and None (Figure 4.7).

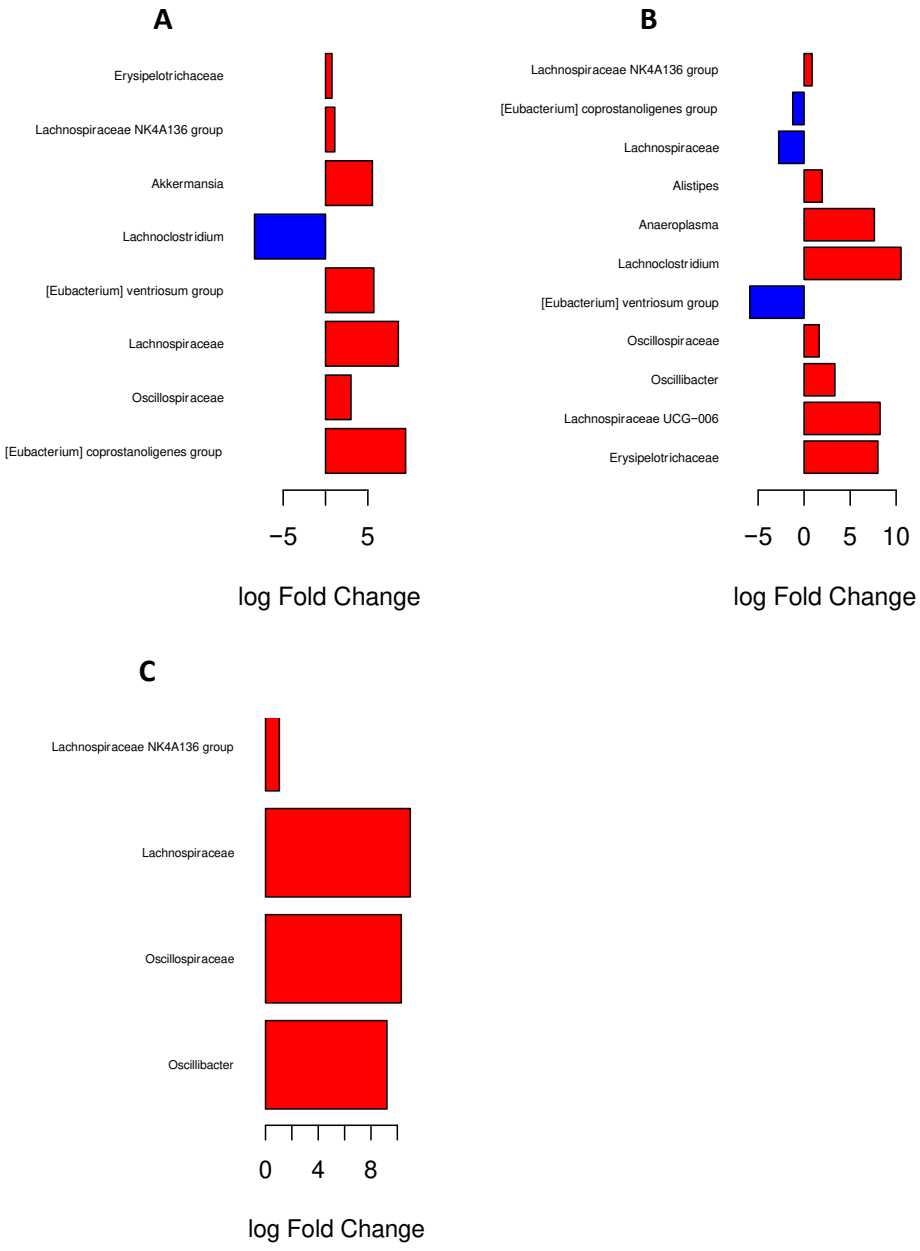

Figure 4.3 A-C. **Log fold change analyses in *Lactobacillus acidophilus* recipients.** Log fold change analyses between treatment groups to represent the significant shifts within the gut microbial communities based on their treatment, specifically between 6GAD85 | 6NCK56 (A), 6GAD85 | 9GAD85 (B), 6GAD85 | 9NCK56 (C).

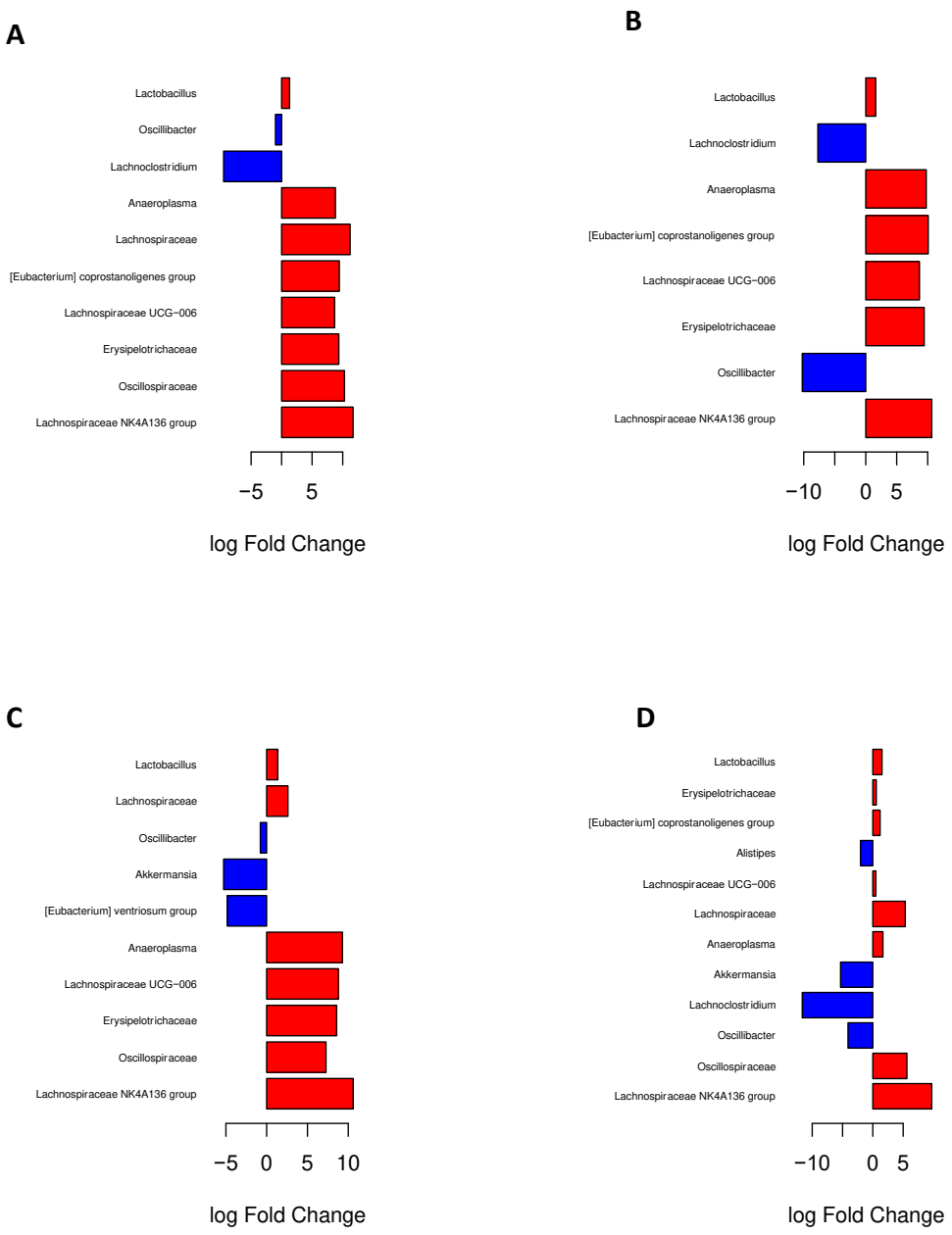

Figure 4.4 A-D. **Log fold change analyses compared to control buffer STI**. Log fold change analyses between treatment groups to represent their gut microbial communities and shifts that occurred by treatment, more specifically between 6NCK56 (A), 9NCK56 (B), 6GAD85 (C), 9GAD85 (D), and control buffer STI group.

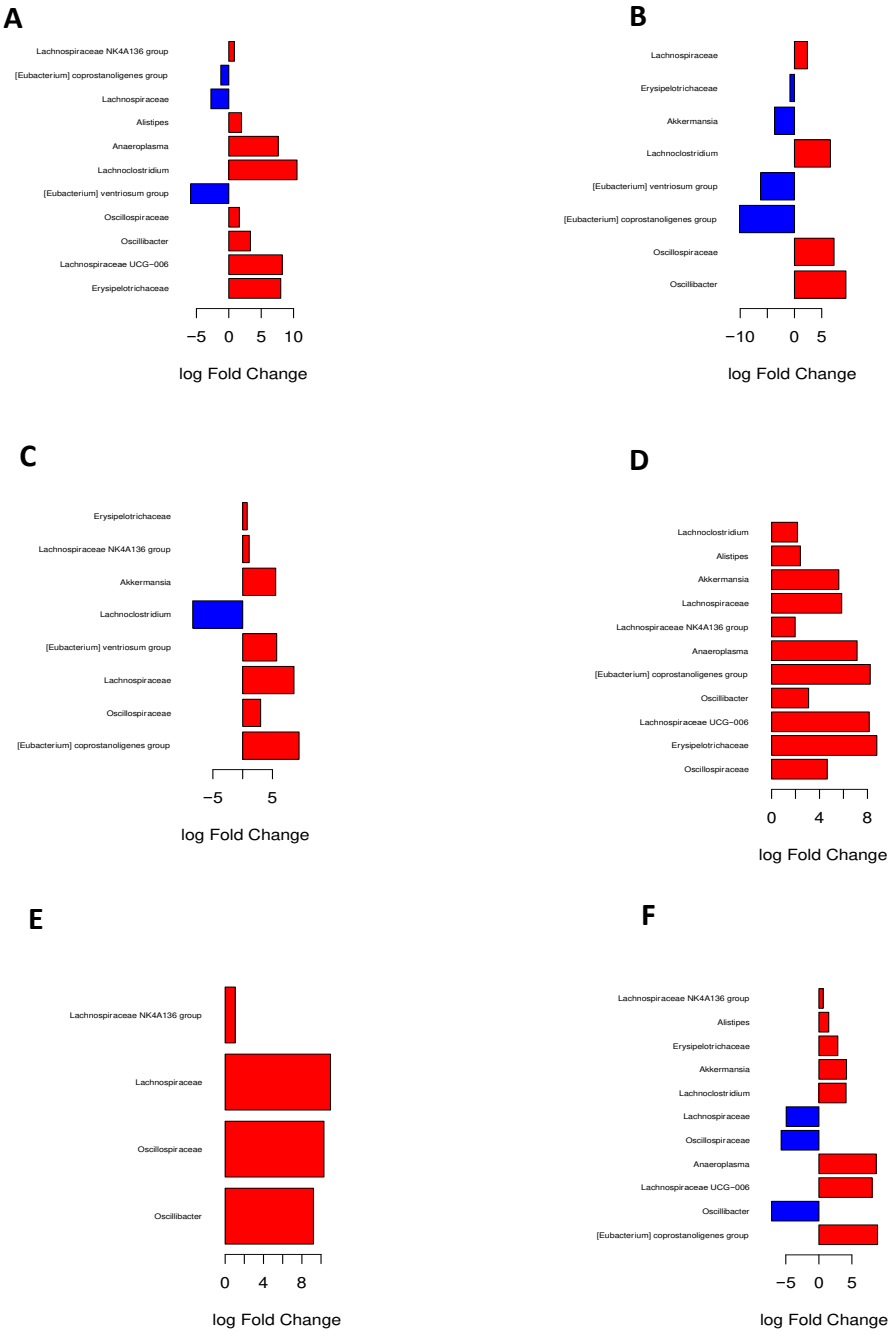

Figure 4.5 A-F **Log fold change analyses between differing dosages of bacteria.** Log fold change analyses between treatment groups to investigate shifts in the gut microbial community, more specifically between (A) 6GAD85 | 9GAD85, (B) 6GAD85 | 9NCK56, (C) 6NCK56 | 6GAD85, (D) 6NCK56 | 9GAD85, (E) 6NCK56 | 9NCK56, (F) 9GAD85 | 9NCK56. Notably there was no significant difference in *Lactobacillus* between all treatment groups that received doses of the wildtype control or the vaccine (NCK56, GAD85).

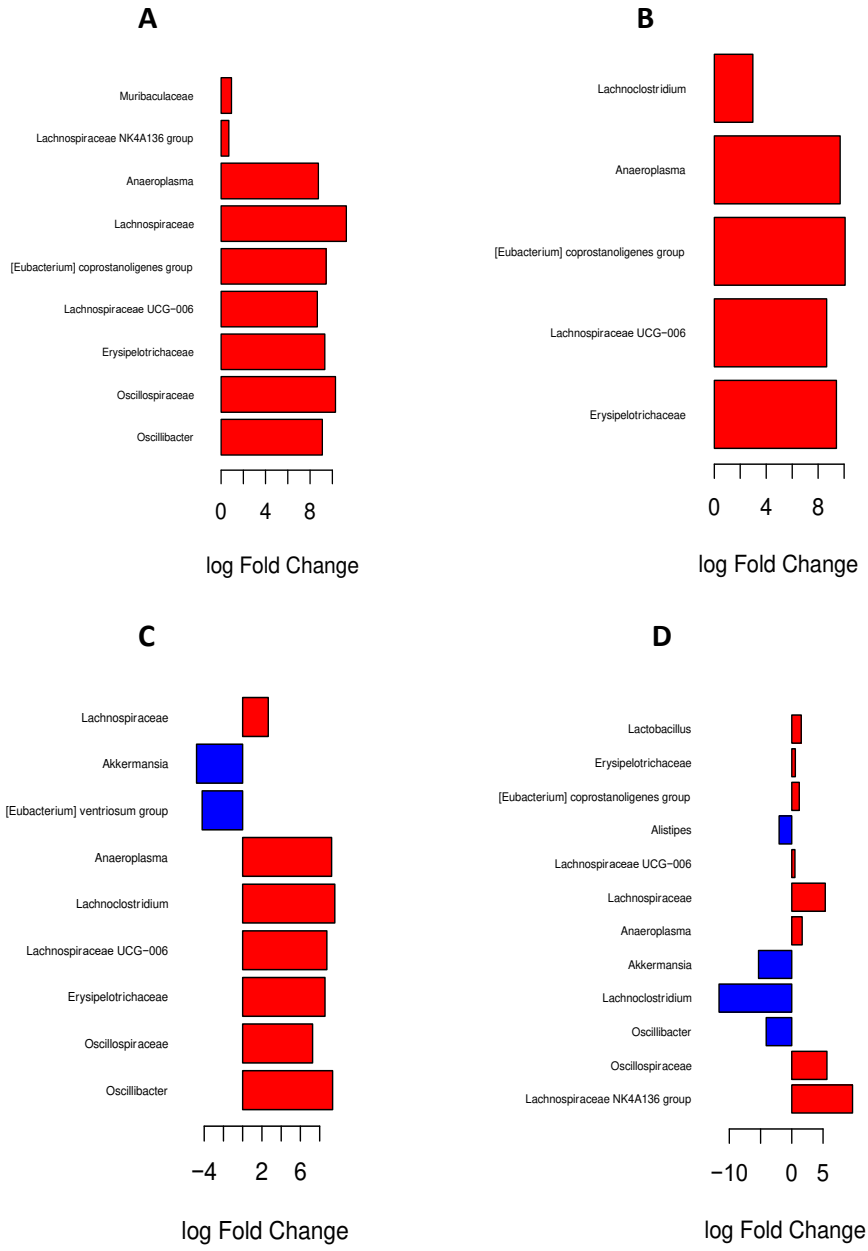

Figure 4.6 A-D. **Log fold change analyses compared to double negative no dose control.** Log fold change analyses between treatment groups to determine how treatment intervention modified the gut microbial community compared to the double negative no dose control group. More specifically, 6NCK56 (A), 9NCK56 (B), 6GAD85 (C), 9GAD85 (D) and the double negative no dose control None.

At the genus level, *Lachnoclostridium* and *Oscillibacter* were significantly increased in STI compared to None which distinguishes changes to the neonatal gut microbiome that result from the STI buffer as our gavage delivery method (Figure 4.7). Since the STI buffer is the delivery buffer for NCK56 and GAD85, it is not surprising that we see a significant increase in *Oscillibacter* in 6NCK56, 6GAD85, 9GAD85 compared to None (Figure 4.5A, C, D), and a significant increase in both *Lachnoclostridium* and *Oscillibacter* in 6GAD85 compared to None (Figure 4.5B). By contrast, *Lachnoclostridium* was significantly increased in STI, 6GAD85, 9GAD85, and 9NCK56 compared to 6NCK56 (Figure 4.3A, Figure 4.6A, Figure 4.4D, Figure 4.4E).

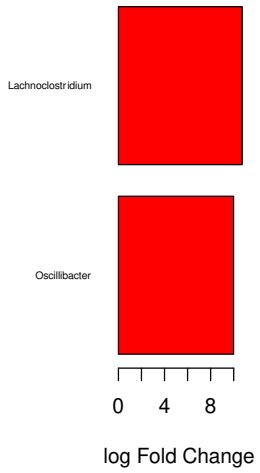

Figure 4.7 **Log fold change analyses between controls.** Log fold change analyses between the delivery buffer control, STI, and the no dose, double negative control, None, to determine how the STI delivery buffer that is used for all NCK56 and GAD85 treatments modified the microbiome.

4.2.3.2: Maternal factors influence neonatal gut microbiome regardless of treatment intervention.

Maternal gut microbiomes were substantially different from one another in richness before the FMT (Figure 4.8). Without post FMT samples in this sequencing run, we cannot confirm how the FMT modified the maternal microbiome prior to the third week of gestation. However, the Bray-Curtis dissimilarity matrix at the Genus level identified that the does are dissimilar to all neonatal groups (Figure 4.9). The doe sample (DOE, FMT) cluster more closely together and all the neonatal treatment groups cluster together (STI, NONE, NCK56, GAD85). Although neonatal microbiomes have been documented to be less diverse than adult microbiomes we wanted to investigate the impact the maternal microbiome has on the neonatal establishment of a gut microbiome. Further, given the influence of the breeding doe in the immunology dataset, we sought to identify if there were litter specific differences in the gut microbiomes. Taken together this suggests that even with a maternal fecal microbiome transplant and equal neonatal treatment intervention, there is a doe effect on the litter gut microbiome. As a result, to study neonates it is critical to include sampling of does in the experimental design and investigative process.

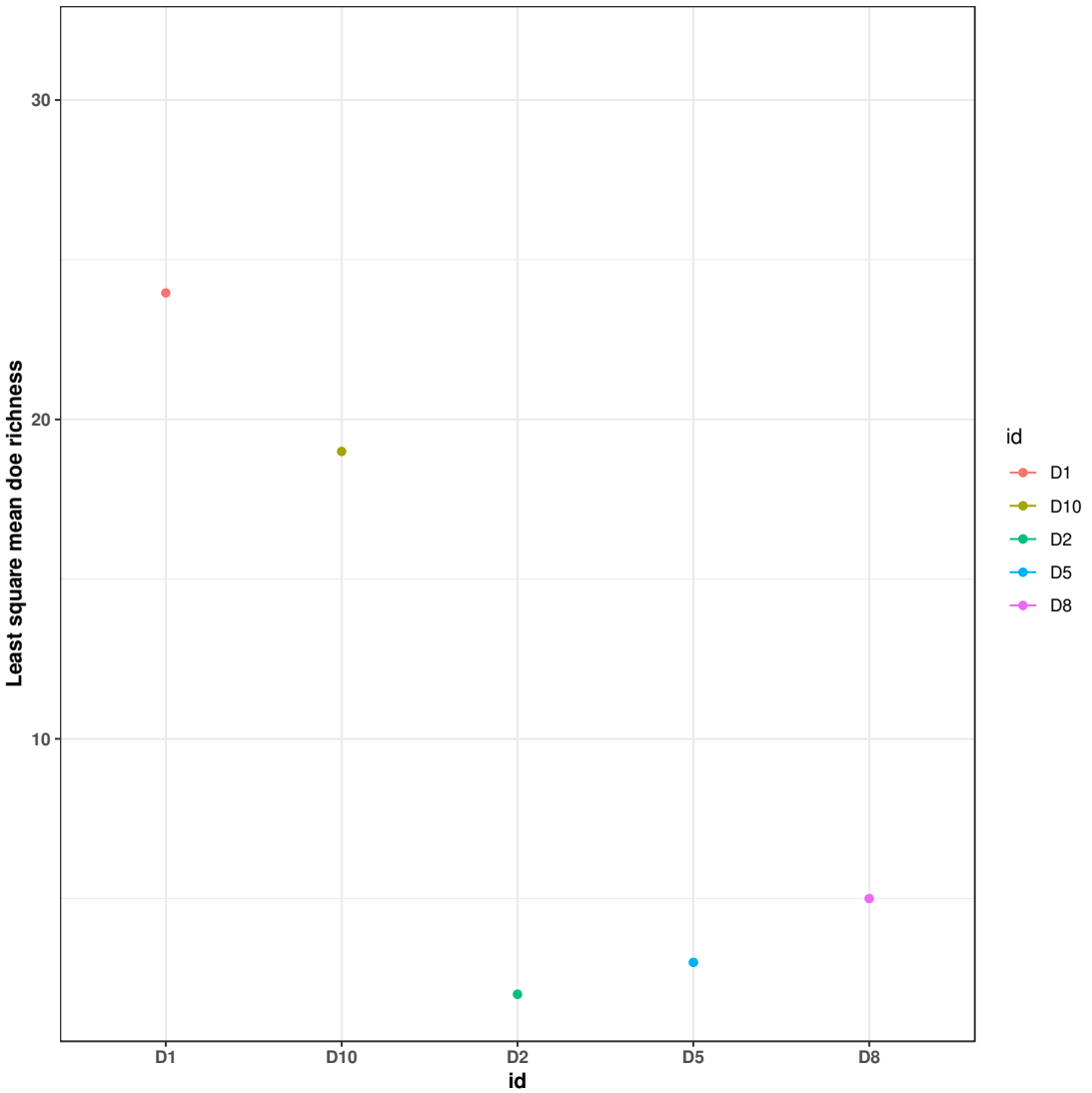

Figure 4.8 **Fecal microbiome transplant modified doe richness.** Richness differs dramatically between different breeding does microbiomes prior to fecal microbiome transplants in the expanded dose neonatal vaccination study (2.2.14.2). This wide variance is significant to consider for normalization of maternal factors while studying neonates.

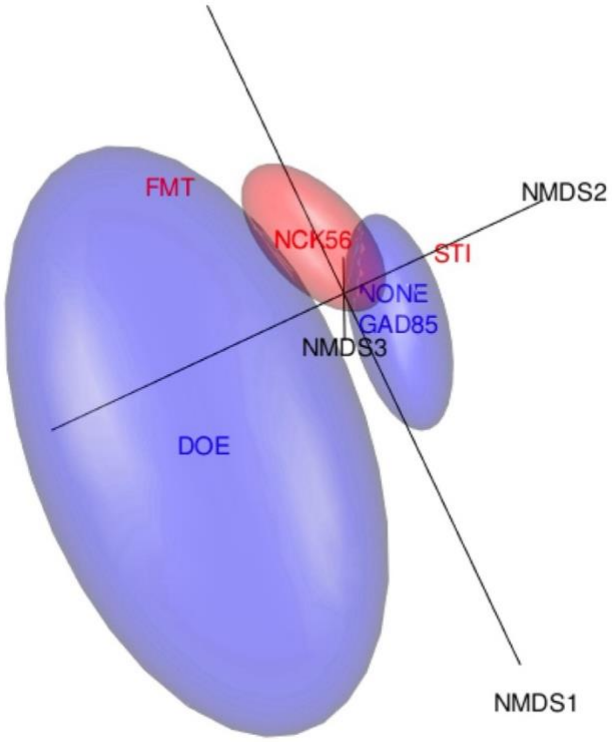

Figure 4.9 **NMDS of neonates and does microbiomes.** NMDS representing the segregation between breeding doe microbiomes (DOE), the doe fecal microbiome transplant gavage material (FMT) and neonatal microbiomes by treatment (NCK56, NONE, GAD85, STI).

4.2.4: GAD85 vaccinated neonates recover quicker from rotavirus challenge and display gut microbiome shifts during challenge.

Neonatal mice received a rotavirus challenge on the day of weaning (21 days of age) to determine if the vaccine (9GAD85) offered protection after two-doses at 7 and 14 days of age (2.2.13.3). Neonatal fecal samples were collected prior to infection and each day following for six days which resulted in 112 samples. Of the total 112 study samples, 105 samples were sequenced and 83 were retained after preprocessing for downstream analysis. Total reads per sample ranged from 1,132 to 89,231.

4.2.4.1: Total IgM and IgG secreting cells increase after rotavirus challenge in the spleen but not Peyer's patches.

After the rotavirus challenge, total IgM and IgG secreting cells increased in GAD85_NR neonates compared to other groups in the spleen, although this was not significant (Figure 4.10 A-B). By contrast, total IgA secreting cells in the spleen increased in NCK56_NR compared to GAD85_NR and STI_NR (Figure 4.10C). Total IgM and IgG secreting cells increased in NCK56_NR and STI_NR treatment groups compared to GAD8_NR in the Peyer's patches (Figure 4.11 A-C). The increased total IgM secreting cells compared to total IgG and IgA secreting cells in neonates in both tissues might be representative of class switching. The germinal centers of Peyer's patches are a key site for generation of class switching and intestinal antibody responses. We did expect an increase in total secreting cells given that all neonates were infected with rotavirus at 21 days of age. To further understand the changes between tissues and treatments we examined the neonatal gut microbiome.

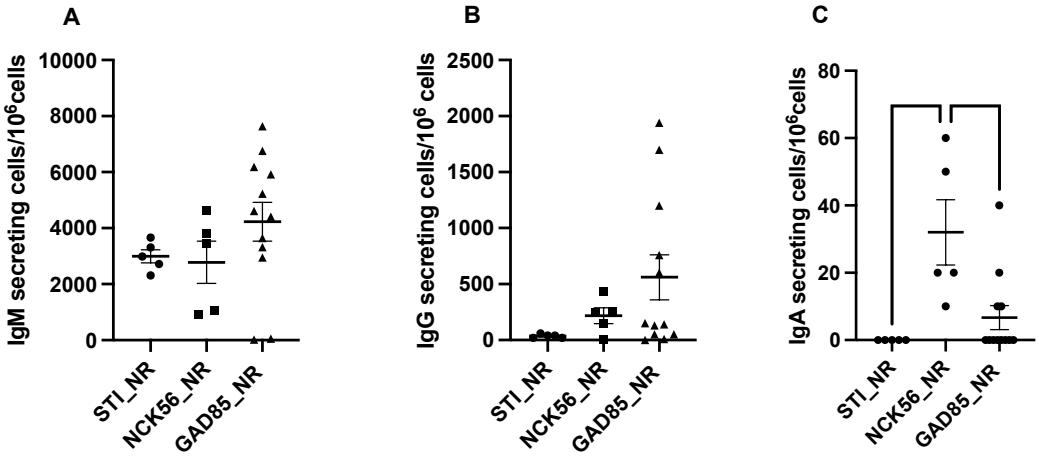

Figure 4.10 **Total IgM, IgG, and IgA secreting cells in the spleen of neonates.** Total (A) IgM, (B) IgG, and (C) IgA secreting cells where * represents significance p=0.0176 and ** represents significance of p=0.0037 in the spleen of neonates. There was not a significant increase in

GAD85_NR in IgM or IgG, but NCK56_NR has a significant increase in IgA in the spleen compared to STI_NR and GAD85_NR.

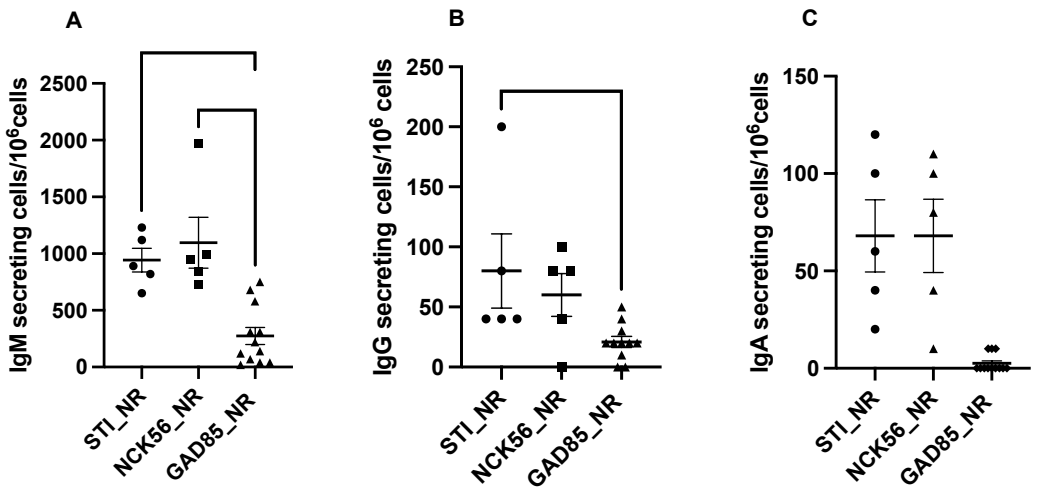

Figure 4.11 **Total IgM, IgG, and IgA secreting cells in the Peyer's patches of neonates.** Total secreting (A) IgM where * represents significance p=0.0109, ** represents significance p=0.0051, (B) IgG * represents significance p=0.0402, and (C) IgA in the Peyer's patches of neonates. GAD85_NR is significantly decreased in total IgM and IgG in Peyer's patches, but IgA is not.

4.2.4.2: Neonatal rotavirus challenge significantly increases fecal antigen shedding for nonvaccinated neonates.

To monitor the infection and recovery, fecal samples were collected before and after neonatal rotavirus infection (2.1.8, 2.1.9). Fecal antigen shedding in challenged NCK56_NR and STI_NR mice peaked 2-5 days post infection and recovered to pre rotavirus infection levels on day 6 post infection. There is an interaction effect between the treatment and timepoint, so analysis was conducted within the interaction ($p<2.2e-16$, Table S4.3). NCK56_NR had significantly increased fecal viral shedding (Figure 4.13) compared to GAD85_NR at 2-, and 3-days post infection, and STI_NR had significantly increased fecal viral shedding compared to GAD85_NR at 5-days post infection (Figure 4.12). This confirms that GAD85 offers neonatal protection because nonvaccinated groups, NCK56_NR and STI_NR, had higher antigen

shedding in their feces. We do note the increased antigen shedding NCK56_NR at 0dpi prior to the rotavirus challenge and the similar pattern of increased NCK56_NR in total secreting IgM and IgG cells in the spleen.

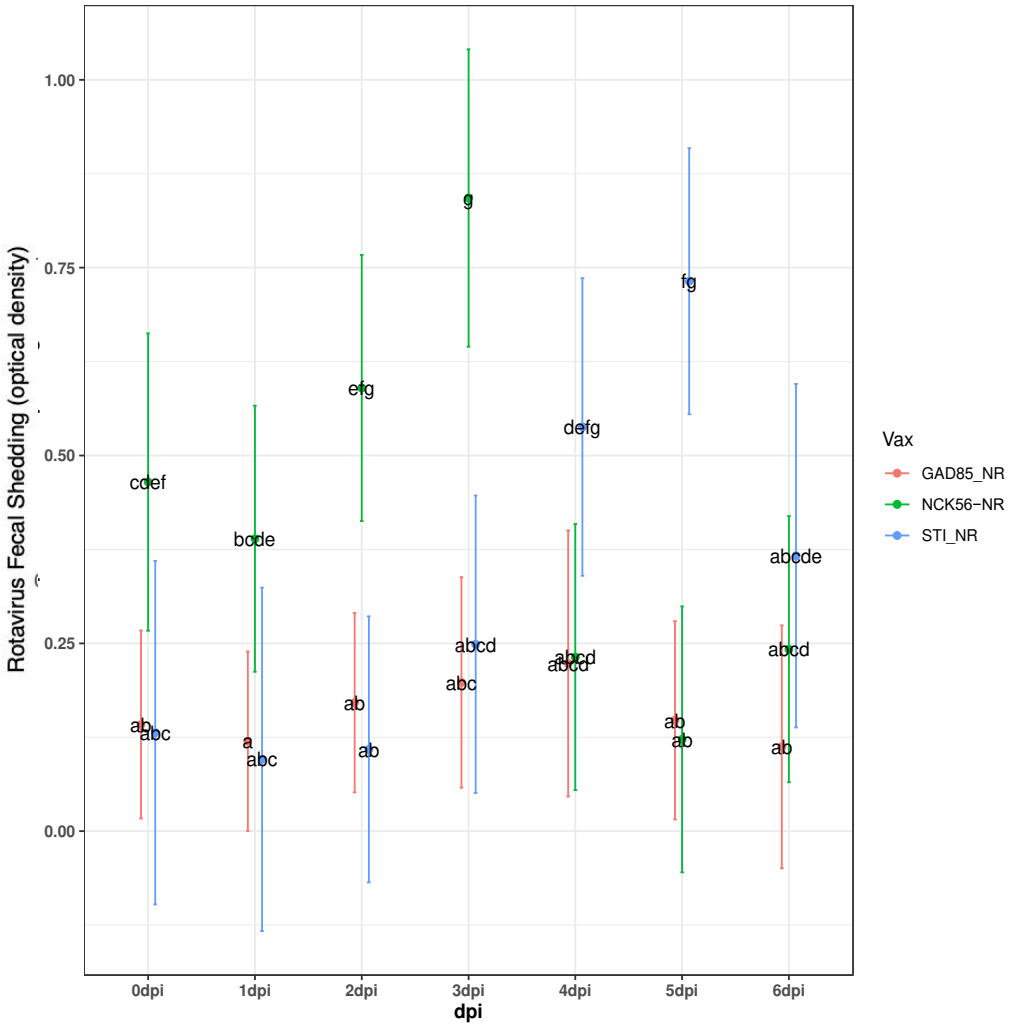

Figure 4.12 **Rotavirus antigen fecal shedding in challenged neonates.** Rotavirus antigen fecal shedding in neonatal mice during rotavirus challenge is increased in NCK56_NR and STI_NR compared to GAD85_NR. Significant differences are denoted on the figure (a,b) at the 0.05 level of significance.

4.2.4.3: Neonatal rotavirus challenge significantly alters the gut microbiome.

InvSimpson diversity peaked one day after rotavirus challenge in STI_NR and NCK56_NR, while it remained unchanged in GAD85_NR (Figure 4.13). Gut microbiome

richness followed the same pattern as InvSimpson (Data not shown). There were no significant changes to Shannon diversity over the rotavirus challenge across treatment groups, although the pattern of gradual decrease over the challenge was consistent (SFigure 4.8, Table S4.4).

Using NMDS based on a Bray-Curtis dissimilarity matrix at the Genus level there was a pattern of microbiome shifts over the course of the seven-day rotavirus challenge (Figure 4.14). NMDS plot also shows that the GAD85_NR is significantly different from NCK56_NR and STI_NR when all timepoints are included (Figure 4.15). Although the neonatal mice recovered from the rotavirus challenge regardless of treatment group based on the return to pre-challenge fecal shedding, their microbiomes never recovered in alpha diversity by 7 days. This suggests that even in the absence of viral shedding there is a shift in the microbial community composition in the gut which may have critical functional implications as the neonate ages and is beyond the scope of 16S sequencing.

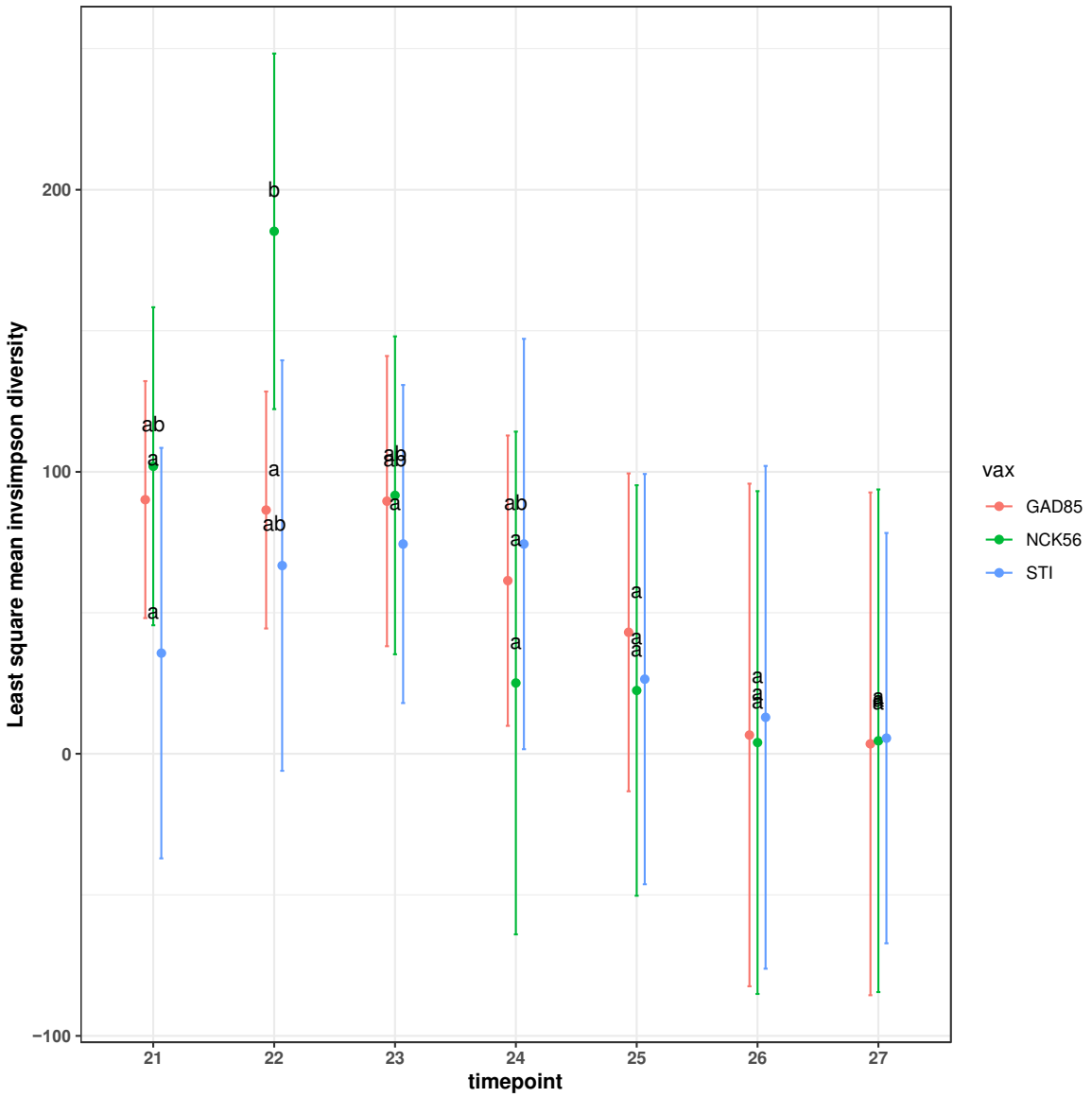

Figure 4.13 **InvSimpson diversity changes during the rotavirus challenge.** InvSimpson is significantly different between treatment groups (STI [STI_NR], NCK56 [NCK56_NR] and GAD85 [GAD85_NR]) one day after rotavirus challenge. Significant differences are denoted on the figure (a, b) at the 0.05 level of significance.

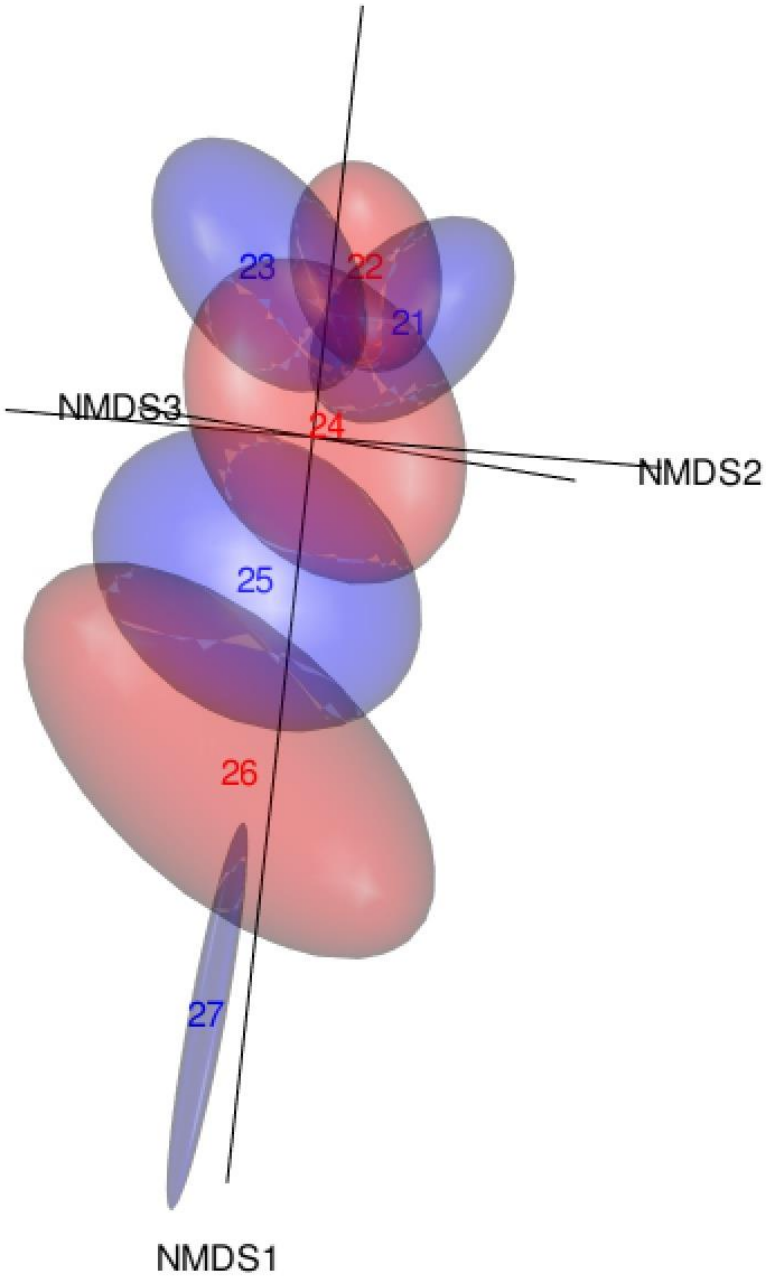

Figure 4.14 **NMDS of microbiome shift over the course of a six-day rotavirus challenge in neonatal mice.** Where 21 is before rotavirus challenge, 22 is one day post challenge, 23 is two days post challenge, 24 is three days post challenge, 25 is four days post challenge, 26 is five days post challenge and 27 is six days post challenge.

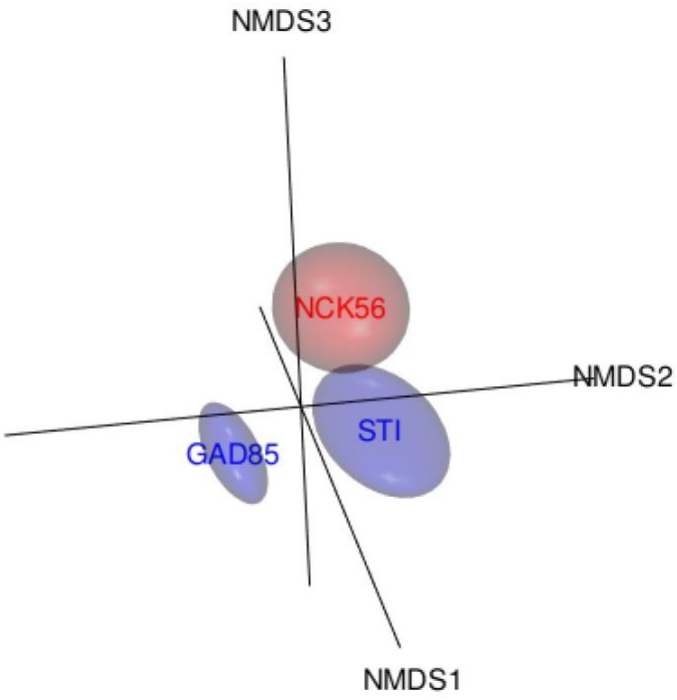

Figure 4.15 **NMDS including all challenge timepoints.** GAD85_NR is more dissimilar to NCK56_NR and STI_NR. The rotavirus challenge modified gut microbiomes of the neonatal treatment groups regardless of which day post challenge, but GAD85_NR was more dissimilar to STI_NR and NCK56_NR.

4.2.5: Investigating maternal infection and neonatal GAD85 vaccination

To determine the role of maternal rotavirus infection prior to gestation, neonates were born to rotavirus infected does (2.2.5, 2.2.13.4). After preprocessing the sample set was too small to complete further analyses for investigating the microbial communities of neonates born to rotavirus infected does.

4.2.5.1: GAD85 vaccinated neonates produce VP8 specific antibody secreting cells even when born to a rotavirus infected doe.

There was an increase in VP8-1 secreting IgM cells in the spleen, MLN and Peyer's patches compared to the wild-type control and the negative control groups (Figure 4.16). This suggests that even with the presumed maternal antibody influence the neonate was exposed to the vaccine and produced rotavirus specific secreting cells. Further, when compared to neonates born to uninfected does, the GAD85_MR neonates have increased VP8-1 specific secreting IgM compared to all other groups (Figure 4.17).

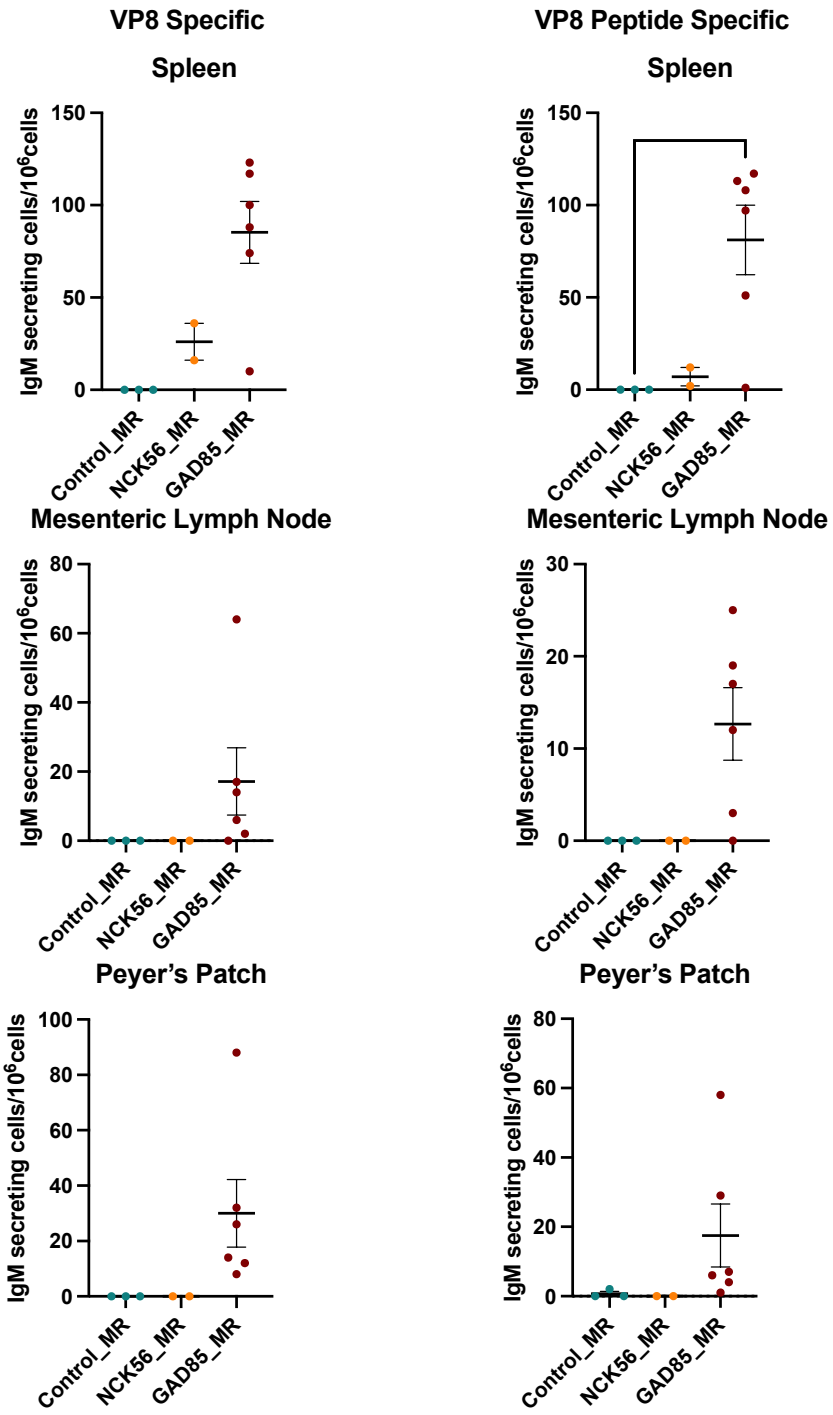

Figure 4.16 **VP8 specific IgM secreting cells in neonates born to rotavirus infected does.** VP8 specific IgM secreting cells in the spleen, mesenteric lymph nodes, and Peyer's patches in neonates that are born to does that were infected with rotavirus prior to gestation. Vaccinated GAD85 neonates have an increase in VP8-1 specific responses even when born to rotavirus infected does. * Represents significance where p=0.0328.

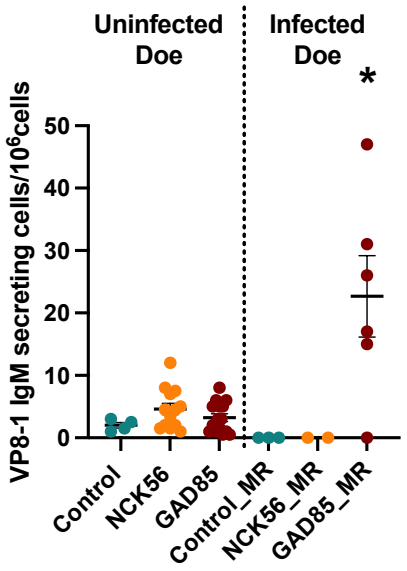

Figure 4.17 **VP8-1 specific IgM secreting cells in the spleen for neonates that are born to infected and uninfected does.** There is a significant increase in the GAD85 neonates born to rotavirus infected does compared to all other groups. *Represents significant of $p<0.001$ compared to all other groups.

4.3: Discussion/Conclusion

These datasets show that in the murine neonatal experimental model it is essential to consider the maternal influence. There are various ways to attempt to normalize and control for the doe/breeder/maternal influence, including fostering pups (39, 35, 40) or maternal fecal microbiome transplant (44, 68, 43). Given the rate and risk of maternal cannibalization of fostered pups (114), we elected to use the fecal microbiome transplant. Does are instinctually protective as delivery approaches (Braden et al., 56) and given the range of gestation we decided to deliver the fecal microbiome transplant at the completion of 2 weeks of gestation, and prior to placing the does into a new clean cage for the third week of gestation and first week of neonatal life. While the conversation continues regarding the mechanisms behind maternal influence on neonatal gut microbiome and immune system development, and maternal interference on neonatal vaccination, the present datasets suggest that investigating neonatal responses to

vaccination requires an experimental design that includes a breeder fecal microbiome transplant to attempt to normalize the perinatal maternal gut microbiome and breeder variance.

Maternal influence has been well documented in neonatal immune development and vaccination (8, 5). Our data suggest that across studies, regardless of if the doe was infected with rotavirus prior to breeding or not, there is a significant difference in the gut microbiome of the neonates depending on the doe and that is not necessarily dependent on the treatment intervention (vaccination or not, neonatal rotavirus challenge or not). While the mechanism of action remains to be elucidated, we suggest evaluation of the maternal breastmilk as the next step in assessing how maternal influence affects neonatal gut microbiome and immune system.

We also considered the role and dosage strategy of the vaccine and control treatment interventions in neonates. The lower wild-type *Lactobacillus acidophilus* dose resulted in more richness than the higher dose. However, the higher dose of the vaccine resulted in increased richness compared to the lower vaccine dose group. While there was not a significant difference in specific antibody secreting cells, the total secreting cells did increase in these two groups with increased richness. Increased neonatal gut microbiome diversity is linked to reduced disease onset of irritable bowel disease, allergies, and obesity as the neonate ages and the microbiome stabilizes (61, 32). Other studies have considered the strategy of oral dosage for neonatal vaccination in mice and humans and found that the composition of the gut microbiota has an influence on immunogenicity of oral rotavirus vaccines (Magwira et al.) In future studies, including analysis of maternal breastmilk and maternal microbiome would be beneficial in

understanding how the microbial environment is establishing homeostasis within the immune system of the gastrointestinal tract, and more specifically the Peyer's patches.

Lower dose 6NCK56 had a significant increase in *Akkermansia*, compared to both high and low dose 6GAD85, and 9GAD85, that had a decrease. *Akkermansia* is generally classified as a beneficial microbe to the gut environment for adults and neonates given its role in colonizing the mucosal layer and prompting metabolic and immune responses including increasing mucus thickness and gut barrier function (27). Reduced *Akkermansia* is observed in patients with irritable bowel syndrome and many clinical and preclinical studies of metabolic disorders and when administered after drug introduction outcome metabolic parameters improve (16). The mucosal lining serves as the first mode of defense against invading pathogens (), thus the presence and maintenance of *Akkermansia* in the gut microbiome is essential. Early life increase in abundance of *Akkermansia spp.* has been associated with long term increased intestinal goblet cell number in infants (28), reduced relative risk of childhood atopy and asthma (17), and neonatal growth as it relates to maternal gestational health (12). However, detection of Akkermansia in early life neonatal gut microbiomes is limited compared to Bacteroides and Lactobacillus groups (11).

On the other hand, the decreased abundance of *Akkermansia* in the vaccinated neonates compared to the lower dose wild type control and double negative no dose control could indicate risk to the gut barrier function and other metabolic and immune responses. Rotavirus infection in neonatal mice has been shown to reduce mucin production in the small intestine and a shift in the ileal microbiome, namely increased *Verrucomicrobiales* specifically *Akkermansia* and decreased

Lactobacillales, one day after infection with recovery at three days after infection (34). Interestingly, there is no report of significant changes in other compartments of the gastrointestinal tract in infected neonates, where samples in these analyses were fecal and similar families are shifting in the microbiome. Contrary to the rotavirus infected neonates, these vaccinated neonates had significantly increased *Lactobacillus* and significantly reduced *Akkermansia* compared to the no dose negative control suggesting an inverse shift at 7 days after the booster dose was delivered. However, the high dose wild type *Lactobacillus* control had a 2-fold significant reduction in *Akkermansia* but no significant shift in *Lactobacillus* compared to the low dose wild type control group. Given that there were no significant differences between these groups in their total or rotavirus specific IgA, IgG, or IgM secreting cells, the shifts between *Akkermansia* and *Lactobacillus* primarily indicate that the gut microbes are shifting and may be influencing vaccination response particularly with the recombinant *Lactobacillus* as a vaccine delivery method.

Further, various studies associate gut dysbiosis and diarrhea with *Lachnoclostridium* in humans (15), piglets (18), and mice (9). This suggests that our delivery buffer is inducing a shift in the neonatal gut microbiome, and the low dose wild type control *Lactobacillus* ameliorates that shift but only when delivered at the lower dose, $1x10^6$ CFU. Further, the better dose selection for neonatal vaccination is the higher dose, $1x10^9$ CFU, because there is no significant increase in *Lachnoclostridium* when compared to the double negative no dose control group. Moreover, decreased *Oscillibacter* has been documented in antibiotic-treated neonatal piglets that have reduced alpha diversity gut microbiomes (24), whereas an increased *Oscillibacter* abundance was seen in a study where lambs were given a breastmilk starter feed supplementation

to enhance gastrointestinal fermentation and promote development (23). Taken together this suggests that the STI buffer used to deliver the bacteria does perturb the neonatal gut microbiome, but when it is being used to deliver our novel recombinant vaccine *Lactobacillus acidophilus* platform the perturbation is coupled with increased abundance of beneficial microbes.

These data further identify that neonatal rotavirus challenge alters the gut microbiome during the six days after challenge. Even though the viral shedding in feces returns to baseline levels, the gut microbial environment remains significantly dissimilar to the baseline pre-challenge gut microbiome. Therefore, we hypothesize that the there is a clear network between the neonatal gut microbiome and neonatal immune development, in response to vaccination, exposure, and recovery of enteric pathogen invasion in the neonatal intestines and warrants further functional analyses.

CHAPTER 5 TOLL-LIKE RECEPTOR 4 DELECTION PARTIALLY PROTECTS MICE FROM HIGH FAT DIET-INDUCED ARTERIAL STIFFENSS DESPITRE PERTURBATION TO THE GUT MICROBIOTA

5.1: Introduction

Obese individuals are more than twice as likely as non-obese individuals to develop cardiovascular disease (CVD) during their lifetime (83). One key process that links obesity to CVD is the development of vascular dysfunction, which can clinically manifest as stiffness of the large elastic arteries. As such, arterial stiffness is an independent predictor of future CVD events and mortality (109). Unhealthy dietary patterns, including consumption of a high fat diet, are implicated in multiple cardiometabolic disruptions, such as glucose intolerance, systemic inflammation, and arterial stiffness (82, 73, 71). High fat diets have also been shown to profoundly impact the gut microbiome, a diverse ecosystem consisting of trillions of bacteria within the gastrointestinal tract that collectively impact nearly every facet of mammalian metabolism (95). Numerous studies, including those from our own laboratory, have suggested that diet-induced changes to the gut microbiome may play a role in downstream cardiometabolic impairments (97, 71, 90).

Although multiple signaling pathways are involved in diet-microbiota-host crosstalk, Cani and colleagues (74, 75) proposed that sub-clinical levels of circulating bacterial lipopolysaccharides (LPS) provide a key mechanistic link between the microbiota, obesity, and downstream disease development. Chronic consumption of a high fat diet can lead to this physiologic state, also known as “metabolic endotoxemia”, by causing gut microbiota perturbations, characterized by disrupted microbial communities, increased intestinal

inflammation, loss of epithelial barrier integrity and translocation of luminal contents into the circulation. LPS can also translocate to the circulation through incorporation into mixed micelles after ingestion of a high fat meal (88, 78, 99, 85). Once in circulation, LPS binds to Tolllike receptor 4 (TLR4) on various cell types to induce a signaling cascade that culminates in inflammation and generation of reactive oxygen species that can drive development of cardiometabolic dysfunction, including arterial stiffness (77).

Our laboratory has observed that the gut microbiota is a critical regulator in the development of obesity-associated arterial stiffness. Specifically, we have demonstrated that antibiotic treatment ameliorates arterial stiffness in western diet-fed mice (71) and that transplantation of an obesity-associated microbiota from obese mice (72) or obese humans (Trikha et al., 2021) is sufficient to increase arterial stiffness in lean mice. In these experiments, increased arterial stiffness was often associated with decreased intestinal barrier function and/or evidence of increased LPS signaling (71, 72). These data led us to further examine the role of TLR4-mediated inflammation in vascular dysfunction by examining the cardiometabolic effects of a high fat diet in TLR4 knockout mice (TLR4-/-). We hypothesized that TLR4-/- mice fed a high fat diet would manifest microbial disruption and impaired gut barrier function like wild-type animals, but given the proinflammatory effects of TLR4 signaling, TLR4-/- mice would be protected from downstream cardiometabolic derangements.

5.2: Materials & Methods

5.2.1: Experimental Design

Eight-week-old male TLR4-/- (KO) and TLR4+/+ littermates (CON) were obtained from The Jackson Laboratory (Bar Harbor, ME) and acclimated for two weeks with ad libitum access

to a purified standard diet (SD; Harlan Laboratories, TD 08485) consisting of 13% fat, 67.9% carbohydrate, and 19.1% protein (% kcal). After two weeks, animals were assigned to either a standard low-fat diet (SD) or a high fat diet (HFD; Harlan Laboratories, TD 06414) consisting of 60.3% fat, 21.4% carbohydrate, and 18.3% protein (% kcal), resulting in the following 4 experimental groups (n=12 per group): 1) TLR4+/+ on SD diet (CON+SD); 2) TLR4+/+ on HFD diet, (CON+HFD); 3) TLR4-/- on SD diet (KO+SD); and 4) TLR4-/- on HFD diet (KO +HFD). Mice remained on assigned diets through 6 months and were cohoused two per cage in a temperature and humidity controlled environment on a 12:12-h light-dark cycle. Food intake and body weight were measured weekly at the time of cage and water changes. All animal procedures were reviewed and approved by the Colorado State University Institutional Animal Care and Use Committee protocol #1369.

5.2.2: Arterial Stiffness

Aortic pulse wave velocity (aPWV) was used to determine in vivo arterial stiffness using a Doppler Flow Velocity System (Indus Instruments, Webster, TX) via methods described previously by our laboratory (71, 89). aPWV (in cm/s) was calculated as aPWV = (distance between the 2 probes)/ (Dtimeabdominal − Dtimecarotid).

5.2.3: Glucose and Insulin tolerance tests

Following a 6h fast, mice received an intraperitoneal injection of 2g/kg dextrose, and blood glucose was assessed at 0, 15, 30, 45, 60, 90, and 120 minutes post-injection using tail-vein blood and AlphaTRAK 2 glucometers (Abbott Laboratories, Chicago, IL). Fasting blood was spun for 5 minutes at 2,000rpm and resultant serum was used for fasting insulin levels via ELISA. For insulin tolerance tests, mice received an intraperitoneal injection of 1.5g/kg insulin

after a 6h fast, and blood glucose was assessed at 0, 15, 60, and 120 minutes post-injection as described above.

5.2.4: *In vivo* intestinal barrier integrity

Animals were water-fasted for 12 hours prior to oral gavage administration of fluorescein isothiocyanate (FITC)-dextran (4,000 mol wt, no. 46944; Sigma-Aldrich; 125 mg/ml for SD fed mice and 150 mg/ml for HFD fed mice). Food was removed immediately after oral gavage and tail vein blood samples were collected after 4 hours for quantification of serum FITC-dextran concentrations. Serum samples were diluted 1:2 in 1X PBS, and fluorescence was measured on a BioTek Synergy 2 Multi-Detection Microplate Reader (BioTek Instruments, Winooski, VT) at 485/20 (excitation) and 528/20 (emission). Serum concentrations were quantified using a standard curve of known FITC-dextran concentrations prepared in a control serum sample from an untreated mouse.

5.2.5: Animal termination and tissue collection

Mice were anesthetized with isoflurane and euthanized by exsanguination via cardiac puncture. Blood was collected in a 0.5 M EDTA-coated syringe (no. 15575020; Invitrogen). Collected blood was added to 2% volume EDTA and plasma was obtained by centrifugation at 2,000 rcf for 10 min at 4°C, and immediately flash frozen in liquid nitrogen. The gastrointestinal tract was excised, and colon length and cecum weight were recorded. Cecal content and colon content were removed from the tissue and flash frozen. Adipose tissue depots (perivascular, subcutaneous, epididymal, and mesenteric depots) were isolated and weighed. Sections of distal colon and proximal small intestine were obtained and flash frozen for further analysis.

5.2.6: Biomarker analysis

Circulating biomarkers associated with intestinal permeability were evaluated in plasma collected by cardiac puncture. Specifically, circulating levels of LPS binding protein (LBP; ALX-850-304/1, Enzo Life Sciences) and zonulin-family peptides (NC1314884, Fisher Scientific) were measured by ELISA. LBP is a soluble acute phase protein that binds and presents LPS to TLR4 and its co-receptor CD14. Zonulin-family peptides are potent regulators of intestinal tight junctions and circulating levels have been associated with "leaky gut", inflammation, and gut dysbiosis (104). Additionally, secretory IgA (sIgA; 50154425, Fisher Scientific) and intestinal alkaline phosphatase (IPA; NC9945170, Fisher Scientific) were measured by ELISA in collected ileal tissues. sIGA and IAP were normalized to total protein, measured by BCA. Intestinal sIgA is secreted in response to luminal pathogens or enterotoxins and IAP dephosphorylates bacterial LPS, reducing its immunogenicity and reduced IAP is associated with loss of gut homeostasis.

5.2.7: DHE staining and analysis

Thoracic aorta (TA) was excised and placed in an ionized solution for removal of perivascular adipose tissue (PVAT). After PVAT removal, a 1-1.5mm section distal to the aortic arch was cut and embedded vertically in optimal cutting temperature (OCT) gel that was flash frozen. Sections were cut at 10μm using a cryostat set to -20°C. 4-5 sections were adhered to each slide and 3-5 slides per mouse were stored at -80°C until staining. 50ml fresh 5 μM DHE (D11347, Thermo Fisher Scientific) staining solution prepared and poured in slide box. 1mg DHE dissolved into 317 μL dimethyl sulfoxide (DMSO) for 10mM stock solution. 25μL DHE stock diluted into 50 mL Milli-Q pure water for 5μM staining solution. Slides were rinsed then

placed in DHE staining solution and incubated for 15 min at room temperature, with limited light exposure. Slides were washed and fluorescent images were acquired. Two to three technical replicates were collected on 2-3 biological replicates for each mouse and replicates were averaged for one mean grey intensity value/area (μm^2).

5.2.8: Microbiota characterization

Fecal DNA was extracted from samples excised from the colon at termination using the FastDNA Stool kit (Catalog 6540400, MP Biomedicals). qPCR amplification of the V4 16S rRNA region was completed following the Earth Microbiome Project protocol using the 515F-806R fusion primers with 12bp Golay barcodes and sequencing adaptors (https://earthmicrobiome.org/protocols-and-standards/16s/). Pooled libraries were sent to the Next Generation Sequencing Facility at Colorado State University and sequenced using 2x250 chemistry on a MiSeq (Illumina Inc, San Diego, CA).

Forward and reverse reads were imported into QIIME2 version 2021.2. Reads were demultiplexed, concatenated, and trimmed to 200 base pairs. Reads were binned into ASVs using the DADA2 pipeline and taxonomic assignments were made using GreenGenes version 13.8. Count tables and taxonomy were imported into MicrobiomeAnalyst (www.microbiomeanalyst.ca) and further curated by removing reads that had fewer than 4 counts and that were present in less than 10% of the samples, which resulted in the removal of 16 low abundance features.

5.2.9: Statistical analyses

Data are presented as either mean ± standard deviation (SD), mean ± standard error of the mean (SEM), or as median (interquartile range (IQR)). Data analysis and visualization was

conducted in GraphPad Prism (version 9). Before statistical analysis, identification and removal of outliers was performed using the ROUT test or Grubbs' test available in GraphPad Prism. To test for differences in outcomes over time, we fit two-way repeated measures ANOVA, followed by Tukey's multiple comparisons tests if indicated. If observations were missing at random time points, we fit linear mixed effect models with individual mice as a random effect and week and group as fixed effects, followed by Tukey's multiple comparisons tests if indicated. To test for differences in outcomes not measured over time, we fit one-way ANOVAs follwed by Tukey's multiple comparisons tests if indicated. Either Welch ANOVA models followed by Dunnett's T3 multiple comparisons tests or Kruskal Wallis tests followed by Dunns multiple comparisons tests were fit if data violated the assumption of homoscedasticitiy or normality, respectively. Microbiome data were statistically analyzed using Kruskal-Wallis test with FDR-corrected (Benjamini, Krieger, Yekutieli method) post-hoc analysis when indicated. Beta-diversity ordination ellipses show the 95% confidence interval for each group and statistical evaluation was conducted using PERMANOVA and PERMDISP to examine differences in centroids and heterogeneity between groups, respectively (69). LEfSe was used to identify taxa that serve as biomarkers for the different experimental conditions (102). A p-value ≤ 0.05 was considered statistically significant.

5.3: Results

5.3.1: TLR4 KO mice are partially protected from diet-induced weight gain

By 4 weeks into the intervention, HFD-fed animals weighed significantly more than SD-fed animals ($p<0.01$ for all pairwise comparisons between HFD and SD; Figure 5.1A). At termination, animals on the HFD weighed significantly more than mice fed SD, regardless of

genotype ($p<0.01$ for all pairwise comparisons between HFD and SD groups; Figure 5.1B); however, the KO+HFD animals weighed significantly less than the CON+HFD animals (52.5 ± 0.8 g. vs. 57.3 ± 1.3g.; $p=0.01$) while weighing significantly more than both SD groups ($p<0.001$) (Figure 5.1B). Changes in body weight could not be explained by changes in food intake, as there were no significant differences in food intake between any two groups (Figure 5.1C). In general, tissue weights and fat depots differed between diet groups, with no differences observed between CON+HFD compared to KO+HFD (Table 5.1). Of note, the KO+SD animals had significantly reduced cecum weight and colon length compared to the CON+SD animals, as well as slightly higher mesenteric adipose tissue weight (Table 5.1).

Table 5.1 Tissue weights and fat depot weights in all mice by treatment.

Liver weight (mg)*	1368.0 ± 42.8 ^{a}	3648.0 ± 237.4^{b}	1449.0 ± 86.6^{a}	3320.0 ± 191.7^{b}	<0.01
Heart weight (mg)*	159.9 ± 6.3^{a,b}	189.3 ± 10.1^{b}	141.2 ± 3.3^{a}	176.7 ± 2.6^{b}	<0.01
Spleen weight (mg)$^{+}$	82.6 (20.6) ^{a}	127.3 (57.6) ^{b}	74.5 (11.5) ^{a}	108.6 (6.4)^{b}	<0.01
Epi Adipose weight (mg)	1096.0 ± 149.3^{a}	1527.0 ± 140.3^{a,b}	1582.0 ± 107.6^{b}	1217 ± 111.5^{a,b}	0.03
SQ Adipose weight (mg)*	350.4 ± 63.0^{a}	2094.0 ± 143.3^{b}	535.9 ± 45.6^{a}	1782.0 ± 70.8^{b}	<0.01
PVAT weight (mg)	43.5 ± 8.0^{a}	96.5 ± 12.1^{b}	53.1 ± 6.1^{a}	90.1 ± 8.5^{b}	<0.01
(log) MAT weight (mg)	2.6 ± 0.05^{a}	3.1 ± 0.04^{b}	2.8 ± 0.03^{c}	3.0 ± 0.04^{b,c}	<0.01
Cecum weight (mg)	395.8 ± 43.0^{a}	247.1 ± 20.3^{b}	288.8 ± 20.5^{b}	241.8 ± 18.3^{b}	<0.01
Colon length (cm)	6.0 ± 0.1^{a}	5.9 ± 0.1^{a,b}	5.4 ± 0.2^{b}	5.6 ± 0.1^{a,b}	<0.01

n=9-12 per group. Data is presented as mean ± SEM unless otherwise stated. Analysis was performed using one-way ANOVA follwed by Tukey's multiple comparisons test unless otherwise stated. *Analysis was performed using Welch ANOVA followed by Dunnett's T3 multiple comparisons test. + Data is presented as median (interquartile range) and analysis was performed using Kruskal Wallis test followed by Dunns multiple comparisons test. Different letters indiciate significant differences between groups ($p<0.05$). Epi Adipose, epididymal adipose tissue; SQ Adipose, subcuteneous adipose tissue; PVAT, perivascular adipose tissue; MAT, mesenteric adipose tissue.

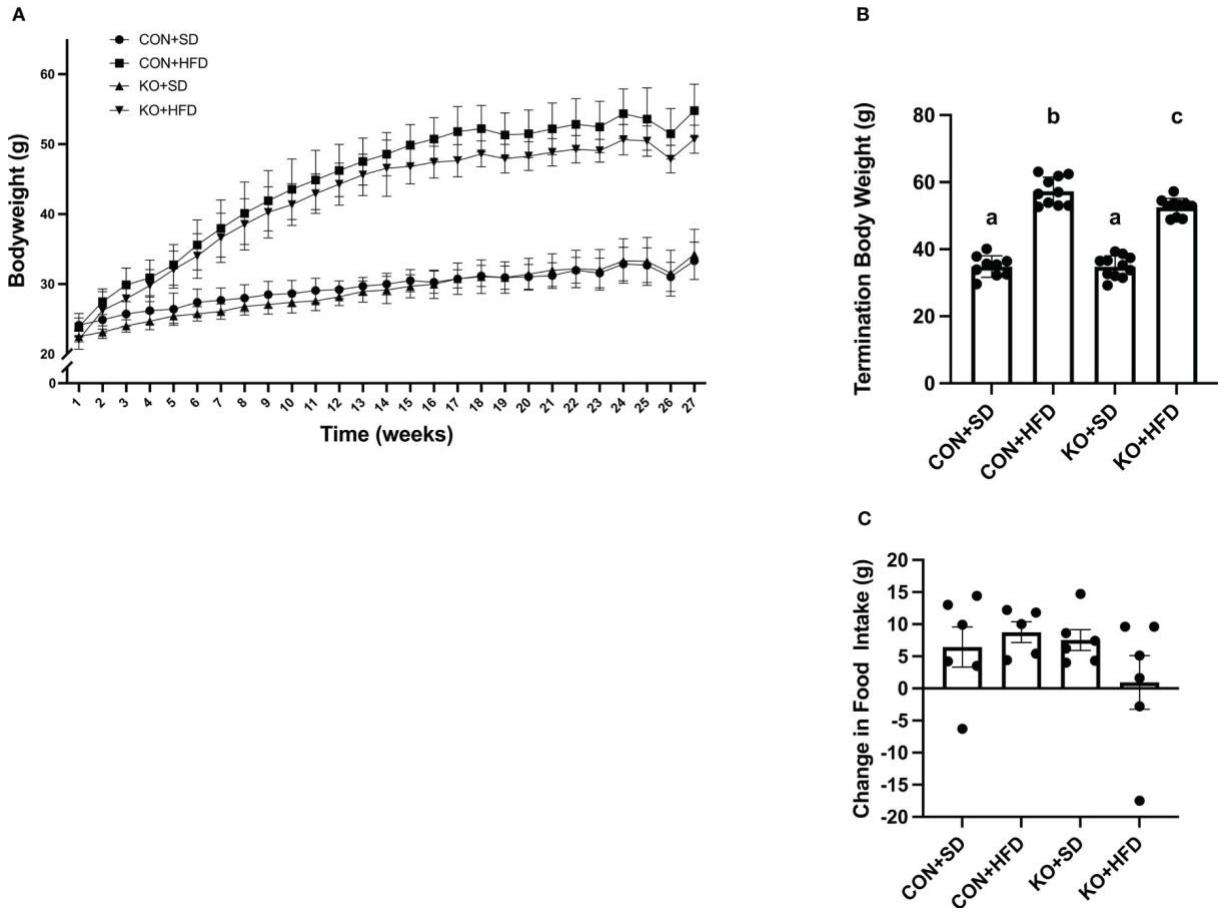

Figure 5.1 A-C **Changes in bodyweight and food intake by treatment group.** There were significant differences in mice fed a standard diet (SD) or high fat diet (HFD) regardless of genotype throughout the course of the study (A) and at termination (B). This occurred independent of food intake (C).

5.3.2: Mice exhibit microbial disruption following a HFD, regardless of genotype

We used 16S rRNA sequencing to characterize diet and genotype-associated differences in the microbiota. Using Kruskal-Wallis tests with FDR <0.05, there were significant differences in all six phyla detected (Figure 5.2A; Table 5.2). Specifically, Pseudomonadota (formerly Proteobacteria) were associated with genotype and were higher in CON mice compared to KO animals. Bacillidota (formerly Firmicutes) were associated with diet and were higher in HFD-fed animals. Verrucomicrobiota were specifically associated with KO+HFD, and both Actinomycetota

(formerly Actinobacteria) and Mycoplasmatota (formerly Tenericutes) were associated with the CON+SD group. Bacteriodota (formerly Bacteroidetes) differences were influenced by both diet and genotype.

In addition to compositional differences between the diet groups, there were also significant differences in several parameters of a-diversity. Specifically, when comparing groups at the genus level, there were significant differences in ASV richness (p-value: 0.041, H= 8.264; Figure 5.2B), Shannon's diversity ($p<0.001$, H=21.191; Figure 5.2C), and Faith's Phylogenetic indices ($p=0.027$; H=9.207; Figure 5.2D), but not in Pileu's Evenness ($p=0.195$, H=4.705; data not shown). In general, the most striking differences was in Shannon's diversity and was driven by higher diversity in the microbiota of the CON+SD group relative to all other groups (Figure 5.2C).

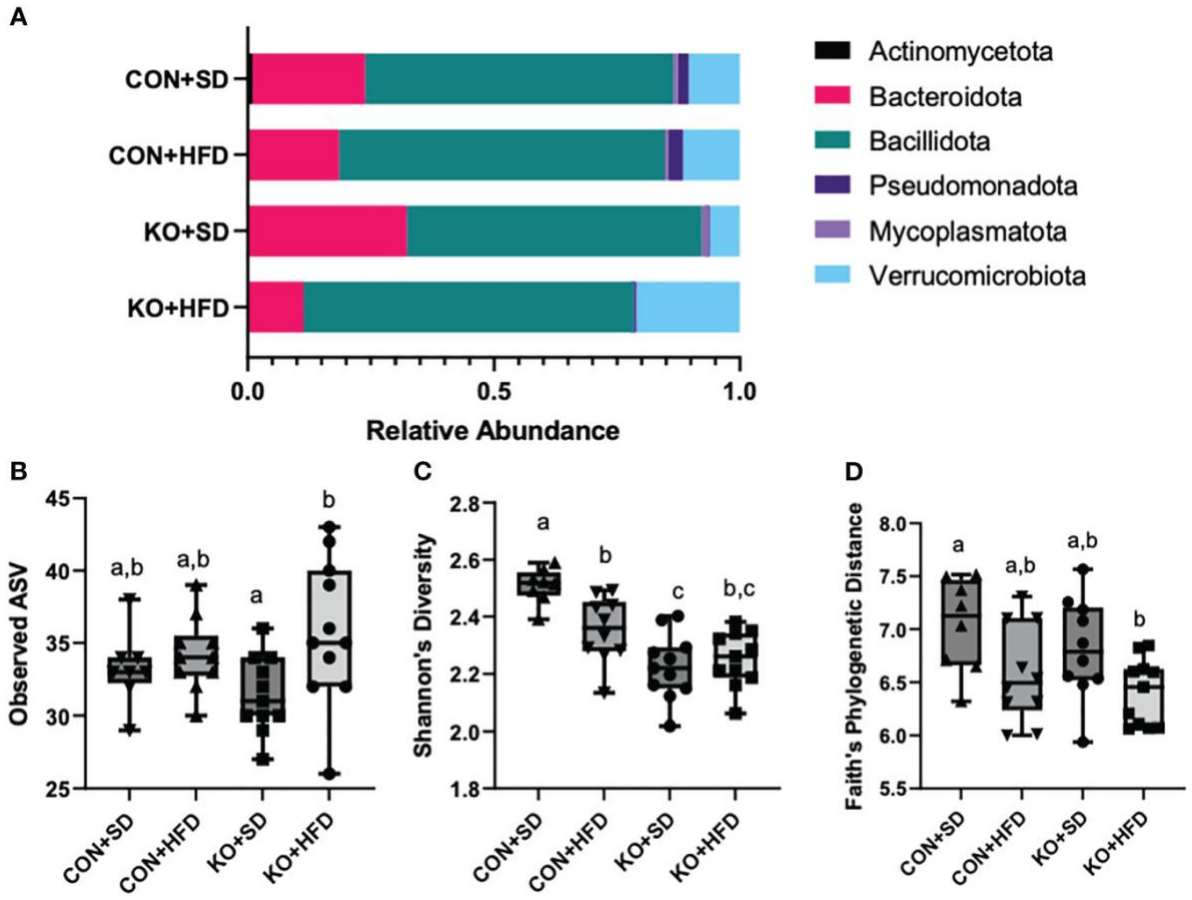

Figure 5.2 **Relative abundance, richness and alpha diversity by treatment group.** There was a significant difference in relative abundance at the phyla level (A) in addition to richness (B), Shannon's diversity (C) and Faith's phylogenetic distance (D).

When visualizing the Bray Curtis distances between the four groups on a Principal Coordinates Analysis (PCoA; PERMANOVA F=11.7, R2=0.494, p<0.001), the KO+SD forms a cluster that is distinctly separate from the other groups along the first axis, which represents 41.4% of the total diversity (Figure 5.3A). Introduction of a HFD produces similar shifts in the microbiota of both the CON and KO mice and there is considerable overlap between the two HFD groups, suggesting that although the SD microbiota differed between the CON and KO mice, dysbiosis was induced in both groups receiving the HFD. There was also a significant difference in the within

group variance (PERMDISP, F=3.4905; p= 0.025), suggesting that the variability in microbial profiles between animals was reduced by the HFD.

Table 5.2 Statistical summary of relative abundances of phyla. There were significant differences in all phyla relative abundances and associated by genotype.

Phylum	P Values	FDR	*H* statistic
Actinomycetota (formerly Actinobacteria)	0.015	0.018	10.461
Bacillota (formerly Firmicutes)	0.002	0.003	15.186
Bacteroidota (formerly Bacteroidetes)	0.003	0.005	13.853
Mycolplasmatota (formerly Tenericutes)	0.024	0.024	9.439
Pseudomonadota (formerly Proteobacteria)	0.001	0.001	19.296
Verrucomicrobiota	0.001	0.003	15.698

Heat trees comparing diet groups (Figure 5.3B) or genotypes (Figure 5.3C) identified microbes associated with specific conditions. Relative to HFD, the SD-fed mice were enriched in Bifidobacteriacae, Anaeroplasmataceae, Bacteriodales, Christensenellaceae, and Erysipelotrichaceae, but had reduced Lactobacillaceae, Verrucomicrobiaceae, and Peptostreptococcacaceae (Figure 5.3B). In comparison, the CON mice were enriched in Actinobacteria, Lactobacillaceae, Alcaligenaceae, Bacteriodaceae, and Rickenellaceae relative to KO mice, which were enriched in Peptococcaceae and Mogibacteraceae (Figure 5.3C).

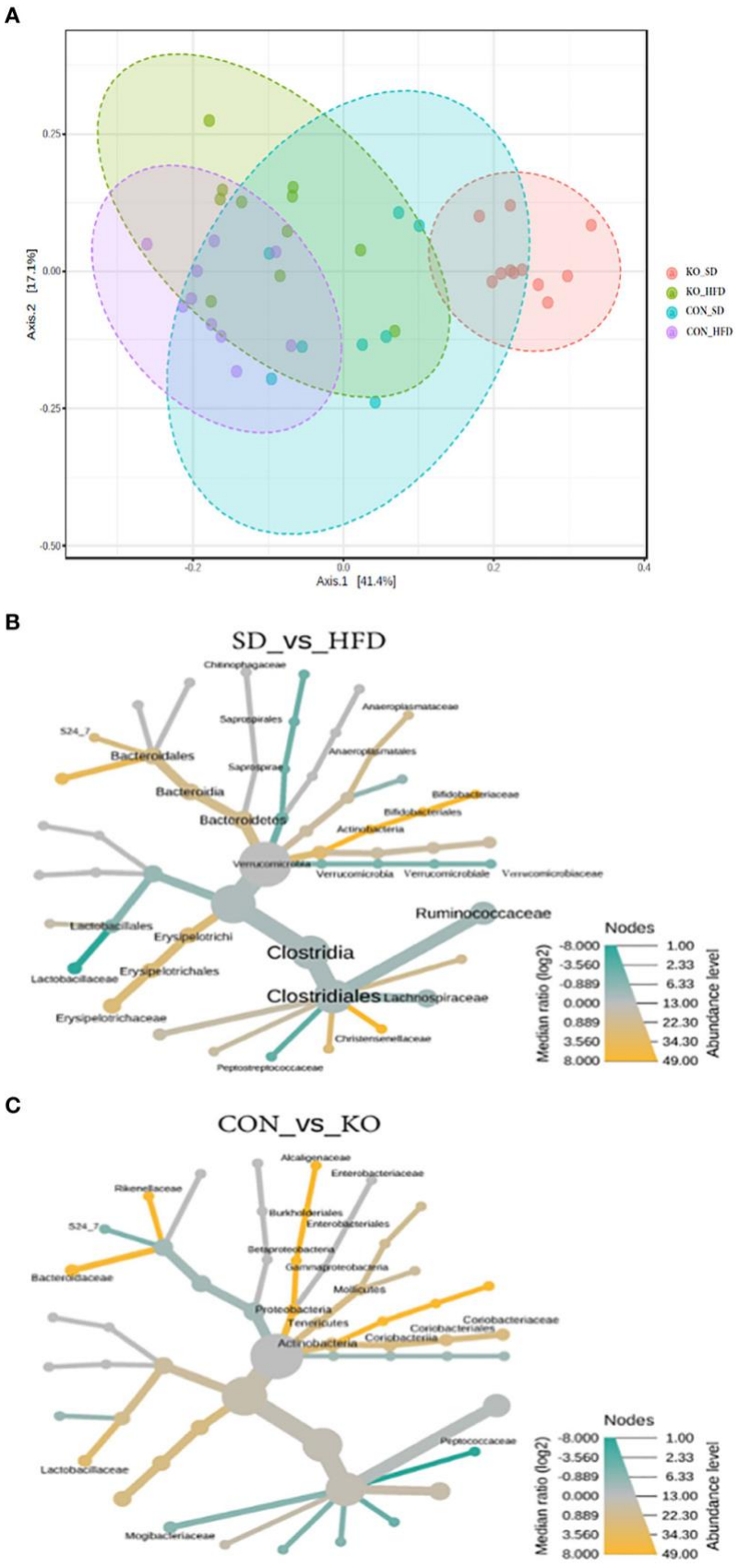
A
0.25
0.00
-0.25
-0.50
Axis.2 [17.1%]
-0.2
0.0
0.2
0.4
Axis.1 [41.4%]
KO_SD
KO_HFD
CON_SD
CON_HFD
B
SD_vs_HFD
Chitinophagaceae
Saprospirales
Anaeroplasmataceae
S24_7
Bacteroidales
Saprospirae
Anaeroplasmatales
Bacteroidia
Bifidobacteriaceae
Bifidobacteriales
Bacteroidetes
Actinobacteria
Verrucomicrobia
Verrucomicrobiae
Verrucomicrobiale
Verrucomicrobiaceae
Ruminococcaceae
Lactobacillales
Erysipelotrichi
Clostridia
Lactobacillaceae
Erysipelotrichales
Clostridiales
Lachnospiraceae
Erysipelotrichaceae
Christensenellaceae
Peptostreptococcaceae
Nodes
Median ratio (log2)
-8.000
-3.560
-0.889
0.000
0.889
3.560
8.000
1.00
2.33
6.33
13.00
22.30
34.30
49.00
Abundance level
C
CON_vs_KO
Alcaligenaceae
Enterobacteriaceae
Rikenellaceae
Burkholderiales
S24_7
Enterobacteriales
Betaproteobacteria
Bacteroidaceae
Gammaproteobacteria
Mollicutes
Proteobacteria
Tenericutes
Coriobacteriaceae
Coriobacteriales
Actinobacteria
Coriobacteriia
Peptococcaceae
Lactobacillaceae
Mogibacteriaceae
Nodes
Median ratio (log2)
-8.000
-3.560
-0.889
0.000
0.889
3.560
8.000
1.00
2.33
6.33
13.00
22.30
34.30
49.00
Abundance level

Figure 5.3 **Heat trees by dietary treatment and genotype illustrate microbe specific interactions.** There were significant differences in specific microbes between the high fat diet and standard diet groups (B) and between the TLR4 knockout genotype and their control (C).

Using LefSE, nine genera were identified as biomarkers that distinguish between the treatment groups (Figure 5.4). Four of these genera: *Ocillospora, Allobaculum, Ruminococcus,* and *Bifidobacterium* were mostly influenced by diet group, while *Bacteroides, Sutterella*, and RC4-4 were linked to genotype (Figure 5.4). *Akkermansia* and *Anaeroplasma* were specifically enriched in KO+HFD relative to other treatment groups (Supplemental Figure 5.2).

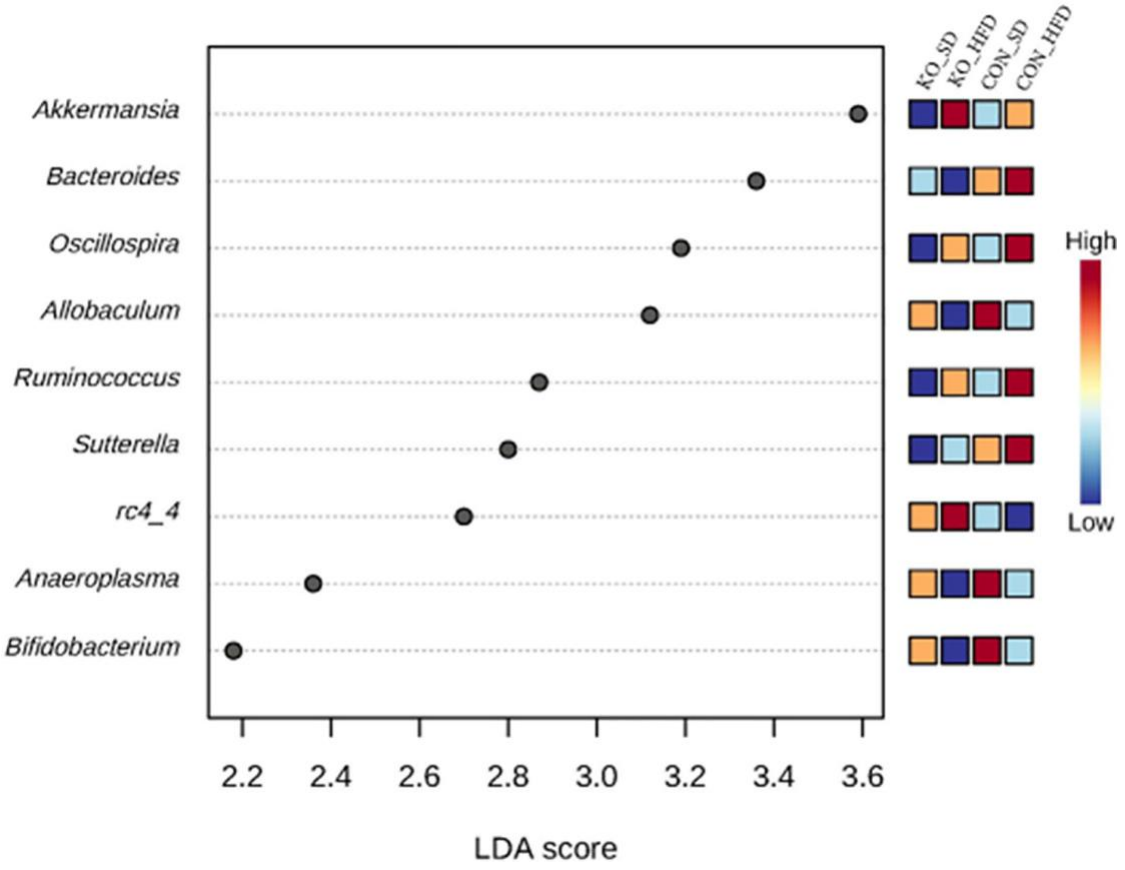

Figure 5.4 **Distinguished biomarkers between treatment groups.** LefSE deteremined the genra most influenced by diet and genotype.

5.3.3: TLR4 KO mice are susceptible to HFD induced intestinal impairments, but partially protected from arterial stiffness

Both CON+HFD and KO+HFD displayed increased intestinal permeability compared to SD-fed animals, indicated by higher circulating levels of FITC after oral gavage (CON+HFD: 1.6 ± 0.1 ug/mL; KO+HFD: 1.3 ± 0.1 ug/mL; CON+SD: 0.4 ± 0.01 ug/mL; KO+SD: 0.4 ± 0.01 ug/mL; $p<0.001$ for all pairwise comparisons between HFD and SD groups; Figure 5.5A). Circulating lipopolysaccharide binding protein (LBP), a proxy measure for circulating endotoxin (101), was also significantly higher in HFD-fed animals regardless of genotype (CON+HFD: 14.7 ± 1.7 ng/mL; KO+HFD: 14.8 ± 1.5 ng/mL; CON+SD: 7.9 ± 0.9 ng/ml; KO+SD: 9.6 ± 1.1 ng/ml; $p<0.05$ for all pairwise comparisons between HFD and SD groups; Figure 5.5B). Plasma zonulin (ZO) (more accurately, zonulin-family peptides (84), and intestinal alkaline phosphatase (IAP), an enzyme that dephosphorylates LPS (70), did not significantly differ between any of the groups (ZO: $p=0.08$, Figure 5.5C; IAP: $p=0.2$, Figure 5.5D). In addition, secretory immunoglobin (sIgA) measured in ileum was also the same across diet and genotype ($p=0.8$; Figure 5.5E).

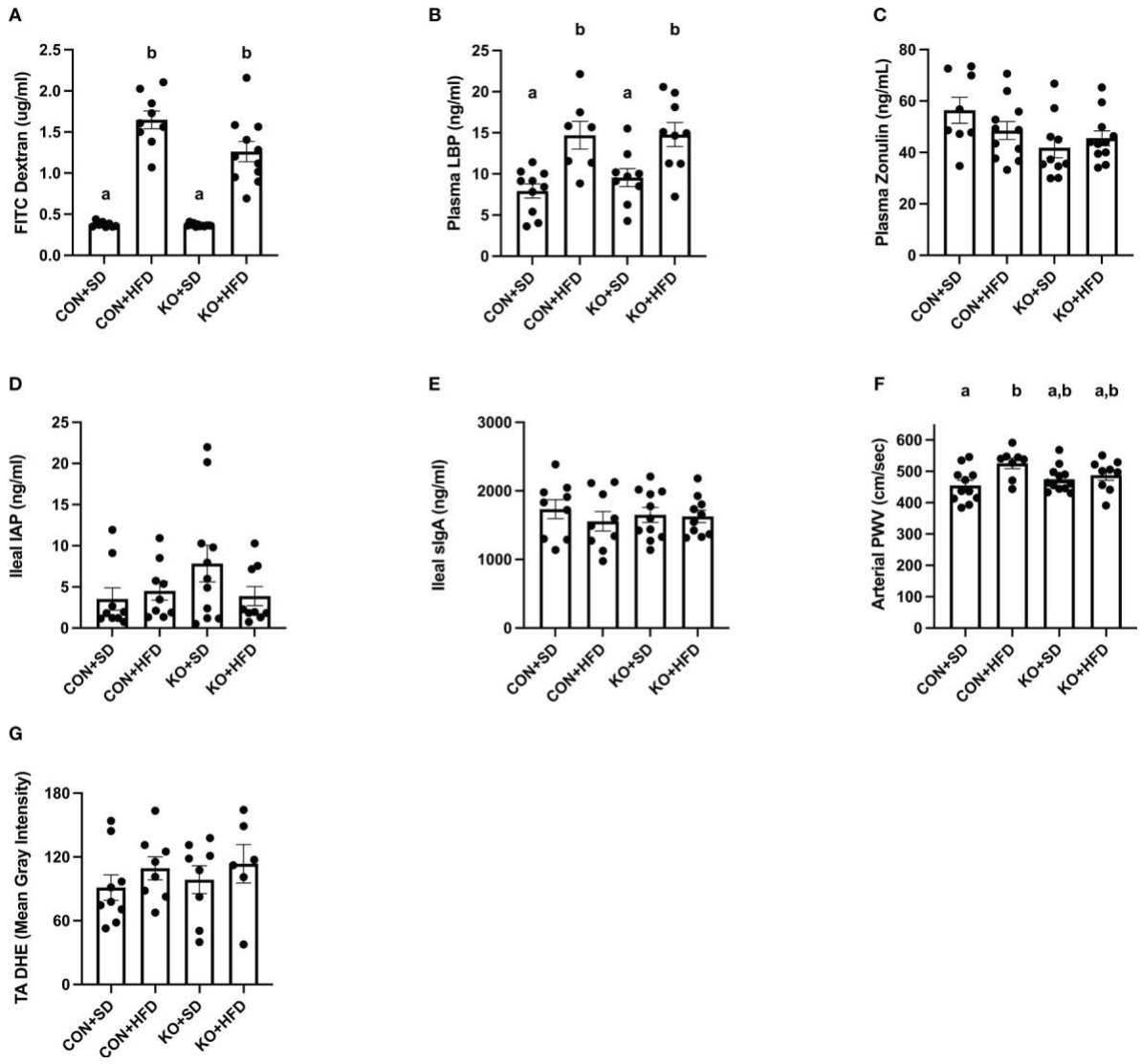

Figure 5.5 **Intestinal permeability and inflammation associated assays.** There was significant gut dysbiosis and intestinal permeability by diet but not genotype (A) which was matched in plasma LPS binding protein (B). There were no significant differences in plasma zonulin (C) or ileal intestinal alkaline phosphatase (D). Ileal sIgA (E) and DHE (G) was not significantly different by diet or genotype but there was a significant increase in control mice fed a high fat diet compared to the control diet (F).

Arterial stiffness was assessed via arterial pulse wave velocity (aPWV). After the 6-month dietary intervention, CON+HFD animals displayed significantly higher aPWV than CON+SD animals (CON+HFD: 525.4 ± 16.5 cm/sec; CON+SD: 455.2 ± 16.5 cm/sec; p=0.02, Figure 5.5F).

However, TLR4 deletion exerted a protective effect against the HFD such that aPWV was not elevated in KO+HFD mice compared to CON+SD or KO+SD, Figure 5.5F). Thoracic aorta DHE intensity was similar in all groups (p=0.6) (Figure 5G). Glucose response (Figure 5.6A) and area under the (AUC) (Figure 5.6B) were significantly higher in all groups compared to the CON+SD cohort. Similarly, insulin responses (Figure 5.6 C, D) were increased in HFD-fed animals compared to CON+SD, while KO+SD was not significantly different from any of the groups.

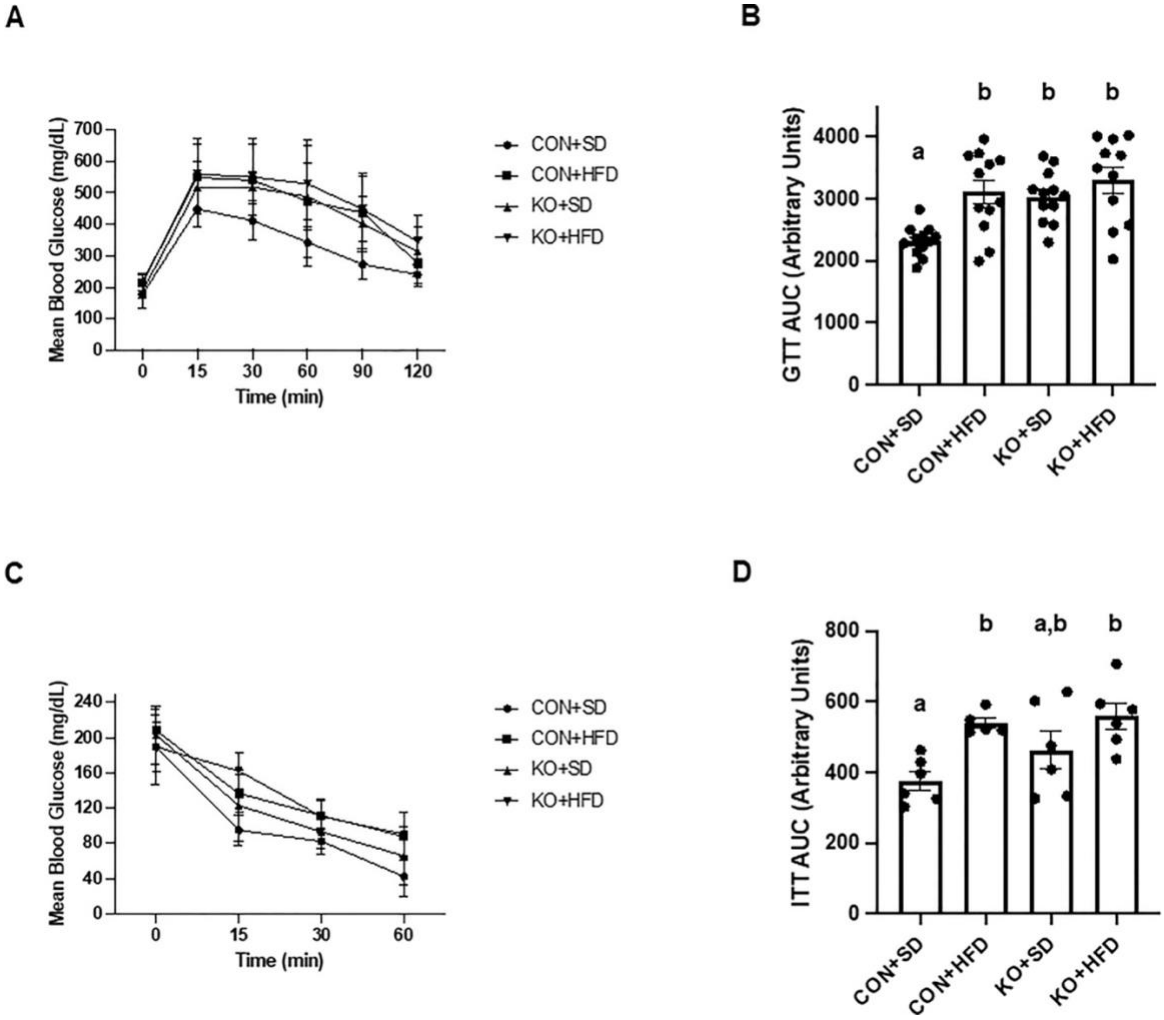

Figure 5.6 **Glucose and insulin responses.** There were no significant differences within timepoints for glucose tolerance tests (GTT) (A) or insulin tolerance tests (ITT) (C) however area under the curve is significantly different for GTT for CON+SD compared to all other groups (B) and ITT with a significant increase for high fat diet fed groups regardless of genotype CON+SD | CON+HFD, CON+SD | KO+HFD (D).

5.4: Discussion

TLRs are critical for pathogen recognition and immune health. One of the primary ligands for TLR4 is bacterial lipopolysaccharide (LPS), a component of the cell wall of all Gram-negative organisms. Translocation of non-pyrogenic levels of LPS from the intestinal lumen into the circulation occurs when disruptions to the gut microbiota result in reduced integrity of the intestinal barrier, a condition termed "metabolic endotoxemia" (76, 75). In turn, activation of TLR4 in immune cells and host tissues generates downstream signaling cascades leading to chronic inflammation. This chronic inflammation has been linked to cardiometabolic disruptions, including arterial stiffness (98, 94). We have demonstrated that suppression of the microbiota reverses arterial stiffness in HFD-fed mice (71). Therefore, we hypothesized that animals lacking TLR4 signaling capacity would be protected from the cardiometabolic consequences of a high fat diet, despite experiencing similar perturbations to the gut microbiota.

Interestingly, we found that TLR4 KO mice had a distinct microbial profile compared to CON littermates, but that introduction of a HFD induced similar microbial changes in both genotypes. Differences in the microbiota of TLR4 KO animals compared to CON littermates on a SD included reduced Shannon's diversity and distinct clustering along the first principal coordinate of an ordination of Bray-Curtis distances. Cuesta et al., recently reported similar patterns of alcohol-induced inflammation in TLR4 KO animals (80). The authors observed that the microbiota of the two genotypes displayed unique responses to ethanol exposure, while we observed very similar changes in response to HFD feeding.

We found that similarity between the two HFD groups was greater than similarity between the TLR4 KO groups on different diets. Specifically, *Ocillospira*, *Ruminoccocus*, and *Bacteroides* were higher in animals consuming HFD, while *Bifidobacterium* and *Allobaculum* were lower. None of the taxa that were increased with HFD are consistently associated with obesity or inflammation; however, L-methionine production by *Ruminococcus* has been associated with cardiovascular phenotypes in obese humans (87). In contrast, numerous studies have linked reduced *Bifidobacterium* to HFD (74, 110, 100) and we have previously reported inverse associations between *Bifidobacterium* and vascular function (71, 72, 107).

In addition to microbial dysbiosis, we also observed increased intestinal permeability in animals fed HFD, regardless of genotype. Although TLR4 is expressed in intestinal epithelial cells (IEL), it has been speculated that the constant exposure to intestinal bacterial LPS necessitates tight regulation of TLR4 activation in the lumen (108). This was confirmed in a recent study by Crame et al., who demonstrated that an intestinal specific KO of TLR4 had no impact on intestinal permeability in the ileum or colon (79). Therefore, it is unsurprising that the TLR4 KO offered no protection against HFD-induced intestinal barrier dysfunction.

Numerous studies have reported protective effects of TLR4 deletion following HFD or nutrient excess (103, 96, 92). Furthermore, Haimovich et al., demonstrated that poor insulin action and metabolic health are key activators of TLR4 signaling (112, 111, 113). Thus, it is plausible that deleting TLR4 in mice could help alleviate the resulting inflammatory effects of a HFD on cardiometabolic health. Interestingly, in the current study, $TLR4^{-/-}$ mice did not display improved glucose metabolism following a HFD. Although the reasons for this discrepancy are

unclear, it should be noted that some previous studies have also failed to demonstrate a protective effect of TLR4 inhibition on aspects of metabolic function (81, 93). Fewer studies have examined the effects of TLR4 signaling on vascular function, and to our knowledge, no studies have determined the effects on arterial stiffness. $TLR4^{-/-}$ deletion or inhibition has been shown to improve endothelial dysfunction in mice caused by angiotensin II delivery or type II diabetes (Liang et al., 2013, 86). Interestingly, and in line with the current study, previous reports have suggested that $TLR4^{-/-}$ mice are partially protected from vascular inflammation and atherosclerosis following a HFD (Kim et al., 2007, Ding et al., 2012). Collectively with the current results, these data suggest that diet-induced vascular disturbances are partially, albeit not entirely, mediated by TLR4 signaling.

Limitations of the current study should be noted. First, the TLR4 knockout model was a whole body knock out and thus it is unclear whether the observed protective effect on arterial stiffness was due to local TLR4 signaling in the vasculature or more remote signaling elsewhere. Tang et al., demonstrated that endothelial-specific TLR4 deletion protected mice from cerebral cavernous malformations, a cause of stroke, thus suggesting that endothelial TLR4 signaling may directly drive vascular dysfunction (105 Second, only male mice were studied. Given that some effects of TLR4 deficiency have been shown to be sex-dependent (91, 106), we cannot extrapolate our findings to beyond male mice. In conclusion, we found that TLR4-/- mice are not protected from the intestinal disturbances of a HFD but are partially protected from the downstream consequences within the vasculature.

Ultimately, our results suggest the importance of TLR4 signaling on the gut microbiota and arterial stiffness. Through the observed differences in the gut microbial composition between TLR4 KO and CON mice, we highlight TLR4 signaling as a potential mediator of the gut

microbial composition while supporting a possible bi-directional relationship between TLR4 signaling and the gut microbiota. Secondly, our data suggest that TLR4 signaling is at least partially responsible for the microbial-provoked arterial stiffening following caloric excess and may play a role in elevated cardiovascular risk associated with obesity, with our future work aiming to understand the specific mechanisms at play.

CHAPTER 6 CONCLUDING REMARKS AND FUTURE DIRECTIONS

6.1: Concluding Remarks

Finding novel therapeutics to target neonatal vulnerability during the first months of life is critical for reducing childhood deaths. Here we discuss the significant role of maternal influence and suggest a novel strategy to be considered for neonatal vaccination.

As reviewed in Chapter 1, successful neonatal vaccination is linked to maternal health outcomes and maternal factors that play a vital role in neonatal development in utero and during the first year of life. There is a need to optimize neonatal vaccination strategies to target the neonatal immune system and circumnavigate maternal influences. In the case of rotavirus, the gastrointestinal tract and gut microbiome must be considered due to the fecal-oral route of transmission and symptomology of severe gastroenteritis. As such, we evaluated a novel rotavirus vaccine platform, recombinant *Lactobacillus acidophilus*, through the maternal and neonatal perspectives including: 1) maternal rotavirus infection, 2) neonatal vaccine treatment with and without adjuvants, 3) neonatal vaccine dosage delivery, 4) neonatal rotavirus challenge. In Chapter 4 we evaluated these aspects independently in pilot studies, considering both immunological output and the impact and influence of the gut microbiome. In Chapter 3 we reproduced these studies in one cohesive experimental design that also offered a non-adjuvant vaccine and the interaction effects of the varying levels of rotavirus exposure (maternal and neonatal). In Chapter 5 we discuss additional roles of the gut microbiome, dysbiosis and Toll like receptor (TLR) 4 presence and activation in cardiometabolic health outcomes.

Alterations to the gut microbiome in cases of infection and maternal health must be considered for vaccines and their associated effectiveness in the neonate. In Chapter 3 we found that there was a significant role of maternal rotavirus infection and neonatal rotavirus challenge in neonatal outcomes. Interestingly, in some cases they were significant independently of one another and in others there was an interaction effect between maternal and neonatal rotavirus exposure. Further, we found that GAD85 performed better as a vaccine in neonates exposed to rotavirus than GAD84, suggesting a significant role for adjuvants in neonatal vaccines. In Chapter 4 we discovered that the fecal microbiome transplant was successful but, perhaps, an insufficient method to control for maternal variation within the context of neonatal study. We suggest consideration of additional normalization methods given that we saw a significant difference within neonatal treatment groups that was associated with the breeding doe for the litter. We found that neonatal gut microbiomes after a rotavirus challenge do not return to pre-challenge communities within 7 days regardless of neonatal treatment group. There were significant differences in the beta diversity of gut microbiomes for neonates that received different treatments, with GAD85 treated neonates more significantly different than STI buffer control and NCK56 wildtype controls. Taken together these results point to the significant role of the impact of the mother and the dynamic nature of the microbiome in mediating vaccination, particularly when considering the use of a mucosal vaccine.

In Chapter 5 we determined that Toll like receptor 4 (TLR4) knock out mice did not gain weight on a high fat diet and had better arterial function than control mice, however introduction of a high fat diet did shift their gut microbiomes in a similar manner to the control mice. We saw increased gut permeability and microbial dysbiosis in mice on a high fat diet regardless of

genotype. Taken together these results point to the significant role of the gut microbiome in impacting inflammation and the downstream biological systems, like cardiometabolic function.

6.2: Future Directions

To sufficiently address the relationship between the gut microbiome and a mucosal vaccine like the one presented in this dissertation, future studies should include additional treatment groups. Antibiotic treated groups (maternal and neonatal) would offer insight into how depletion or manipulating of the gut microbiome during the peripartum and postpartum timeframes influences neonatal vaccination responses. In addition, cross-fostering neonates to germ free does could be considered to determine more specifically the interaction of maternal microbiome and neonatal outcomes. More sequencing research into maternal microbiomes would strengthen the understanding of what maternal parameters most greatly influence neonatal gut microbiome development, including examination of the gut, vaginal, skin, and breastmilk microbiomes in conjunction with the neonatal microbiome. Another route to evaluate the high association of neonatal outcome and their breeding doe would be to include additional maternal analysis of rotavirus specific secretion in tissues and in breastmilk. This may provide additional normalization options to parse apart the neonatal outcomes in a way that is more independent of the mother.

More specific to this work, further analyses of the gut microbiome of neonates and does in Chapter 3 would provide insight into the immunology datasets. Specifically, if rotavirus infection irreversibly manipulated the neonate gut microbiomes during the seven-day rotavirus

challenge like we saw in Chapter 4, and how rotavirus infection influenced the maternal gut microbiome during the seven days after infection and before breeding. Understanding the microbial environment in does and neonates would be valuable information for the neonatal immunology outcomes presented in Chapter 3. Additionally, this analysis would include the new value that is previously undocumented in this dataset: rotavirus challenged neonates that were born to a rotavirus infected doe. Additional sequencing of samples collection during the first 16 days of life in neonates presented in Chapter 4 could also improve understanding of how the use of a recombinant probiotic as method for vaccine delivery is adjusting neonatal gut microbiomes and downstream, the neonatal immune systems.

REFERENCES

1. Berrington, J. E., Stewart, C. J., Embleton, N. D., & Cummings, S. P. (2013). Gut microbiota in preterm infants: Assessment and relevance to health and disease. *Archives of Disease in Childhood - Fetal and Neonatal Edition*, *98*(4), F286–F290. https://doi.org/10.1136/archdischild-2012-302134
2. De Filippo, C., Cavalieri, D., Di Paola, M., Ramazzotti, M., Poullet, J. B., Massart, S., Collini, S., Pieraccini, G., & Lionetti, P. (2010). Impact of diet in shaping gut microbiota revealed by a comparative study in children from Europe and rural Africa. *Proceedings of the National Academy of Sciences*, *107*(33), 14691–14696. https://doi.org/10.1073/pnas.1005963107
3. Dominguez-Bello, M. G., Costello, E. K., Contreras, M., Magris, M., Hidalgo, G., Fierer, N., & Knight, R. (2010). Delivery mode shapes the acquisition and structure of the initial microbiota across multiple body habitats in newborns. *Proceedings of the National Academy of Sciences*, *107*(26), 11971–11975. https://doi.org/10.1073/pnas.1002601107
4. Kanehisa, M., Goto, S., Furumichi, M., Tanabe, M., & Hirakawa, M. (2010). KEGG for representation and analysis of molecular networks involving diseases and drugs. *Nucleic Acids Research*, *38*(suppl_1), D355–D360. https://doi.org/10.1093/nar/gkp896
5. Macpherson, A. J., de Agüero, M. G., & Ganal-Vonarburg, S. C. (2017). How nutrition and the maternal microbiota shape the neonatal immune system. *Nature Reviews Immunology*, *17*(8), 508–517. https://doi.org/10.1038/nri.2017.58
6. Mai, V., Torrazza, R. M., Ukhanova, M., Wang, X., Sun, Y., Li, N., Shuster, J., Sharma, R., Hudak, M. L., & Neu, J. (2013). Distortions in Development of Intestinal Microbiota Associated with Late Onset Sepsis in Preterm Infants. *PLoS ONE*, *8*(1), e52876. https://doi.org/10.1371/journal.pone.0052876
7. Matamoros, S., Gras-Leguen, C., Le Vacon, F., Potel, G., & de La Cochetiere, M.-F. (2013). Development of intestinal microbiota in infants and its impact on health. *Trends in Microbiology*, *21*(4), 167–173. https://doi.org/10.1016/j.tim.2012.12.001
8. Nyangahu, D. D., & Jaspan, H. B. (2019). Influence of maternal microbiota during pregnancy on infant immunity. *Clinical and Experimental Immunology*, *198*(1), 47–56. https://doi.org/10.1111/cei.13331
9. Adams, S. H., Wright, R., Piccolo, B. D., Moody, B., Sikes, J., Avaritt, N., Chintapalli, S. V., & Ou, X. (2022). C-section increases cecal abundance of the archetypal bile acid and glucocorticoid modifying *Lachnoclostridium [clostridium] scindens* in mice. *Physiological Reports*, *10*(13). https://doi.org/10.14814/phy2.15363
10. Alexander, C., & Rietschel, E. T. (2001). Bacterial lipopolysaccharides and innate immunity. *Journal of Endotoxin Research*, *7*(3), 167–202.
11. Arboleya, S., Binetti, A., Salazar, N., Fernández, N., Solís, G., Hernández-Barranco, A., Margolles, A., Los Reyes-Gavilán, C. G., & Gueimonde, M. (2012). Establishment and development of intestinal microbiota in preterm neonates. *FEMS Microbiology Ecology*, *79*(3), 763–772. https://doi.org/10.1111/j.1574-6941.2011.01261.x
12. Berry, A. S. F., Pierdon, M. K., Misic, A. M., Sullivan, M. C., O'Brien, K., Chen, Y., Murray, S. J., Ramharack, L. A., Baldassano, R. N., Parsons, T. D., & Beiting, D. P. (2021). Remodeling of the maternal gut microbiome during pregnancy is shaped by parity. *Microbiome*, *9*(1), 146. https://doi.org/10.1186/s40168-021-01089-8
13. Bouskra, D., Brézillon, C., Bérard, M., Werts, C., Varona, R., Boneca, I. G., & Eberl, G.

(2008). Lymphoid tissue genesis induced by commensals through NOD1 regulates intestinal homeostasis. *Nature*, *456*(7221), 507–510. https://doi.org/10.1038/nature07450
14. Chattha, K. S., Vlasova, A. N., Kandasamy, S., Esseili, M. A., Siegismund, C., Rajashekara, G., & Saif, L. J. (2013). Probiotics and colostrum/milk differentially affect neonatal humoral immune responses to oral rotavirus vaccine. *Vaccine*, *31*(15), 1916–1923. https://doi.org/10.1016/j.vaccine.2013.02.020
15. Clancy, R. M., Marion, M. C., Ainsworth, H. C., Chang, M., Howard, T. D., Izmirly, P. M., Masson, M., Buyon, J. P., & Langefeld, C. D. (2022). Gut dysbiosis and the clinical spectrum in anti-Ro positive mothers of children with neonatal lupus. *Gut Microbes*, *14*(1), 2081474. https://doi.org/10.1080/19490976.2022.2081474
16. Derrien, M., Belzer, C., & De Vos, W. M. (2017). Akkermansia muciniphila and its role in regulating host functions. *Microbial Pathogenesis*, *106*, 171–181. https://doi.org/10.1016/j.micpath.2016.02.005
17. Fujimura, K. E., Sitarik, A. R., Havstad, S., Lin, D. L., Levan, S., Fadrosh, D., Panzer, A. R., LaMere, B., Rackaityte, E., Lukacs, N. W., Wegienka, G., Boushey, H. A., Ownby, D. R., Zoratti, E. M., Levin, A. M., Johnson, C. C., & Lynch, S. V. (2016). Neonatal gut microbiota associates with childhood multisensitized atopy and T cell differentiation. *Nature Medicine*, *22*(10), 1187–1191. https://doi.org/10.1038/nm.4176
18. Han, C., Dai, Y., Liu, B., Wang, L., Wang, J., & Zhang, J. (2019). Diversity analysis of intestinal microflora between healthy and diarrheal neonatal piglets from the same litter in different regions. *Anaerobe*, *55*, 136–141. https://doi.org/10.1016/j.anaerobe.2018.12.001
19. Harris, V., Ali, A., Fuentes, S., Korpela, K., Kazi, M., Tate, J., Parashar, U., Wiersinga, W. J., Giaquinto, C., De Weerth, C., & De Vos, W. M. (2018). Rotavirus vaccine response correlates with the infant gut microbiota composition in Pakistan. *Gut Microbes*, *9*(2), 93–101. https://doi.org/10.1080/19490976.2017.1376162
20. Harris, V. C., Armah, G., Fuentes, S., Korpela, K. E., Parashar, U., Victor, J. C., Tate, J., De Weerth, C., Giaquinto, C., Wiersinga, W. J., Lewis, K. D. C., & De Vos, W. M. (2017). Significant Correlation Between the Infant Gut Microbiome and Rotavirus Vaccine Response in Rural Ghana. *The Journal of Infectious Diseases*, *215*(1), 34–41. https://doi.org/10.1093/infdis/jiw518
21. Isolauri, E., Joensuu, J., Suomalainen, H., Luomala, M., & Vesikari, T. (1995). Improved immunogenicity of oral D x RRV reassortant rotavirus vaccine by Lactobacillus casei GG. *Vaccine*, *13*(3), 310–312. https://doi.org/10.1016/0264-410X(95)93319-5
22. Kimura, I., Miyamoto, J., Ohue-Kitano, R., Watanabe, K., Yamada, T., Onuki, M., Aoki, R., Isobe, Y., Kashihara, D., Inoue, D., Inaba, A., Takamura, Y., Taira, S., Kumaki, S., Watanabe, M., Ito, M., Nakagawa, F., Irie, J., Kakuta, H., … Hase, K. (2020). Maternal gut microbiota in pregnancy influences offspring metabolic phenotype in mice. *Science*, *367*(6481), eaaw8429. https://doi.org/10.1126/science.aaw8429
23. Liu, J., Bian, G., Sun, D., Zhu, W., & Mao, S. (2017). Starter Feeding Supplementation Alters Colonic Mucosal Bacterial Communities and Modulates Mucosal Immune Homeostasis in Newborn Lambs. *Frontiers in Microbiology*, *8*. https://doi.org/10.3389/fmicb.2017.00429
24. Ma, X., Xu, T., Qian, M., Zhang, Y., Yang, Z., & Han, X. (2022). Faecal microbiota transplantation alleviates early-life antibiotic-induced gut microbiota dysbiosis and mucosa injuries in a neonatal piglet model. *Microbiological Research*, *255*, 126942. https://doi.org/10.1016/j.micres.2021.126942

25. Macpherson, A. J., & Harris, N. L. (2004). Interactions between commensal intestinal bacteria and the immune system. *Nature Reviews Immunology*, *4*(6), 478–485. https://doi.org/10.1038/nri1373
26. Needham, B. D., Carroll, S. M., Giles, D. K., Georgiou, G., Whiteley, M., & Trent, M. S. (2013). Modulating the innate immune response by combinatorial engineering of endotoxin. *Proceedings of the National Academy of Sciences*, *110*(4), 1464–1469. https://doi.org/10.1073/pnas.1218080110
27. Ottman, N., Geerlings, S. Y., Aalvink, S., De Vos, W. M., & Belzer, C. (2017). Action and function of Akkermansia muciniphila in microbiome ecology, health and disease. *Best Practice & Research Clinical Gastroenterology*, *31*(6), 637–642. https://doi.org/10.1016/j.bpg.2017.10.001
28. Ribo, S., Sánchez-Infantes, D., Martinez-Guino, L., García-Mantrana, I., Ramon-Krauel, M., Tondo, M., Arning, E., Nofrarías, M., Osorio-Conles, Ó., Fernández-Pérez, A., González-Torres, P., Cebrià, J., Gavaldà-Navarro, A., Chenoll, E., Isganaitis, E., Villarroya, F., Vallejo, M., Segalés, J., Jiménez-Chillarón, J. C., … Lerin, C. (2021). Increasing breast milk betaine modulates *Akkermansia* abundance in mammalian neonates and improves long-term metabolic health. *Science Translational Medicine*, *13*(587), eabb0322. https://doi.org/10.1126/scitranslmed.abb0322
29. Sun, X., Guo, N., Li, J., Yan, X., He, Z., Li, D., Jin, M., Xie, G., Pang, L., Zhang, Q., Liu, N., & Duan, Z.-J. (2016). Rotavirus infection and histo-blood group antigens in the children hospitalized with diarrhoea in China. *Clinical Microbiology and Infection*, *22*(8), 740.e1-740.e3. https://doi.org/10.1016/j.cmi.2016.06.007
30. Twitchell, E. L., Tin, C., Wen, K., Zhang, H., Becker-Dreps, S., Azcarate-Peril, M. A., Vilchez, S., Li, G., Ramesh, A., Weiss, M., Lei, S., Bui, T., Yang, X., Schultz-Cherry, S., & Yuan, L. (2016). Modeling human enteric dysbiosis and rotavirus immunity in gnotobiotic pigs. *Gut Pathogens*, *8*(1), 51. https://doi.org/10.1186/s13099-016-0136-y
31. Wen, K., Li, G., Bui, T., Liu, F., Li, Y., Kocher, J., Lin, L., Yang, X., & Yuan, L. (2012). High dose and low dose Lactobacillus acidophilus exerted differential immune modulating effects on T cell immune responses induced by an oral human rotavirus vaccine in gnotobiotic pigs. *Vaccine*, *30*(6), 1198–1207. https://doi.org/10.1016/j.vaccine.2011.11.107
32. Chong, Clara, Frank Bloomfield, and Justin O'Sullivan. "Factors Affecting Gastrointestinal Microbiome Development in Neonates." *Nutrients* 10, no. 3 (February 28, 2018): 274. https://doi.org/10.3390/nu10030274.
33. Clark, Andrew, Kevin Van Zandvoort, Stefan Flasche, Colin Sanderson, Julie Bines, Jacqueline Tate, Umesh Parashar, and Mark Jit. "Efficacy of Live Oral Rotavirus Vaccines by Duration of Follow-up: A Meta-Regression of Randomised Controlled Trials." *The Lancet Infectious Diseases* 19, no. 7 (July 2019): 717–27. https://doi.org/10.1016/S1473-3099(19)30126-4.
34. Engevik, Melinda A., Lori D. Banks, Kristen A. Engevik, Alexandra L. Chang-Graham, Jacob L. Perry, Diane S. Hutchinson, Nadim J. Ajami, Joseph F. Petrosino, and Joseph M. Hyser. "Rotavirus Infection Induces Glycan Availability to Promote Ileum-Specific Changes in the Microbiome Aiding Rotavirus Virulence." *Gut Microbes* 11, no. 5 (September 2, 2020): 1324–47. https://doi.org/10.1080/19490976.2020.1754714.
35. Fleming, Alison S., Gary W. Kraemer, Andrea Gonzalez, Vedran Lovic, Stephanie Rees, and Angel Melo. "Mothering Begets Mothering." *Pharmacology Biochemistry and Behavior* 73, no. 1 (August 2002): 61–75. https://doi.org/10.1016/S0091-3057(02)00793-1.

36. Fonseca, Wendy, Carrie-Anne Malinczak, Kei Fujimura, Danny Li, Kathryn McCauley, Jia Li, Shannon K.K. Best, et al. “Maternal Gut Microbiome Regulates Immunity to RSV Infection in Offspring.” *Journal of Experimental Medicine* 218, no. 11 (November 1, 2021): e20210235. https://doi.org/10.1084/jem.20210235.
37. Garcia-Flores, Valeria, Roberto Romero, Amy-Eunice Furcron, Dustyn Levenson, Jose Galaz, Chengrui Zou, Sonia S. Hassan, et al. “Prenatal Maternal Stress Causes Preterm Birth and Affects Neonatal Adaptive Immunity in Mice.” *Frontiers in Immunology* 11 (February 26, 2020): 254. https://doi.org/10.3389/fimmu.2020.00254.
38. Gilfillan, Darby, Allison C. Vilander, Meichen Pan, Yong Jun Goh, Sarah O’Flaherty, Ningguo Feng, Bridget E. Fox, et al. “Lactobacillus Acidophilus Expressing Murine Rotavirus VP8 and Mucosal Adjuvants Induce Virus-Specific Immune Responses.” *Vaccines* 11, no. 12 (November 28, 2023): 1774. https://doi.org/10.3390/vaccines11121774.
39. Hennessy, Michael B., Jerry Vogt, and Seymour Levine. “Strain of Foster Mother Determines Long-Term Effects of Early Handling: Evidence for Maternal Mediation.” *Physiological Psychology* 10, no. 1 (March 1982): 153–57. https://doi.org/10.3758/BF03327019.
40. Heun-Johnson, Hanke, and Pat Levitt. “Early-Life Stress Paradigm Transiently Alters Maternal Behavior, Dam-Pup Interactions, and Offspring Vocalizations in Mice.” *Frontiers in Behavioral Neuroscience* 10 (July 5, 2016). https://doi.org/10.3389/fnbeh.2016.00142.
41. Kalbermatter, Cristina, Nerea Fernandez Trigo, Sandro Christensen, and Stephanie C. Ganal-Vonarburg. “Maternal Microbiota, Early Life Colonization and Breast Milk Drive Immune Development in the Newborn.” *Frontiers in Immunology* 12 (May 13, 2021): 683022. https://doi.org/10.3389/fimmu.2021.683022.
42. Kimura, Ikuo, Junki Miyamoto, Ryuji Ohue-Kitano, Keita Watanabe, Takahiro Yamada, Masayoshi Onuki, Ryo Aoki, et al. “Maternal Gut Microbiota in Pregnancy Influences Offspring Metabolic Phenotype in Mice.” *Science* 367, no. 6481 (February 28, 2020): eaaw8429. https://doi.org/10.1126/science.aaw8429.
43. Korpela, Katri, and Willem M. De Vos. “Infant Gut Microbiota Restoration: State of the Art.” *Gut Microbes* 14, no. 1 (December 31, 2022): 2118811. https://doi.org/10.1080/19490976.2022.2118811.
44. Korpela, Katri, Otto Helve, Kaija-Leena Kolho, Terhi Saisto, Kirsi Skogberg, Evgenia Dikareva, Vedran Stefanovic, Anne Salonen, Sture Andersson, and Willem M. De Vos. “Maternal Fecal Microbiota Transplantation in Cesarean-Born Infants Rapidly Restores Normal Gut Microbial Development: A Proof-of-Concept Study.” *Cell* 183, no. 2 (October 2020): 324-334.e5. https://doi.org/10.1016/j.cell.2020.08.047.
45. Le Doare, Kirsty, Beth Holder, Aisha Bassett, and Pia S. Pannaraj. “Mother’s Milk: A Purposeful Contribution to the Development of the Infant Microbiota and Immunity.” *Frontiers in Immunology* 9 (February 28, 2018): 361. https://doi.org/10.3389/fimmu.2018.00361.
46. Lim, Ai Ing, Taryn McFadden, Verena M. Link, Seong-Ji Han, Rose-Marie Karlsson, Apollo Stacy, Taylor K. Farley, et al. “Prenatal Maternal Infection Promotes Tissue-Specific Immunity and Inflammation in Offspring.” *Science* 373, no. 6558 (August 27, 2021): eabf3002. https://doi.org/10.1126/science.abf3002.
47. Miyoshi, Jun, Alexandria M. Bobe, Sawako Miyoshi, Yong Huang, Nathaniel Hubert, Tom O. Delmont, A. Murat Eren, Vanessa Leone, and Eugene B. Chang. “Peripartum Antibiotics Promote Gut Dysbiosis, Loss of Immune Tolerance, and Inflammatory Bowel Disease in

Genetically Prone Offspring." *Cell Reports* 20, no. 2 (July 2017): 491–504. https://doi.org/10.1016/j.celrep.2017.06.060.
48. Morein, B., G. Blomqvist, and K. Hu. "Immune Responsiveness in the Neonatal Period." *Journal of Comparative Pathology* 137 (July 2007): S27–31. https://doi.org/10.1016/j.jcpa.2007.04.008.
49. Moreira, Virgínia B., Vânia G.M. Mattaraia, Mariana V. Rodrigues, Cynthia Z. De Albuquerque, and Ana Silvia A.M.T. Moura. "Parental Behavior and Anxiety in Isogenic and Outbred Mice given Access to Two Types of Nesting Materials." *Applied Animal Behaviour Science* 215 (June 2019): 68–76. https://doi.org/10.1016/j.applanim.2019.03.012.
50. Nguyen, Quang N., Jonathon E. Himes, David R. Martinez, and Sallie R. Permar. "The Impact of the Gut Microbiota on Humoral Immunity to Pathogens and Vaccination in Early Infancy." Edited by Deborah A. Hogan. *PLOS Pathogens* 12, no. 12 (December 22, 2016): e1005997. https://doi.org/10.1371/journal.ppat.1005997.
51. Noakes, P. S. "Maternal Smoking Is Associated with Impaired Neonatal Toll-like-Receptor-Mediated Immune Responses." *European Respiratory Journal* 28, no. 4 (October 1, 2006): 721–29. https://doi.org/10.1183/09031936.06.00050206.
52. Nunez, Natalia, Louis Réot, and Elisabeth Menu. "Neonatal Immune System Ontogeny: The Role of Maternal Microbiota and Associated Factors. How Might the Non-Human Primate Model Enlighten the Path?" *Vaccines* 9, no. 6 (June 1, 2021): 584. https://doi.org/10.3390/vaccines9060584.
53. O'Neill, Ian J., Rocio Sanchez Gallardo, Radka Saldova, Eileen F. Murphy, Paul D. Cotter, Fionnuala M. McAuliffe, and Douwe Van Sinderen. "Maternal and Infant Factors That Shape Neonatal Gut Colonization by Bacteria." *Expert Review of Gastroenterology & Hepatology* 14, no. 8 (August 2, 2020): 651–64. https://doi.org/10.1080/17474124.2020.1784725.
54. Orije, Marjolein R.P., Kirsten Maertens, Véronique Corbière, Nasamon Wanlapakorn, Pierre Van Damme, Elke Leuridan, and Françoise Mascart. "The Effect of Maternal Antibodies on the Cellular Immune Response after Infant Vaccination: A Review." *Vaccine* 38, no. 1 (January 2020): 20–28. https://doi.org/10.1016/j.vaccine.2019.10.025.
55. Otero, Claire E., Stephanie N. Langel, Maria Blasi, and Sallie R. Permar. "Maternal Antibody Interference Contributes to Reduced Rotavirus Vaccine Efficacy in Developing Countries." Edited by Andrew Mehle. *PLOS Pathogens* 16, no. 11 (November 19, 2020): e1009010. https://doi.org/10.1371/journal.ppat.1009010.
56. Pardon, Marie-Christine, Priscille Gérardin, Chantal Joubert, Fernando Pérez-Diaz, and Charles Cohen-Salmon. "Influence of Prepartum Chronic Ultramild Stress on Maternal Pup Care Behavior in Mice." *Biological Psychiatry* 47, no. 10 (May 2000): 858–63. https://doi.org/10.1016/S0006-3223(99)00253-X.
57. Parker, Edward P. K., Christina Bronowski, Kulandaipalayam Natarajan C. Sindhu, Sudhir Babji, Blossom Benny, Noelia Carmona-Vicente, Nedson Chasweka, et al. "Impact of Maternal Antibodies and Microbiota Development on the Immunogenicity of Oral Rotavirus Vaccine in African, Indian, and European Infants." *Nature Communications* 12, no. 1 (December 15, 2021): 7288. https://doi.org/10.1038/s41467-021-27074-1.
58. Pasolli, Edoardo, Francesca De Filippis, Italia E. Mauriello, Fabio Cumbo, Aaron M. Walsh, John Leech, Paul D. Cotter, Nicola Segata, and Danilo Ercolini. "Large-Scale Genome-Wide Analysis Links Lactic Acid Bacteria from Food with the Gut Microbiome." *Nature Communications* 11, no. 1 (May 25, 2020): 2610. https://doi.org/10.1038/s41467-020-16438-

8.
59. Pasquale, Alberta, Scott Preiss, Fernanda Silva, and Nathalie Garçon. “Vaccine Adjuvants: From 1920 to 2015 and Beyond.” *Vaccines* 3, no. 2 (April 16, 2015): 320–43. https://doi.org/10.3390/vaccines3020320.
60. Renson, Patricia, Christelle Fablet, Mathieu Andraud, Valérie Normand, Arnaud Lebret, Frédéric Paboeuf, Nicolas Rose, and Olivier Bourry. “Maternally-Derived Neutralizing Antibodies Reduce Vaccine Efficacy against Porcine Reproductive and Respiratory Syndrome Virus Infection.” *Vaccine* 37, no. 31 (July 2019): 4318–24. https://doi.org/10.1016/j.vaccine.2019.06.045.
61. Romani, Lorenza, Federica Del Chierico, Maria Chiriaco, Silvia Foligno, Sofia Reddel, Guglielmo Salvatori, Cristina Cifaldi, et al. “Gut Mucosal and Fecal Microbiota Profiling Combined to Intestinal Immune System in Neonates Affected by Intestinal Ischemic Injuries.” *Frontiers in Cellular and Infection Microbiology* 10 (February 25, 2020): 59. https://doi.org/10.3389/fcimb.2020.00059.
62. Romano-Keeler, Joann, and Jörn-Hendrik Weitkamp. “Maternal Influences on Fetal Microbial Colonization and Immune Development.” *Pediatric Research* 77, no. 1–2 (January 2015): 189–95. https://doi.org/10.1038/pr.2014.163.
63. Rotroff, Daniel M., Bonnie R. Joubert, Skylar W. Marvel, Siri E. Håberg, Michael C. Wu, Roy M. Nilsen, Per M. Ueland, Wenche Nystad, Stephanie J. London, and Alison Motsinger-Reif. “Maternal Smoking Impacts Key Biological Pathways in Newborns through Epigenetic Modification in Utero.” *BMC Genomics* 17, no. 1 (December 2016): 976. https://doi.org/10.1186/s12864-016-3310-1.
64. Sanidad, Katherine Z., Mohammed Amir, Aparna Ananthanarayanan, Anvita Singaraju, Nicholas B. Shiland, Hanna S. Hong, Nobuhiko Kamada, Naohiro Inohara, Gabriel Núñez, and Melody Y. Zeng. “Maternal Gut Microbiome–Induced IgG Regulates Neonatal Gut Microbiome and Immunity.” *Science Immunology* 7, no. 72 (June 24, 2022): eabh3816. https://doi.org/10.1126/sciimmunol.abh3816.
65. Solís, G., C.G. De Los Reyes-Gavilan, N. Fernández, A. Margolles, and M. Gueimonde. “Establishment and Development of Lactic Acid Bacteria and Bifidobacteria Microbiota in Breast-Milk and the Infant Gut.” *Anaerobe* 16, no. 3 (June 2010): 307–10. https://doi.org/10.1016/j.anaerobe.2010.02.004.
66. Szatraj, K., A.K. Szczepankowska, and M. Chmielewska-Jeznach. “Lactic Acid Bacteria - Promising Vaccine Vectors: Possibilities, Limitations, Doubts.” *Journal of Applied Microbiology* 123, no. 2 (August 2017): 325–39. https://doi.org/10.1111/jam.13446.
67. Villarreal Pérez, Jesús Zacarías, José Manuel Ramírez Aranda, Manuel De La O Cavazos, Michelle De J. Zamudio Osuna, José Perales Dávila, María Romelia Ballesteros Elizondo, Marco Vinicio Gómez Meza, Francisco Javier García Elizondo, and Azucena M. Rodríguez González. “Randomized Clinical Trial of the Safety and Immunogenicity of the Tdap Vaccine in Pregnant Mexican Women.” *Human Vaccines & Immunotherapeutics* 13, no. 1 (January 2, 2017): 128–35. https://doi.org/10.1080/21645515.2016.1232786.
68. Xu, Rongying, Jiajia Wan, Chunhui Lin, and Yong Su. “Effects of Early Intervention with Antibiotics and Maternal Fecal Microbiota on Transcriptomic Profiling Ileal Mucusa in Neonatal Pigs.” *Antibiotics* 9, no. 1 (January 18, 2020): 35. https://doi.org/10.3390/antibiotics9010035.
69. Anderson, M. J. (2001). A new method for non-parametric multivariate analysis of variance. *Austral Ecology*, *26*(1), 32–46. https://doi.org/10.1111/j.1442-9993.2001.01070.pp.x

70. Bates, J. M., Akerlund, J., Mittge, E., & Guillemin, K. (2007). Intestinal Alkaline Phosphatase Detoxifies Lipopolysaccharide and Prevents Inflammation in Zebrafish in Response to the Gut Microbiota. *Cell Host & Microbe*, *2*(6), 371–382. https://doi.org/10.1016/j.chom.2007.10.010
71. Battson, M. L., Lee, D. M., Jarrell, D. K., Hou, S., Ecton, K. E., Weir, T. L., & Gentile, C. L. (2018). Suppression of gut dysbiosis reverses Western diet-induced vascular dysfunction. *American Journal of Physiology-Endocrinology and Metabolism*, *314*(5), E468–E477. https://doi.org/10.1152/ajpendo.00187.2017
72. Battson, M. L., Lee, D. M., Li Puma, L. C., Ecton, K. E., Thomas, K. N., Febvre, H. P., Chicco, A. J., Weir, T. L., & Gentile, C. L. (2019). Gut microbiota regulates cardiac ischemic tolerance and aortic stiffness in obesity. *American Journal of Physiology-Heart and Circulatory Physiology*, *317*(6), H1210–H1220. https://doi.org/10.1152/ajpheart.00346.2019
73. Brown, J. M., & Hazen, S. L. (2015). The Gut Microbial Endocrine Organ: Bacterially Derived Signals Driving Cardiometabolic Diseases. *Annual Review of Medicine*, *66*(1), 343–359. https://doi.org/10.1146/annurev-med-060513-093205
74. Cani, P. D., Amar, J., Iglesias, M. A., Poggi, M., Knauf, C., Bastelica, D., Neyrinck, A. M., Fava, F., Tuohy, K. M., Chabo, C., Waget, A., Delmée, E., Cousin, B., Sulpice, T., Chamontin, B., Ferrières, J., Tanti, J.-F., Gibson, G. R., Casteilla, L., … Burcelin, R. (2007). Metabolic Endotoxemia Initiates Obesity and Insulin Resistance. *Diabetes*, *56*(7), 1761–1772. https://doi.org/10.2337/db06-1491
75. Cani, P. D., Bibiloni, R., Knauf, C., Waget, A., Neyrinck, A. M., Delzenne, N. M., & Burcelin, R. (2008). Changes in Gut Microbiota Control Metabolic Endotoxemia-Induced Inflammation in High-Fat Diet–Induced Obesity and Diabetes in Mice. *Diabetes*, *57*(6), 1470–1481. https://doi.org/10.2337/db07-1403
76. Cani, P. D., Neyrinck, A. M., Fava, F., Knauf, C., Burcelin, R. G., Tuohy, K. M., Gibson, G. R., & Delzenne, N. M. (2007). Selective increases of bifidobacteria in gut microflora improve high-fat-diet-induced diabetes in mice through a mechanism associated with endotoxaemia. *Diabetologia*, *50*(11), 2374–2383. https://doi.org/10.1007/s00125-007-0791-0
77. Ciesielska, A., Matyjek, M., & Kwiatkowska, K. (2021). TLR4 and CD14 trafficking and its influence on LPS-induced pro-inflammatory signaling. *Cellular and Molecular Life Sciences*, *78*(4), 1233–1261. https://doi.org/10.1007/s00018-020-03656-y
78. Clemente-Postigo, M., Queipo-Ortuño, M. I., Murri, M., Boto-Ordoñez, M., Perez-Martinez, P., Andres-Lacueva, C., Cardona, F., & Tinahones, F. J. (2012). Endotoxin increase after fat overload is related to postprandial hypertriglyceridemia in morbidly obese patients. *Journal of Lipid Research*, *53*(5), 973–978. https://doi.org/10.1194/jlr.P020909
79. Crame, E. E., Bowen, J. M., Secombe, K. R., Coller, J. K., François, M., Leifert, W., & Wardill, H. R. (2021). Epithelial-Specific TLR4 Knockout Challenges Current Evidence of TLR4 Homeostatic Control of Gut Permeability. *Inflammatory Intestinal Diseases*, *6*(4), 199–209. https://doi.org/10.1159/000519200
80. Cuesta, C. M., Pascual, M., Pérez-Moraga, R., Rodríguez-Navarro, I., García-García, F., Ureña-Peralta, J. R., & Guerri, C. (2021). TLR4 Deficiency Affects the Microbiome and Reduces Intestinal Dysfunctions and Inflammation in Chronic Alcohol-Fed Mice. *International Journal of Molecular Sciences*, *22*(23), 12830. https://doi.org/10.3390/ijms222312830
81. Dalby, M. J., Aviello, G., Ross, A. W., Walker, A. W., Barrett, P., & Morgan, P. J. (2018). Diet induced obesity is independent of metabolic endotoxemia and TLR4 signalling, but

markedly increases hypothalamic expression of the acute phase protein, SerpinA3N. *Scientific Reports*, *8*(1), 15648. https://doi.org/10.1038/s41598-018-33928-4
82. David, L. A., Maurice, C. F., Carmody, R. N., Gootenberg, D. B., Button, J. E., Wolfe, B. E., Ling, A. V., Devlin, A. S., Varma, Y., Fischbach, M. A., Biddinger, S. B., Dutton, R. J., & Turnbaugh, P. J. (2014). Diet rapidly and reproducibly alters the human gut microbiome. *Nature*, *505*(7484), 559–563. https://doi.org/10.1038/nature12820
83. Eckel, R. H., & Krauss, R. M. (1998). American Heart Association Call to Action: Obesity as a Major Risk Factor for Coronary Heart Disease. *Circulation*, *97*(21), 2099–2100. https://doi.org/10.1161/01.CIR.97.21.2099
84. Fasano, A. (2021). Zonulin measurement conundrum: Add confusion to confusion does not lead to clarity. *Gut*, *70*(10), 2007.2-2008. https://doi.org/10.1136/gutjnl-2020-323367
85. Fuke, N., Nagata, N., Suganuma, H., & Ota, T. (2019). Regulation of Gut Microbiota and Metabolic Endotoxemia with Dietary Factors. *Nutrients*, *11*(10), 2277. https://doi.org/10.3390/nu11102277
86. Hernanz, R., Martínez-Revelles, S., Palacios, R., Martín, A., Cachofeiro, V., Aguado, A., García-Redondo, L., Barrús, M. T., De Batista, P. R., Briones, A. M., Salaices, M., & Alonso, M. J. (2015). Toll-like receptor 4 contributes to vascular remodelling and endothelial dysfunction in angiotensin II -induced hypertension. *British Journal of Pharmacology*, *172*(12), 3159–3176. https://doi.org/10.1111/bph.13117
87. Kurilshikov, A., Van Den Munckhof, I. C. L., Chen, L., Bonder, M. J., Schraa, K., Rutten, J. H. W., Riksen, N. P., De Graaf, J., Oosting, M., Sanna, S., Joosten, L. A. B., Van Der Graaf, M., Brand, T., Koonen, D. P. Y., Van Faassen, M., LifeLines DEEP Cohort Study, BBMRI Metabolomics Consortium, Slagboom, P. E., Xavier, R. J., Kuipers, F., … Fu, J. (2019). Gut Microbial Associations to Plasma Metabolites Linked to Cardiovascular Phenotypes and Risk: A Cross-Sectional Study. *Circulation Research*, *124*(12), 1808–1820. https://doi.org/10.1161/CIRCRESAHA.118.314642
88. Laugerette, F., Vors, C., Géloën, A., Chauvin, M.-A., Soulage, C., Lambert-Porcheron, S., Peretti, N., Alligier, M., Burcelin, R., Laville, M., Vidal, H., & Michalski, M.-C. (2011). Emulsified lipids increase endotoxemia: Possible role in early postprandial low-grade inflammation. *The Journal of Nutritional Biochemistry*, *22*(1), 53–59. https://doi.org/10.1016/j.jnutbio.2009.11.011
89. Lee, D. M., Battson, M. L., Jarrell, D. K., Hou, S., Ecton, K. E., Weir, T. L., & Gentile, C. L. (2018). SGLT2 inhibition via dapagliflozin improves generalized vascular dysfunction and alters the gut microbiota in type 2 diabetic mice. *Cardiovascular Diabetology*, *17*(1), 62. https://doi.org/10.1186/s12933-018-0708-x
90. Lee, D. M., Ecton, K. E., Trikha, S. R. J., Wrigley, S. D., Thomas, K. N., Battson, M. L., Wei, Y., Johnson, S. A., Weir, T. L., & Gentile, C. L. (2020). Microbial metabolite indole-3-propionic acid supplementation does not protect mice from the cardiometabolic consequences of a Western diet. *American Journal of Physiology-Gastrointestinal and Liver Physiology*, *319*(1), G51–G62. https://doi.org/10.1152/ajpgi.00375.2019
91. Li, Y., Zhu, S., Xie, K., Feng, X., Chen, L., Wu, X., Sun, Z., Shu, G., Wang, S., Zhu, C., Gao, P., Jiang, Q., & Wang, L. (2022). TLR4 in Tph2 neurons modulates anxiety-related behaviors in a sex-dependent manner. *Neuropharmacology*, *216*, 109175. https://doi.org/10.1016/j.neuropharm.2022.109175
92. Lin, H.-Y., Weng, S.-W., Shen, F.-C., Chang, Y.-H., Lian, W.-S., Hsieh, C.-H., Chuang, J.-H., Lin, T.-K., Liou, C.-W., Chang, C.-S., Lin, C.-Y., Su, Y.-J., & Wang, P.-W. (2020).

Abrogation of Toll-Like Receptor 4 Mitigates Obesity-Induced Oxidative Stress, Proinflammation, and Insulin Resistance Through Metabolic Reprogramming of Mitochondria in Adipose Tissue. *Antioxidants & Redox Signaling*, *33*(2), 66–86. https://doi.org/10.1089/ars.2019.7737

93. Moser, V. A., Uchoa, M. F., & Pike, C. J. (2018). TLR4 inhibitor TAK-242 attenuates the adverse neural effects of diet-induced obesity. *Journal of Neuroinflammation*, *15*(1), 306. https://doi.org/10.1186/s12974-018-1340-0
94. Mozos, I., Malainer, C., Horbańczuk, J., Gug, C., Stoian, D., Luca, C. T., & Atanasov, A. G. (2017). Inflammatory Markers for Arterial Stiffness in Cardiovascular Diseases. *Frontiers in Immunology*, *8*, 1058. https://doi.org/10.3389/fimmu.2017.01058
95. Ojeda, P., Bobe, A., Dolan, K., Leone, V., & Martinez, K. (2016). Nutritional modulation of gut microbiota—The impact on metabolic disease pathophysiology. *The Journal of Nutritional Biochemistry*, *28*, 191–200. https://doi.org/10.1016/j.jnutbio.2015.08.013
96. Poggi, M., Bastelica, D., Gual, P., Iglesias, M. A., Gremeaux, T., Knauf, C., Peiretti, F., Verdier, M., Juhan-Vague, I., Tanti, J. F., Burcelin, R., & Alessi, M. C. (2007). C3H/HeJ mice carrying a toll-like receptor 4 mutation are protected against the development of insulin resistance in white adipose tissue in response to a high-fat diet. *Diabetologia*, *50*(6), 1267–1276. https://doi.org/10.1007/s00125-007-0654-8
97. Qiao, Y., Sun, J., Ding, Y., Le, G., & Shi, Y. (2013). Alterations of the gut microbiota in high-fat diet mice is strongly linked to oxidative stress. *Applied Microbiology and Biotechnology*, *97*(4), 1689–1697. https://doi.org/10.1007/s00253-012-4323-6
98. Roman, M. J., Devereux, R. B., Schwartz, J. E., Lockshin, M. D., Paget, S. A., Davis, A., Crow, M. K., Sammaritano, L., Levine, D. M., Shankar, B.-A., Moeller, E., & Salmon, J. E. (2005). Arterial Stiffness in Chronic Inflammatory Diseases. *Hypertension*, *46*(1), 194–199. https://doi.org/10.1161/01.HYP.0000168055.89955.db
99. Ryu, J.-K., Kim, S. J., Rah, S.-H., Kang, J. I., Jung, H. E., Lee, D., Lee, H. K., Lee, J.-O., Park, B. S., Yoon, T.-Y., & Kim, H. M. (2017). Reconstruction of LPS Transfer Cascade Reveals Structural Determinants within LBP, CD14, and TLR4-MD2 for Efficient LPS Recognition and Transfer. *Immunity*, *46*(1), 38–50. https://doi.org/10.1016/j.immuni.2016.11.007
100. Schellekens, H., Torres-Fuentes, C., Van De Wouw, M., Long-Smith, C. M., Mitchell, A., Strain, C., Berding, K., Bastiaanssen, T. F. S., Rea, K., Golubeva, A. V., Arboleya, S., Verpaalen, M., Pusceddu, M. M., Murphy, A., Fouhy, F., Murphy, K., Ross, P., Roy, B. L., Stanton, C., … Cryan, J. F. (2021). Bifidobacterium longum counters the effects of obesity: Partial successful translation from rodent to human. *EBioMedicine*, *63*, 103176. https://doi.org/10.1016/j.ebiom.2020.103176
101. Schumann, R. R., & Zweigner, J. (1999). A Novel Acute-Phase Marker: Lipopolysaccharide Binding Protein (LBP). *Cclm*, *37*(3), 271–274. https://doi.org/10.1515/CCLM.1999.047
102. Segata, N., Izard, J., Waldron, L., Gevers, D., Miropolsky, L., Garrett, W. S., & Huttenhower, C. (2011). Metagenomic biomarker discovery and explanation. *Genome Biology*, *12*(6), R60. https://doi.org/10.1186/gb-2011-12-6-r60
103. Shi, H., Kokoeva, M. V., Inouye, K., Tzameli, I., Yin, H., & Flier, J. S. (2006). TLR4 links innate immunity and fatty acid–induced insulin resistance. *Journal of Clinical Investigation*, *116*(11), 3015–3025. https://doi.org/10.1172/JCI28898
104. Tajik, N., Frech, M., Schulz, O., Schälter, F., Lucas, S., Azizov, V., Dürholz, K., Steffen,

F., Omata, Y., Rings, A., Bertog, M., Rizzo, A., Iljazovic, A., Basic, M., Kleyer, A., Culemann, S., Krönke, G., Luo, Y., Überla, K., … Zaiss, M. M. (2020). Targeting zonulin and intestinal epithelial barrier function to prevent onset of arthritis. *Nature Communications*, *11*(1), 1995. https://doi.org/10.1038/s41467-020-15831-7

105. Tang, A. T., Choi, J. P., Kotzin, J. J., Yang, Y., Hong, C. C., Hobson, N., Girard, R., Zeineddine, H. A., Lightle, R., Moore, T., Cao, Y., Shenkar, R., Chen, M., Mericko, P., Yang, J., Li, L., Tanes, C., Kobuley, D., Võsa, U., … Kahn, M. L. (2017). Endothelial TLR4 and the microbiome drive cerebral cavernous malformations. *Nature*, *545*(7654), 305–310. https://doi.org/10.1038/nature22075

106. Tirelle, P., Salaün, C., Kauffmann, A., Bôle-Feysot, C., Guérin, C., Huré, M., Goichon, A., Amamou, A., Breton, J., Do Rego, J.-L., Déchelotte, P., Achamrah, N., & Coëffier, M. (2022). Intestinal Epithelial Toll-like Receptor 4 Deficiency Modifies the Response to the Activity-Based Anorexia Model in a Sex-Dependent Manner: A Preliminary Study. *Nutrients*, *14*(17), 3607. https://doi.org/10.3390/nu14173607

107. Trikha, S. R. J., Lee, D. M., Ecton, K. E., Wrigley, S. D., Vazquez, A. R., Litwin, N. S., Thomas, K. N., Wei, Y., Battson, M. L., Johnson, S. A., Kuhn, K. A., Colgan, S. P., Gentile, C. L., & Weir, T. L. (2021). Transplantation of an obesity-associated human gut microbiota to mice induces vascular dysfunction and glucose intolerance. *Gut Microbes*, *13*(1), 1940791. https://doi.org/10.1080/19490976.2021.1940791

108. Villena, J., & Kitazawa, H. (2014). Modulation of Intestinal TLR4-Inflammatory Signaling Pathways by Probiotic Microorganisms: Lessons Learned from Lactobacillus jensenii TL2937. *Frontiers in Immunology*, *4*. https://doi.org/10.3389/fimmu.2013.00512

109. Vlachopoulos, C., Aznaouridis, K., & Stefanadis, C. (2010). Prediction of Cardiovascular Events and All-Cause Mortality With Arterial Stiffness. *Journal of the American College of Cardiology*, *55*(13), 1318–1327. https://doi.org/10.1016/j.jacc.2009.10.061

110. Wang, B., Kong, Q., Li, X., Zhao, J., Zhang, H., Chen, W., & Wang, G. (2020). A High-Fat Diet Increases Gut Microbiota Biodiversity and Energy Expenditure Due to Nutrient Difference. *Nutrients*, *12*(10), 3197. https://doi.org/10.3390/nu12103197

111. Zhang, Z., Amorosa, L. F., Coyle, S. M., Macor, M. A., Birnbaum, M. J., Lee, L. Y., & Haimovich, B. (2016). Insulin-Dependent Regulation of mTORC2-Akt-FoxO Suppresses TLR4 Signaling in Human Leukocytes: Relevance to Type 2 Diabetes. *Diabetes*, *65*(8), 2224–2234. https://doi.org/10.2337/db16-0027

112. Zhang, Z., Amorosa, L. F., Coyle, S. M., Macor, M. A., Lubitz, S. E., Carson, J. L., Birnbaum, M. J., Lee, L. Y., & Haimovich, B. (2015). Proteolytic Cleavage of AMPKα and Intracellular MMP9 Expression Are Both Required for TLR4-Mediated mTORC1 Activation and HIF-1α Expression in Leukocytes. *The Journal of Immunology*, *195*(5), 2452–2460. https://doi.org/10.4049/jimmunol.1500944

113. Zhang, Z., Amorosa, L. F., Petrova, A., Coyle, S., Macor, M., Nair, M., Lee, L. Y., & Haimovich, B. (2019). TLR4 counteracts BVRA signaling in human leukocytes via differential regulation of AMPK, mTORC1 and mTORC2. *Scientific Reports*, *9*(1), 7020. https://doi.org/10.1038/s41598-019-43347-8

114. Weber, E. M., Algers, B., Würbel, H., Hultgren, J., & Olsson, I. A. S. (2013). Influence of strain and parity on the risk of litter loss in laboratory mice. *Reproduction in Domestic Animals*, *48*(2), 292-296.

115. Crawford, S. E., Ramani, S., Tate, J. E., Parashar, U. D., Svensson, L., Hagbom, M., ... & Estes, M. K. (2017). Rotavirus infection. *Nature Reviews Disease Primers*, *3*(1), 1-16.

116. Bolger, A. M., Lohse, M., & Usadel, B. (2014). Trimmomatic: A flexible trimmer for Illumina Sequence Data. *Bioinformatics*, btu170.
117. Quast C, Pruesse E, Yilmaz P, Gerken J, Schweer T, Yarza P, Peplies J, Glöckner FO (2013) The SILVA ribosomal RNA gene database project: improved data processing and web-based tools.
118. Oksanen J, Simpson G, Blanchet F, Kindt R, Legendre P, Minchin P, O'Hara R, Solymos P, Stevens M, Szoecs E, Wagner H, Barbour M, Bedward M, Bolker B, Borcard D, Carvalho G, Chirico M, De Caceres M, Durand S, Evangelista H, FitzJohn R, Friendly M, Furneaux B, Hannigan G, Hill M, Lahti L, McGlinn D, Ouellette M, Ribeiro Cunha E, Smith T, Stier A, Ter Braak C, Weedon J (2022). _vegan: Community Ecology Package_. R package version 2.6-4, <https://CRAN.R-project.org/package=vegan>.
119. Posit team (2024). RStudio: Integrated Development Environment for R. Posit Software, PBC, Boston, MA. URL http://www.posit.co/.
120. Oksanen J, Simpson G, Blanchet F, Kindt R, Legendre P, Minchin P, O'Hara R, Solymos P, Stevens M, Szoecs E, Wagner H, Barbour M, Bedward M, Bolker B, Borcard D, Carvalho G, Chirico M, De Caceres M, Durand S, Evangelista H, FitzJohn R, Friendly M, Furneaux B, Hannigan G, Hill M, Lahti L, McGlinn D, Ouellette M, Ribeiro Cunha E, Smith T, Stier A, Ter Braak C, Weedon J (2022). _vegan: Community Ecology Package_. R package version 2.6-4, <https://CRAN.R-project.org/package=vegan>.
121. H. Wickham. ggplot2: Elegant Graphics for Data Analysis. Springer-Verlag New York, 2016.
122. phyloseq: An R package for reproducible interactive analysis and graphics of microbiome census data. Paul J. McMurdie and Susan Holmes (2013) PLoS ONE 8(4):e61217.
123. Ewels, P., Magnusson, M., Lundin, S., & Käller, M. (2016). MultiQC: Summarize analysis results for multiple tools and samples in a single report. *Bioinformatics*, *32*(19), 3047–3048. https://doi.org/10.1093/bioinformatics/btw354
124. Benjamin Callahan <Benjamin. J.Callahan@Gmail.Com>, P. (2017). *Dada2* [Computer software]. [object Object]. https://doi.org/10.18129/B9.BIOC.DADA2
125. Paulson JN, Stine OC, Bravo HC, Pop M (2013). "Differential abundance analysis for microbial marker-gene surveys." _Nat Meth_, *advance online publication*. doi:10.1038/nmeth.2658 <https://doi.org/10.1038/nmeth.2658>, <http://www.nature.com/nmeth/journal/vaop/ncurrent/abs/nmeth.2658.html>.
126. Summary of WHO Prequalified Rotavirus Vaccines: WHO; 2017 [updated March 2021. Available from: https://iris.who.int/bitstream/handle/10665/344642/WHO-IVB-2021.03-eng.pdf?sequence=]
127. Brosseau, C., Selle, A., Duval, A., Misme-Aucouturier, B., Chesneau, M., Brouard, S., Cherbuy, C., Cariou, V., Bouchaud, G., Mincham, K. T., Strickland, D. H., Barbarot, S., & Bodinier, M. (2021). Prebiotic Supplementation During Pregnancy Modifies the Gut Microbiota and Increases Metabolites in Amniotic Fluid, Driving a Tolerogenic Environment In Utero. *Frontiers in Immunology*, *12*, 712614. https://doi.org/10.3389/fimmu.2021.712614
128. Albrecht, M., & Arck, P. C. (2020). Vertically Transferred Immunity in Neonates: Mothers, Mechanisms and Mediators. *Frontiers in Immunology*, *11*, 555. https://doi.org/10.3389/fimmu.2020.00555
129. Marchant, A., Sadarangani, M., Garand, M., Dauby, N., Verhasselt, V., Pereira, L.,

Bjornson, G., Jones, C. E., Halperin, S. A., Edwards, K. M., Heath, P., Openshaw, P. J., Scheifele, D. W., & Kollmann, T. R. (2017). Maternal immunisation: Collaborating with mother nature. *The Lancet Infectious Diseases*, *17*(7), e197–e208. https://doi.org/10.1016/S1473-3099(17)30229-3

130. Maertens, K., Caboré, R. N., Huygen, K., Hens, N., Van Damme, P., & Leuridan, E. (2016). Pertussis vaccination during pregnancy in Belgium: Results of a prospective controlled cohort study. *Vaccine*, *34*(1), 142–150. https://doi.org/10.1016/j.vaccine.2015.10.100
131. Pou, C., Nkulikiyimfura, D., Henckel, E., Olin, A., Lakshmikanth, T., Mikes, J., Wang, J., Chen, Y., Bernhardsson, A. K., Gustafsson, A., Bohlin, K., & Brodin, P. (2019). The repertoire of maternal anti-viral antibodies in human newborns. *Nature Medicine*, *25*(4), 591–596. https://doi.org/10.1038/s41591-019-0392-8
132. Cetin Coban, S., Temel, F., Duman, P., Cosgun, Y., Ozarslan, F., Kayman, T., Guven, S., Bezirganoglu, H., Gunes, O., Yilmaz Ciftdogan, D., Karadagli, E. E., Kaya, C., & Kara, A. (2019). Prevalence of Protective Measles Virus Antibody Levels in Umbilical Cord Blood Samples and Sera of Mothers and Transplacental Transport Ratio in Turkey. *Japanese Journal of Infectious Diseases*, *72*(3), 185–192. https://doi.org/10.7883/yoken.JJID.2018.387
133. White et al 2012
134. Hassiotou, F., Hepworth, A. R., Metzger, P., Tat Lai, C., Trengove, N., Hartmann, P. E., & Filgueira, L. (2013). Maternal and infant infections stimulate a rapid leukocyte response in breastmilk. *Clinical & Translational Immunology*, *2*(4), e3. https://doi.org/10.1038/cti.2013.1
135. Vidal, K., Labéta, M. O., Schiffrin, E. J., & Donnet-Hughes, A. (2001). Soluble CD14 in human breast milk and its role in innate immune responses. *Acta Odontologica Scandinavica*, *59*(5), 330–334. https://doi.org/10.1080/000163501750541219
136. Lamberti, L. M., Fischer Walker, C. L., Noiman, A., Victora, C., & Black, R. E. (2011). Breastfeeding and the risk for diarrhea morbidity and mortality. *BMC Public Health*, *11*(S3), S15. https://doi.org/10.1186/1471-2458-11-S3-S15
137. Maruyama, K., Hida, M., Kohgo, T., & Fukunaga, Y. (2009). Changes in salivary and fecal secretory IgA in infants under different feeding regimens. *Pediatrics International*, *51*(3), 342–345. https://doi.org/10.1111/j.1442-200X.2008.02748.x
138. Patel, M., Glass, R. I., Jiang, B., Santosham, M., Lopman, B., & Parashar, U. (2013). A Systematic Review of Anti-Rotavirus Serum IgA Antibody Titer as a Potential Correlate of Rotavirus Vaccine Efficacy. *The Journal of Infectious Diseases*, *208*(2), 284–294. https://doi.org/10.1093/infdis/jit166
139. Caballero-Flores, G., Sakamoto, K., Zeng, M. Y., Wang, Y., Hakim, J., Matus-Acuña, V., Inohara, N., & Núñez, G. (2019). Maternal Immunization Confers Protection to the Offspring against an Attaching and Effacing Pathogen through Delivery of IgG in Breast Milk. *Cell Host & Microbe*, *25*(2), 313-323.e4. https://doi.org/10.1016/j.chom.2018.12.015
140. Jones, C., Pollock, L., Barnett, S. M., Battersby, A., & Kampmann, B. (2014). The relationship between concentration of specific antibody at birth and subsequent response to primary immunization. *Vaccine*, *32*(8), 996–1002. https://doi.org/10.1016/j.vaccine.2013.11.104
141. Karlsson, M. C. I., Getahun, A., & Heyman, B. (2001). FcγRIIB in IgG-Mediated Suppression of Antibody Responses: Different Impact In Vivo and In Vitro. *The Journal of Immunology*, *167*(10), 5558–5564. https://doi.org/10.4049/jimmunol.167.10.5558
142. Georges-Courbot, M. C., Monges, J., Siopathis, M. R., Roungou, J. B., Gresenguet, G.,

Belec, L., Bouquety, J. C., Lanckriet, C., Cadoz, M., Hessel, L., Gouvea, V., Clark, F., & Georges, A. J. (1991). Evaluation of the efficacy of a low-passage bovine rotavirus (strain WC3) vaccine in children in Central Africa. *Research in Virology*, *142*(5), 405–411. https://doi.org/10.1016/0923-2516(91)90008-Q

143. Chilengi, R., Simuyandi, M., Beach, L., Mwila, K., Becker-Dreps, S., Emperador, D. M., Velasquez, D. E., Bosomprah, S., & Jiang, B. (2016). Association of Maternal Immunity with Rotavirus Vaccine Immunogenicity in Zambian Infants. *PLOS ONE*, *11*(3), e0150100. https://doi.org/10.1371/journal.pone.0150100
144. Moon, S.-S., Groome, M. J., Velasquez, D. E., Parashar, U. D., Jones, S., Koen, A., Van Niekerk, N., Jiang, B., & Madhi, S. A. (2016). Prevaccination Rotavirus Serum IgG and IgA Are Associated With Lower Immunogenicity of Live, Oral Human Rotavirus Vaccine in South African Infants. *Clinical Infectious Diseases*, *62*(2), 157–165. https://doi.org/10.1093/cid/civ828
145. Yang, H., Luo, G., Zeng, Y., Li, Y., Yu, S., Zhao, B., An, R., Zhang, S., Wang, Y., Li, T., Ge, S., & Xia, N. (2019). The distinct impact of maternal antibodies on the immunogenicity of live and recombinant rotavirus vaccines. *Vaccine*, *37*(30), 4061–4067. https://doi.org/10.1016/j.vaccine.2019.05.086
146. Lozupone, C. A., Stombaugh, J. I., Gordon, J. I., Jansson, J. K., & Knight, R. (2012). Diversity, stability and resilience of the human gut microbiota. *Nature*, *489*(7415), 220–230. https://doi.org/10.1038/nature11550
147. Arboleya, S., Sánchez, B., Milani, C., Duranti, S., Solís, G., Fernández, N., De Los Reyes-Gavilán, C. G., Ventura, M., Margolles, A., & Gueimonde, M. (2015). Intestinal Microbiota Development in Preterm Neonates and Effect of Perinatal Antibiotics. *The Journal of Pediatrics*, *166*(3), 538–544. https://doi.org/10.1016/j.jpeds.2014.09.041
148. Tormo-Badia, N., Håkansson, Å., Vasudevan, K., Molin, G., Ahrné, S., & Cilio, C. M. (2014). Antibiotic Treatment of Pregnant Non-Obese Diabetic Mice Leads to Altered Gut Microbiota and Intestinal Immunological Changes in the Offspring. *Scandinavian Journal of Immunology*, *80*(4), 250–260. https://doi.org/10.1111/sji.12205
149. Sahl, J. W., Matalka, M. N., & Rasko, D. A. (2012). Phylomark, a Tool To Identify Conserved Phylogenetic Markers from Whole-Genome Alignments. *Applied and Environmental Microbiology*, *78*(14), 4884–4892. https://doi.org/10.1128/AEM.00929-12
150. Ward, R. E., Ninonuevo, M., Mills, D. A., Lebrilla, C. B., & German, J. B. (2006). In vitro fermentation of breast milk oligosaccharides by Bifidobacterium infantis and Lactobacillus gasseri. *Applied and environmental microbiology*, *72*(6), 4497-4499.Sela, D. A., & Mills, D. A. (2010). Nursing our microbiota: Molecular linkages between bifidobacteria and milk oligosaccharides. *Trends in Microbiology*, *18*(7), 298–307. https://doi.org/10.1016/j.tim.2010.03.008
151. Yu, Z.-T., Chen, C., Kling, D. E., Liu, B., McCoy, J. M., Merighi, M., Heidtman, M., & Newburg, D. S. (2013). The principal fucosylated oligosaccharides of human milk exhibit prebiotic properties on cultured infant microbiota. *Glycobiology*, *23*(2), 169–177. https://doi.org/10.1093/glycob/cws138
152. Li, M., Monaco, M. H., Wang, M., Comstock, S. S., Kuhlenschmidt, T. B., Fahey Jr, G. C., Miller, M. J., Kuhlenschmidt, M. S., & Donovan, S. M. (2014). Human milk oligosaccharides shorten rotavirus-induced diarrhea and modulate piglet mucosal immunity and colonic microbiota. *The ISME Journal*, *8*(8), 1609–1620. https://doi.org/10.1038/ismej.2014.10

153. Humphrey, J. H. (2009). Child undernutrition, tropical enteropathy, toilets, and handwashing. *The Lancet*, *374*(9694), 1032–1035. https://doi.org/10.1016/S0140-6736(09)60950-8
154. Guerrant, R. L., Oriá, R. B., Moore, S. R., Oriá, M. O., & Lima, A. A. (2008). Malnutrition as an enteric infectious disease with long-term effects on child development: Nutrition Reviews©, Vol. 66, No. 9. *Nutrition Reviews*, *66*(9), 487–505. https://doi.org/10.1111/j.1753-4887.2008.00082.x
155. Korpe, P. S., Liu, Y., Siddique, A., Kabir, M., Ralston, K., Ma, J. Z., Haque, R., & Petri, W. A. (2013). Breast Milk Parasite-Specific Antibodies and Protection From Amebiasis and Cryptosporidiosis in Bangladeshi Infants: A Prospective Cohort Study. *Clinical Infectious Diseases*, *56*(7), 988–992. https://doi.org/10.1093/cid/cis1044
156. Heikkila, M. P., & Saris, P. E. J. (2003). Inhibition of Staphylococcus aureus by the commensal bacteria of human milk. *Journal of Applied Microbiology*, *95*(3), 471–478. https://doi.org/10.1046/j.1365-2672.2003.02002.x
157. Jost, T., Lacroix, C., Braegger, C. P., Rochat, F., & Chassard, C. (2014). Vertical mother–neonate transfer of maternal gut bacteria via breastfeeding. *Environmental Microbiology*, *16*(9), 2891–2904. https://doi.org/10.1111/1462-2920.12238
158. Jost, T., Lacroix, C., Braegger, C., & Chassard, C. (2013). Assessment of bacterial diversity in breast milk using culture-dependent and culture-independent approaches. *British Journal of Nutrition*, *110*(7), 1253–1262. https://doi.org/10.1017/S0007114513000597
159. Martín, V., Maldonado-Barragán, A., Moles, L., Rodriguez-Baños, M., Campo, R. D., Fernández, L., Rodríguez, J. M., & Jiménez, E. (2012). Sharing of Bacterial Strains Between Breast Milk and Infant Feces. *Journal of Human Lactation*, *28*(1), 36–44. https://doi.org/10.1177/0890334411424729
160. aLawley, T. D., & Walker, A. W. (2013). Intestinal colonization resistance. *Immunology*, *138*(1), 1-11.

APPENDIX

Supplemental Table 0.1 **Fecal Antigen ELISA Buffers**

Botto	*5%*	*Carnation skim milk in 1xPBS + 1% Kathon*
	1%	*1:5 dilution of blotto*
CBC Coating buffer	*1L ultrapure water*	*Adjust pH to 9.6*
	0.015mol/L NaCO2	
	0.035mol/L NaHCO3	

Supplemental Table 0.2 **Sample Collection & Processing Buffers**

Wash/Culture Media (CTL Media)	*ACK lysing buffer*	*Collection & Processing Media*
405mL Gibco RMPI-1640 wihtout L-glutamine	0.15mol/L NH_4Cl	490mL RPMI 1640 w/o L-glutamine, GIBCO
2% L-glutamine (Gibco)	0. 001mol/L $KHCO_3$	1% HEPES
1% HEPES	0. 0001mol/L Na_2EDTA	1% Pen/Strep
1% Pen/Strep	Add to 800 ml H_2O and adjust pH to 7.2	0.1% Gentamicin (10mg/mL, Gibco 15700-064)
50mL Fetal Bovine Serum		
0.1% 2-ME		
1% 1N NaOH		
1% Sodium Pyruvate		
1% MEM Non-essential amino acids		
2% MEM essential amino acids		

Supplemental Table 0.3 Pilot study *Lactobacillus acidophilus* strains

Strain Name	Strain contents	Dose delivered (per 50µL)
6NCK56	Wild type *Lactobacillus acidophilus*	$1x10^6$ CFU
9NCK56	Wild type *Lactobacillus acidophilus*	$1x10^9$ CFU
6GAD85	VP8-1, VP8Pep, FliC, FimH	$1x10^6$ CFU
9GAD85	VP8-1, VP8Pep, FliC, FimH	$1x10^9$ CFU

Supplemental Table 0.4 **Split plot randomization for breeding: Expanded Dose Neonatal Vaccination Study**

Sire	Treatment	Neonatal Dose	Doe	Breeding Round
	STI	$1x10^6$ CFU	D1	1
	9NCK56	$1x10^9$ CFU	D2	1
	9GAD85	$1x10^9$ CFU	D7	2
S1	6NCK56	$1x10^6$ CFU	D8	2
	6NCK56	$1x10^6$ CFU	D3	1
	9GAD85	$1x10^9$ CFU	D4	1
	STI	$1x10^9$ CFU	D9	2
S2	6GAD85	$1x10^6$ CFU	D10	2
	6GAD85	$1x10^6$ CFU	D5	1
	None	none	D6	1
S3	9NCK56	$1x10^9$ CFU	D11	2

Supplemental Table 0.5 **Maternal Antibody Influence Neonatal Vaccination & Challenge Study breeding randomization***indicates that doe was rebreed and successfully produce additional litters **indicates that doe was rebreed and did not successfully produce any litter

Sire	Treatment	Maternal Infection	Doe	Breeding Round
S1	GAD 85	N	UD17	1
	NCK56	N	UD25*	1
	GAD84	Y	RD7*	2
	STI	Y	RD15	2
S2	GAD84	N	UD21	1
	STI	N	UD29*	1
	GAD 85	Y	RD3*	2
	NCK56	Y	RD11	2
S3	GAD 85	N	UD18	1
	STI	N	UD30	1
	GAD84	Y	RD8**	2
	NCK56	Y	RD12**	2
S4	GAD84	N	UD22	1
	NCK56	N	UD26	1
	GAD 85	Y	RD4*	2
	STI	Y	RD16**	2
S5	GAD 85	Y	RD1	1
	NCK56	Y	RD9*	1
S6	GAD84	Y	RD5	1
	STI	Y	RD13*	1
S7	GAD 85	Y	RD2	1
	GAD84	Y	RD6	1
S8	NCK56	Y	RD10	1
	STI	Y	RD14	1
S9	GAD 85	N	UD19	2
	STI	N	UD31	2
S10	GAD 85	N	UD20	2
	GAD84	N	UD23	2
S11	GAD84	N	UD24	2
	NCK56	N	UD27	2
S12	NCK56	N	UD28	2
	STI	N	UD32	2

Chapter 3 Supplemental Tables & Figures:

Supplemental Table 0.6 ANOVA Table for the comparison between neonates within timepoint and treatment levels for Maternal Antibody Study, * represents significance at p<0.05 level of significance, ** represents significance at p<0.01, *** represents significance at p<0.001.

Response: Doe Fecal Shedding					
	Df	Sum Sq	Mean Sq	F value	Pr(>F)
Doe Infection	1	0.00617	0.006168	0.3579	0.5509
Days Post Infection (dpi)	7	0.27159	0.038798	2.2515	0.0352
*Doe Infection * dpi*	7	0.07723	0.011033	0.6403	0.7217
Residuals	111	1.91279	0.017232		
Response: Doe Rotavirus IgG Serum Titer					
	Df	Sum Sq	Mean Sq	F value	Pr(>F)
Doe Infection	1	0.16820	0.0168200	16.4071	0.0001247***
Days Post Infection (dpi)	2	0.031867	0.0159337	15.5426	2.315e-6***
*Doe Infection * dpi*	2	0.017805	0.0089025	8.6839	0.0004095***
Residuals	74	0.075863	0.0010252		

Supplemental Table 0.7 ANOVA Table for the comparison between neonates within timepoint and treatment levels for Maternal Antibody Study, * represents significance at p<0.05 level of significance, ** represents significance at p<0.01, *** represents significance at p<0.001.

Response: Fecal Shedding					
	Df	Sum Sq	Mean Sq	F value	Pr(>F)
Timepoint	6	5.2496	0.87493	6.9051	8.969e-7***

Treatment	4	0.5544	0.13860	1.0939	0.3602
*Treatment*Timepoint*	18	2.1917	0.12176	0.9610	0.5059
Residuals	237	30.0296	0.12671		

Supplemental Table 0.8 ANOVA Table for the comparison between maternal infection and neonatal challenge for VP8-1 IgM spleen in Maternal Antibody Study, * represents significance at p<0.05 level of significance, ** represents significance at p<0.01, *** represents significance at p<0.001.

VP8-1 Spleen ELISA					
Response: VP81 IgM					
	Df	Sum Sq	Mean Sq	F value	Pr(>F)
Maternal Infection	1	3.172	3.1723	5.7126	**0.0183***
Neonatal Challenge	1	0.4591	0.8267	0.3649	0.28740
*Maternal Infection * Neonatal Challenge*	1	0.122	0.1223	0.2202	0.6397
Residuals	128	71.081	0.5553		
Response: VP81 IgM					
	Df	Sum Sq	Mean Sq	F value	Pr(>F)
Maternal Infection	1	3.172	3.1723	6.1144	0.01476
Treatment	3	1.978	0.6593	1.2709	0.28740

*Maternal Infection * Treatment*	3	5.350	1.7833	3.4371	**0.01904***
Residuals	124	64.335	0.5188		
Response: VP81 IgM					
	Df	Sum Sq	Mean Sq	F value	Pr(>F)
Treatment	3	2.169	0.72290	1.3191	0.27123
Neonatal Challenge	1	0.248	0.24769	0.4520	0.50265
*Treatment * Neonatal Challenge*	3	4.462	1.48741	2.7141	**0.04775***
Residuals	124	67.956	0.54803		

Supplemental Table 0.9 ANOVA Table for the comparison between maternal infection and neonatal challenge for VP8-1 IgG spleen in Maternal Antibody Study, * represents significance at p<0.05 level of significance, ** represents significance at p<0.01, *** represents significance at p<0.001.

VP8-1 Spleen ELISA					
Response: VP81 IgG					
	Df	Sum Sq	Mean Sq	F value	Pr(>F)
Maternal Infection	1	0.0003852	0.00038518	4.3159	**0.03976***
Neonatal Challenge	1	0.0001983	0.00019834	2.2224	0.13848
*Maternal Infection * Neonatal Challenge*	1	0.0000680	0.00006796	0.7615	0.38451
Residuals	128	0.0114235	0.00008925		
Response: VP81 IgG					
	Df	Sum Sq	Mean Sq	F value	Pr(>F)
Maternal Infection	1	0.0004118	0.00041177	4.7622	**0.03098***
Treatment	3	0.0003045	0.00010151	1.1740	0.32247
*Maternal Infection * Treatment*	3	0.0006369	0.00021231	2.4554	0.06625
Residuals	124	0.0107218	0.00008647		
Response: VP81 IgG					
	Df	Sum Sq	Mean Sq	F value	Pr(>F)
Treatment	3	0.0003984	1.3280E-4	1.4653	0.2273

Neonatal Challenge	1	0.0001983	1.9834E-4	2.1885	0.1416
*Treatment * Neonatal Challenge*	3	0.0002404	8.0118E-5	0.8840	0.4514
Residuals	124	0.0112379	9.0628E-5		

Supplemental Table 0.10 ANOVA Table for the comparison between maternal infection and neonatal challenge for total IgG MLN in Maternal Antibody Study, * represents significance at p<0.05 level of significance, ** represents significance at p<0.01, *** represents significance at p<0.001.

Total MLN ELISA					
Response: Total IgG					
	Df	Sum Sq	Mean Sq	F value	Pr(>F)
Maternal Infection	1	61800	61800	2.2042	0.1401
Neonatal Challenge	2	5450	2725	0.0972	0.9075
*Maternal Infection * Neonatal Challenge*	2	15321	7660	0.2732	0.7614
Residuals	127	3560782	28038		
Response: Total IgG					
	Df	Sum Sq	Mean Sq	F value	Pr(>F)
Maternal Infection	1	63276	63276	2.3676	0.1264
Treatment	3	106216	35045	1.3248	0.2693
*Maternal Infection * Treatment*	3	133164	44388	1.6609	0.1789

Residuals	125	3340696	26726		
Response: Total IgG					
	Df	Sum Sq	Mean Sq	F value	Pr(>F)
Treatment	3	106724	35575	1.3029	0.2766
Neonatal Challenge	2	5450	2725	0.0998	0.9051
*Treatment * Neonatal Challenge*	4	172724	43181	1.5815	0.1834
Residuals	123	3358455	27305		

Supplemental Table 0.11 ANOVA Table for the comparison between maternal infection and neonatal challenge for Total IgM MLN in Maternal Antibody Study, * represents significance at p<0.05 level of significance, ** represents significance at p<0.01, *** represents significance at p<0.001.

Total MLN ELISA					
Response: Total IgM					
	Df	Sum Sq	Mean Sq	F value	Pr(>F)
Maternal Infection	1	107	107	0.0002	0.99011
Neonatal Challenge	2	3293392	1646696	2.3719	0.09739
*Maternal Infection * Neonatal Challenge*	2	3689084	1844542	2.6569	0.07404
Residuals	128	88865143	694259		
Response: Total IgM					
	Df	Sum Sq	Mean Sq	F value	Pr(>F)
Maternal Infection	1	44	44	0.0001	0.99373
Treatment	3	1535199	511733	0.7236	0.53971
*Maternal Infection * Treatment*	3	5204182	1734727	2.4529	0.06638
Residuals	126	89108302	707209		
Response: Total IgM					
	Df	Sum Sq	Mean Sq	F value	Pr(>F)
Treatment	3	1327740	442580	0.6226	0.6017
Neonatal Challenge	2	3293392	1646696	2.3166	0.1029
*Treatment * Neonatal Challenge*	4	3086103	771526	1.0854	0.3667

Residuals	124	88140492	710810		

Supplemental Table 0.12 ANOVA Table for the comparison between maternal infection and neonatal challenge for VP8-1 IgG MLN in Maternal Antibody Study, * represents significance at p<0.05 level of significance, ** represents significance at p<0.01, *** represents significance at p<0.001.

VP8-1 MLN ELISA					
Response: VP81 IgG					
	Df	Sum Sq	Mean Sq	F value	Pr(>F)
Maternal Infection	1	0.0003852	0.00038518	4.3159	**0.03976***
Neonatal Challenge	1	0.0001983	0.00019834	2.2224	0.13848
*Maternal Infection * Neonatal Challenge*	1	0.0000680	0.00006796	0.7615	0.38451
Residuals	128	0.0114235	0.00008925		
Response: VP81 IgG					
	Df	Sum Sq	Mean Sq	F value	Pr(>F)
Maternal Infection	1	0.0003239	0.00032386	1.4711	0.2274
Treatment	3	0.0005770	0.00019234	0.8736	0.4567
*Maternal Infection * Treatment*	3	0.0011914	0.0039712	1.8038	0.1498
Residuals	127	0.0279597	0.00022016		
Response: VP81 IgG					
	Df	Sum Sq	Mean Sq	F value	Pr(>F)
Treatment	3	0.0004924	0.00016413	0.7305	0.5356
Neonatal Challenge	1	0.0000132	0.00001325	0.0590	0.8085
*Treatment * Neonatal Challenge*	3	0.0010132	0.00033775	1.5033	0.2169
Residuals	127	0.0285330	0.00022467		

Supplemental Table 0.13 ANOVA Table for the comparison between maternal infection and neonatal challenge for spleen in Maternal Antibody Study, * represents significance at p<0.05 level of significance, ** represents significance at p<0.01, *** represents significance at p<0.001.

VP8-1 Spleen Spot Intensity					
Response: VP81 IgM					
	Df	Sum Sq	Mean Sq	F value	Pr(>F)
Maternal Infection	1	0.09841	0.098412	3.9393	**0.04983***
Neonatal Challenge	1	0.10066	0.100661	4.0293	**0.04689***
*Maternal Infection * Neonatal Challenge*	1	0.01735	0.017355	0.6947	0.40618
Residuals	124	3.09781	0.024982		
Response: VP81 IgG					
	Df	Sum Sq	Mean Sq	F value	Pr(>F)
Maternal Infection	1	0.000317	0.003172	0.5413	0.4635313
Neonatal Challenge	1	0.007150	0.0071495	12.1982	**0.0006989*****
*Maternal Infection * Neonatal Challenge*	1	0.000483	0.0004831	0.8242	0.3660233
Residuals	106	0.062128	0.0005861		
Response: VP81 IgA					
	Df	Sum Sq	Mean Sq	F value	Pr(>F)
Maternal Infection	2	0.0003101	0.00015503	0.9243	0.4001
Neonatal Challenge	1	0.0000056	0.00000562	0.0335	0.8551
*Maternal Infection * Neonatal Challenge*	1	0.0003794	0.00037937	2.2618	0.1357
Residuals	103	0.0172761	0.00016773		

Supplemental Table 0.14 ANOVA Table for the comparison between maternal infection and neonatal challenge for MLN in Maternal Antibody Study, * represents significance at p<0.05 level of significance, ** represents significance at p<0.01, *** represents significance at p<0.001.

VP8-1 MLN Spot Intensity					
Response: VP81 IgM					
	Df	Sum Sq	Mean Sq	F value	Pr(>F)
Maternal Infection	1	0.00020	0.000205	0.0185	0.89213
Neonatal Challenge	1	0.01500	0.014999	1.3524	0.24710
*Maternal Infection * Neonatal Challenge*	1	0.04837	0.048367	4.3609	**0.03882***
Residuals	124	1.37528	0.011091		
Response: VP81 IgG					
	Df	Sum Sq	Mean Sq	F value	Pr(>F)
Maternal Infection	1	0.0000579	0.00005790	0.3951	0.530980
Neonatal Challenge	1	0.0016053	0.00160527	10.9547	**0.001277****
*Maternal Infection * Neonatal Challenge*	1	0.0000878	0.00008780	0.5991	0.440630
Residuals	106	0.0155330	0.0014654		
Response: VP81 IgA					
	Df	Sum Sq	Mean Sq	F value	Pr(>F)
Maternal Infection	2	0.0000524	2.6206e-5	0.3768	0.6870
Neonatal Challenge	1	0.0000465	4.6485e-5	0.6684	0.4155
*Maternal Infection * Neonatal Challenge*	1	0.0001564	1.5644e-4	2.2497	0.1367
Residuals	103	0.0071628	6.9542e-5		

Supplemental Table 0.15 ANOVA Table for the comparison between maternal infection and neonatal challenge for Peyer's patches in Maternal Antibody Study, * represents significance at p<0.05 level of significance, ** represents significance at p<0.01, *** represents significance at p<0.001.

VP8-1 Peyer's patches Spot Intensity					
Response: VP81 IgM					
	Df	Sum Sq	Mean Sq	F value	Pr(>F)
Maternal Infection	1	0.10849	0.108486	8.6799	**0.003844****
Neonatal Challenge	1	0.05837	0.058373	4.6704	**0.032609***
*Maternal Infection * Neonatal Challenge*	1	0.01567	0.015668	1.2535	0.265040
Residuals	124	1.54982	0.012499		
Response: VP81 IgG					
	Df	Sum Sq	Mean Sq	F value	Pr(>F)
Maternal Infection	1	0.000094	0.0000944	0.1559	0.693776
Neonatal Challenge	1	0.005497	0.0054969	9.0727	**0.003245****
*Maternal Infection * Neonatal Challenge*	1	0.000158	0.0001577	0.2602	0.611016
Residuals	106	0.064223	0.0006059		
Response: VP81 IgA					
	Df	Sum Sq	Mean Sq	F value	Pr(>F)
Maternal Infection	2	0.0013691	0.00068453	4.9490	**0.008867****
Neonatal Challenge	1	0.0000007	0.00000068	0.0049	0.944107
*Maternal Infection * Neonatal Challenge*	1	0.0003473	0.00034735	2.5112	0.116103
Residuals	103	0.142466	0.00013832		

Supplemental Table 0.16 ANOVA Table for the comparison between maternal infection and neonatal challenge for total IgA MLN in Maternal Antibody Study, * represents significance at p<0.05 level of significance, ** represents significance at p<0.01, *** represents significance at p<0.001.

Total MLN ELISA					
Response: Total IgA					
	Df	Sum Sq	Mean Sq	F value	Pr(>F)
Maternal Infection	1	0	0.1	0.003	0.9871
Neonatal Challenge	2	23451	11725.6	32.9453	**2.764e-12*** **
*Maternal Infection * Neonatal Challenge*	2	323	161.6	0.4539	0.6361
Residuals	129	45912	355.9		
Response: Total IgA					
	Df	Sum Sq	Mean Sq	F value	Pr(>F)
Maternal Infection	1	2	1.89	0.0039	0.95005
Treatment	3	4658	1552.53	3.2450	**0.02424***
*Maternal Infection * Treatment*	3	4266	1422.11	2.9724	**0.03430***
Residuals	127	60761	478.43		
Response: Total IgA					
	Df	Sum Sq	Mean Sq	F value	Pr(>F)
Treatment	3	2394	798.0	2.4618	0.06568
Neonatal Challenge	2	23451	11725.6	36.1728	**4.029e-13*** **
*Treatment * Neonatal Challenge*	4	3322	830.6	2.5622	**0.04165***
Residuals	125	40519	324.2		

Supplemental Table 0.17 ANOVA Table for the comparison between maternal infection and neonatal challenge for total IgG spleen in Maternal Antibody Study, * represents significance at p<0.05 level of significance, ** represents significance at p<0.01, *** represents significance at p<0.001.

Total Spleen ELISA					
Response: Total IgG					
	Df	Sum Sq	Mean Sq	F value	Pr(>F)
Maternal Infection	1	1431123	1431123	4.7277	**0.03152***
Neonatal Challenge	1	514089	514089	1.6983	0.19485
*Maternal Infection * Neonatal Challenge*	1	392075	392075	1.2952	0.25721
Residuals	128	38746528	302707		
Response: Total IgG					
	Df	Sum Sq	Mean Sq	F value	Pr(>F)
Maternal Infection	1	1512826	1512826	5.3683	**0.02215***
Treatment	3	1566362	522121	1.8527	0.14111
*Maternal Infection * Treatment*	3	3060237	1020079	3.6197	**0.01509***
Residuals	124	34944390	281810		
Response: Total IgG					
	Df	Sum Sq	Mean Sq	F value	Pr(>F)
Treatment	3	1732393	577464	1.9698	0.12196
Neonatal Challenge	1	514089	514089	1.7537	0.18785
*Treatment * Neonatal Challenge*	3	2486526	828842	2.8273	**0.04135***
Residuals	124	36350807	293152		

Supplemental Table 0.18 ANOVA Table for the comparison between maternal infection and neonatal challenge for total IgA MLN cell supernatant in Maternal Antibody Study, * represents significance at p<0.05 level of significance, ** represents significance at p<0.01, *** represents significance at p<0.001.

Total MLN ELISA					
Response: Total IgA					
	Df	Sum Sq	Mean Sq	F value	Pr(>F)
Maternal Infection	1	0	0.1	0.003	0.9871
Neonatal Challenge	2	23451	11725.6	32.9453	**2.764e-12*** **
*Maternal Infection * Neonatal Challenge*	2	323	161.6	0.4539	0.6361
Residuals	129	45912	355.9		
Response: Total IgA					
	Df	Sum Sq	Mean Sq	F value	Pr(>F)
Maternal Infection	1	2	1.89	0.0039	0.95005
Treatment	3	4658	1552.53	3.2450	**0.02424***
*Maternal Infection * Treatment*	3	4266	1422.11	2.9724	**0.03430***
Residuals	127	60761	478.43		
Response: Total IgA					
	Df	Sum Sq	Mean Sq	F value	Pr(>F)
Treatment	3	2394	798.0	2.4618	0.06568
Neonatal Challenge	2	23451	11725.6	36.1728	**4.029e-13*** **
*Treatment * Neonatal Challenge*	4	3322	830.6	2.5622	**0.04165***
Residuals	125	40519	324.2		

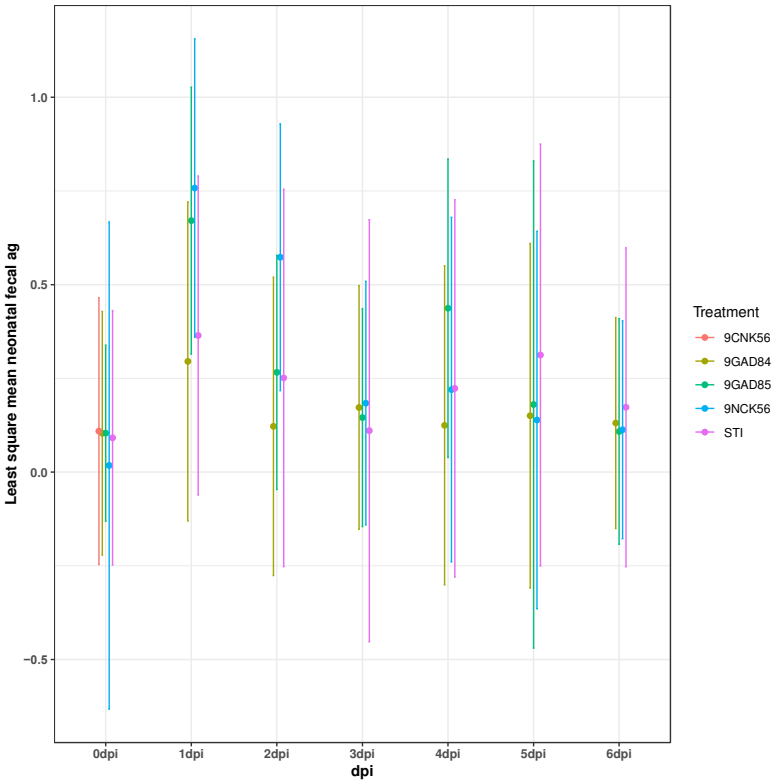

Supplemental Figure 0.1 Neonatal fecal antigen shedding was not significantly different between treatment groups over the six days after rotavirus challenge.

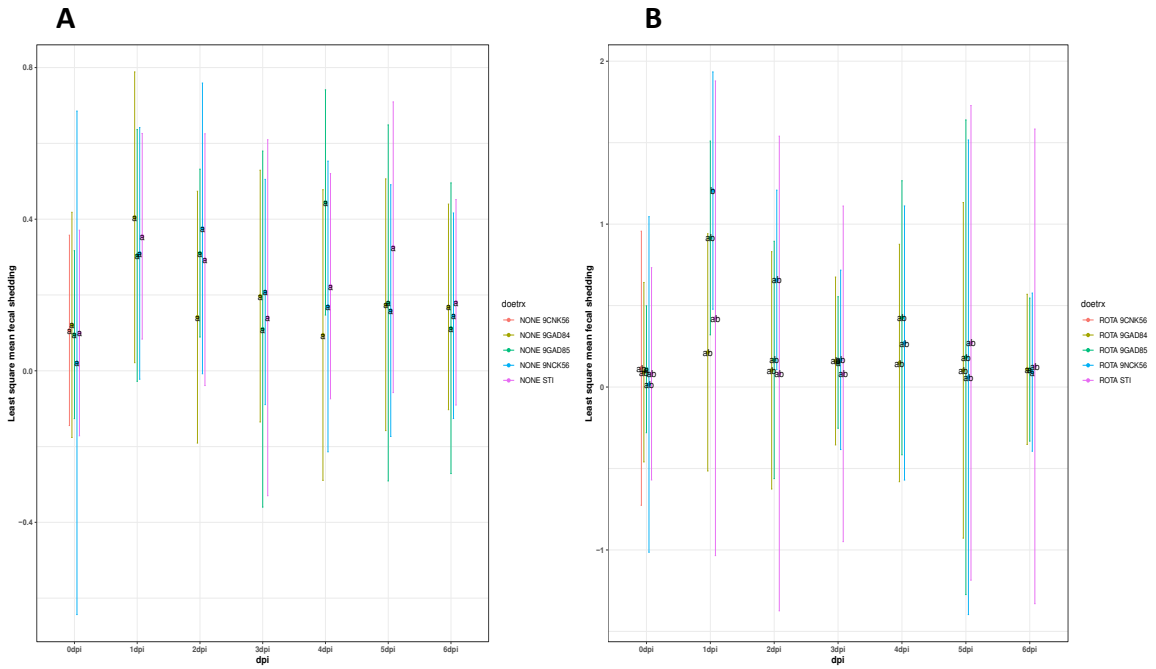

Supplemental Figure 0.2 A-B. Neonatal fecal antigen shedding was not significantly different between treatment groups born to uninfected does (A), NCK56 was the treatment group responsible for the significant fecal shedding in neonates born to rotavirus infected does (B) over the six days after rotavirus challenge.

Supplemental Figure 0.3 Sequencing depth for samples included in Pilot Neonate Vaccination Study analysis (2.2.13.1). Samples included neonates at early timepoints (ie. 10 days of age) and older timepoint after treatments (16 days of age) in addition to doe samples before and after fecal microbiome transplant.

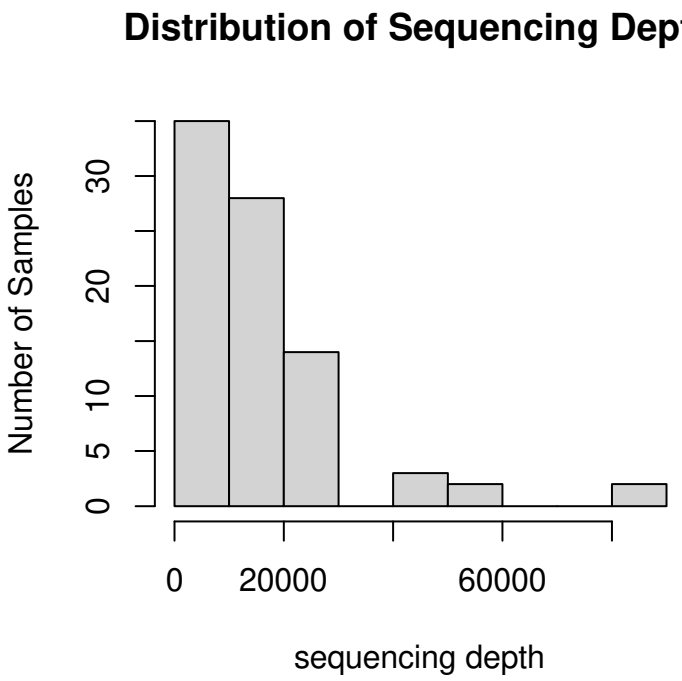

Supplemental Figure 0.4 Sequencing depth of samples included in Expanded Dose Neonate Vaccination Study (2.2.13.2). Samples included neonatal samples that received different doses of treatments including the no dose control (None), the buffer control (STI), the wildtype controls (6NCK56, 9NCK56) and the vaccine (6GAD85, 9GAD85). Doe samples from before the fecal microbiome transplant were included in this analyses.

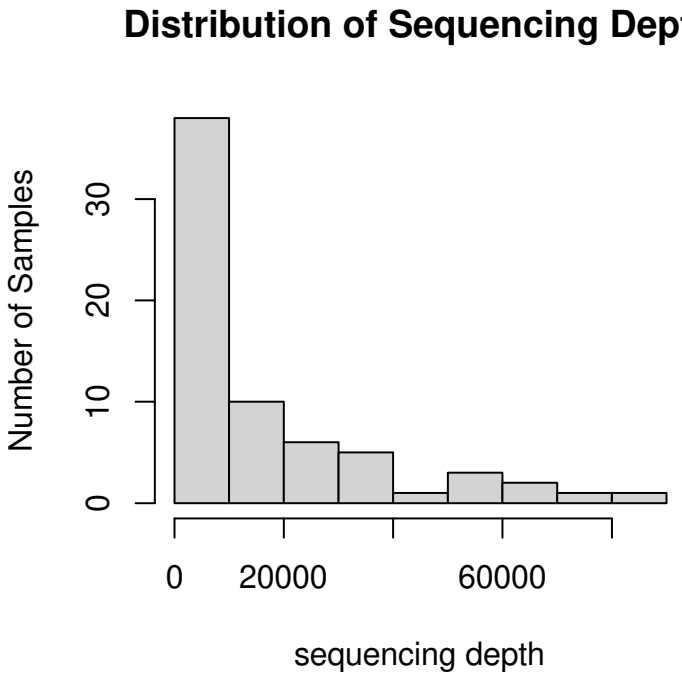

Supplemental Figure 0.5 Seuqnecing depth of samples included in Pilot Neonate Vaccination and Challenge Study (2.2.13.3). Samples included neoantal timepoints prior to the rotavirus challenge (21 days of age) and each day following for six days of the rotavirus challenge (22-27 days of age) to determine how rotaivrus challenge to varying treatments (STI, NCK56, GAD85) modified the gut microbiome in neonates.

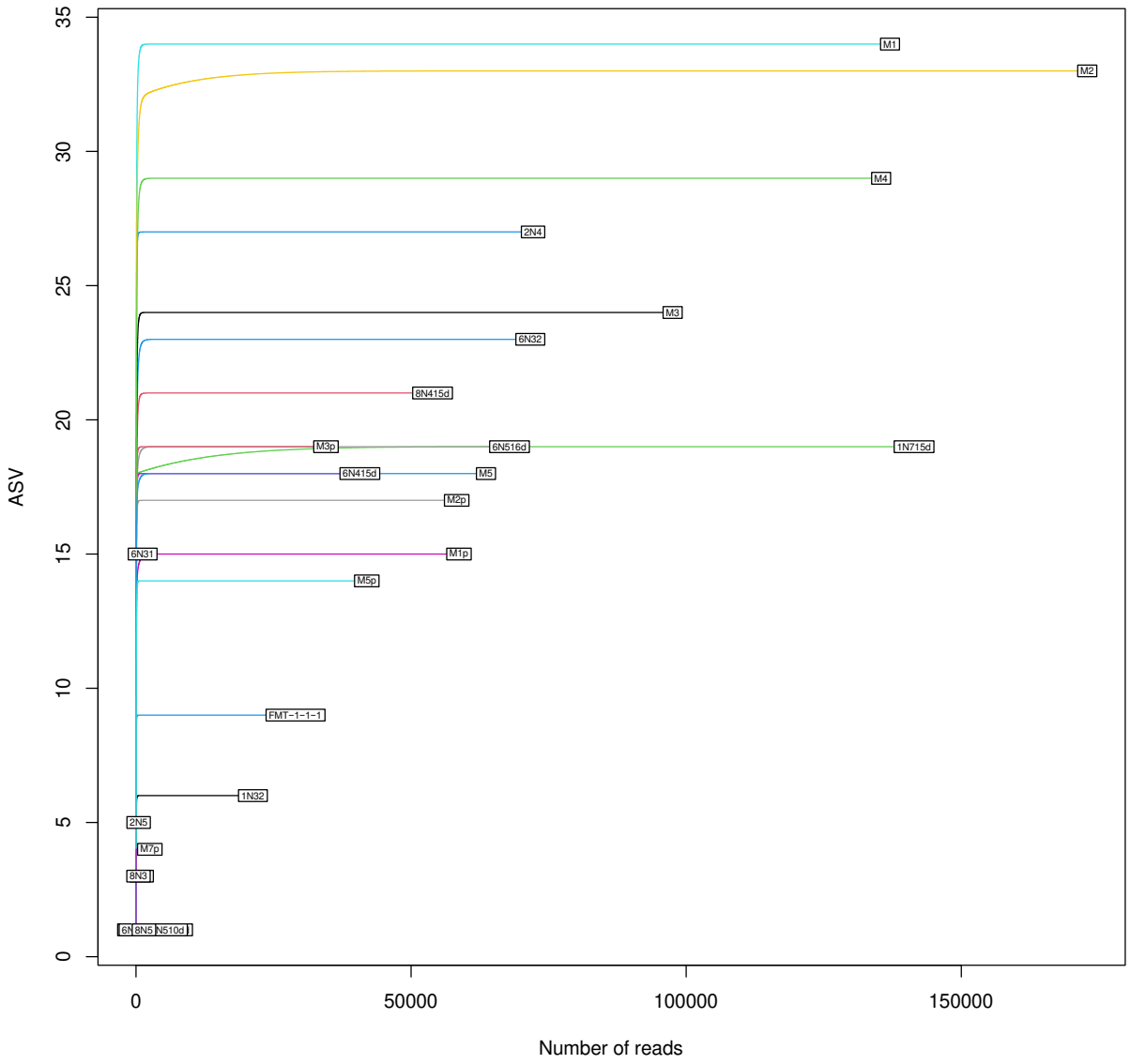

Supplemental Figure 0.6 Rarefaction curve for samples included in Pilot Neonate Vaccination Study analysis (2.2.13.1). Samples included neonates at early timepoints (ie. 10 days of age) and older timepoint after treatments (16 days of age) in addition to doe samples before and after fecal microbiome transplant.

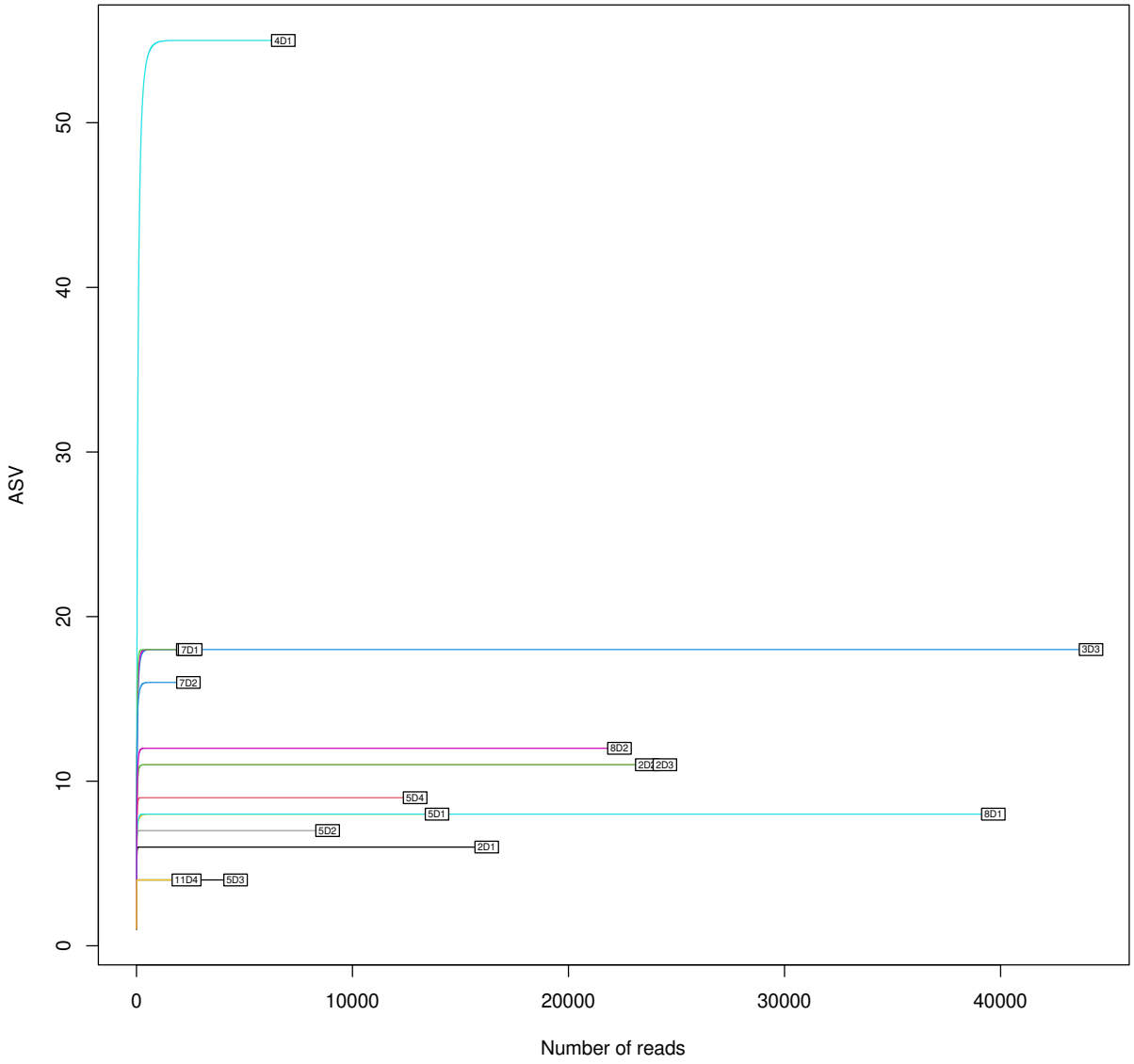

Supplemental Figure 0.7 Rarefaction curve for samples sequenced in Expanded Dose Neonate Vaccination Study (2.2.13.2). Samples included neonatal samples that received different doses of treatments including the no dose control (None), the buffer control (STI), the wildtype controls (6NCK56, 9NCK56) and the vaccine (6GAD85, 9GAD85). Doe samples from before the fecal microbiome transplant were included in this analyses.

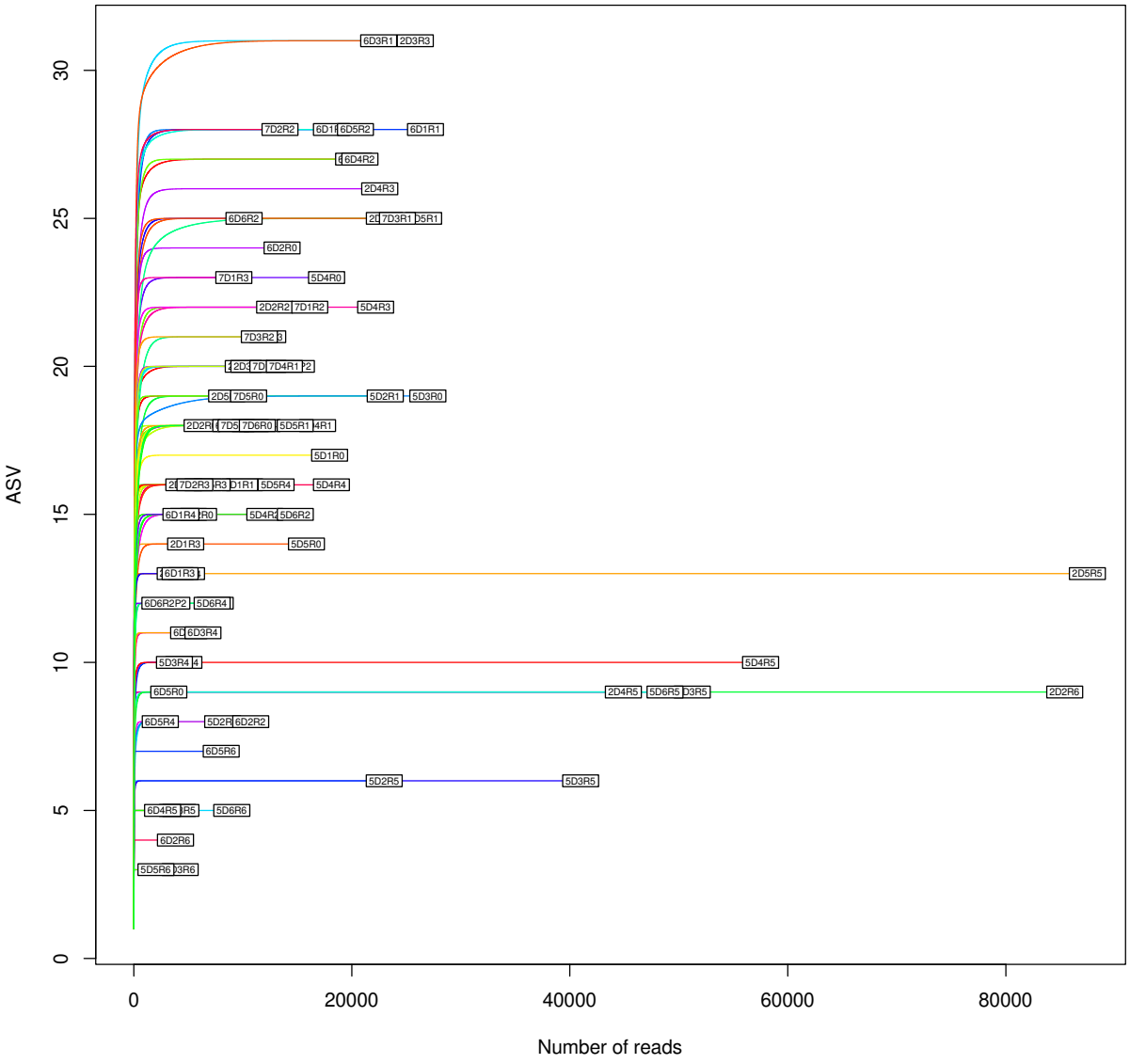

Supplemental Figure 0.8 Rarefaction curves for samples included in Pilot Neonate Vaccination and Challenge Study (2.2.13.3). Samples included neoantal timepoints prior to the rotavirus challenge (21 days of age) and each day following for six days of the rotavirus challenge (22-27 days of age) to determine how rotaivrus challenge to varying treatments (STI, NCK56, GAD85) modified the gut microbiome in neonates.

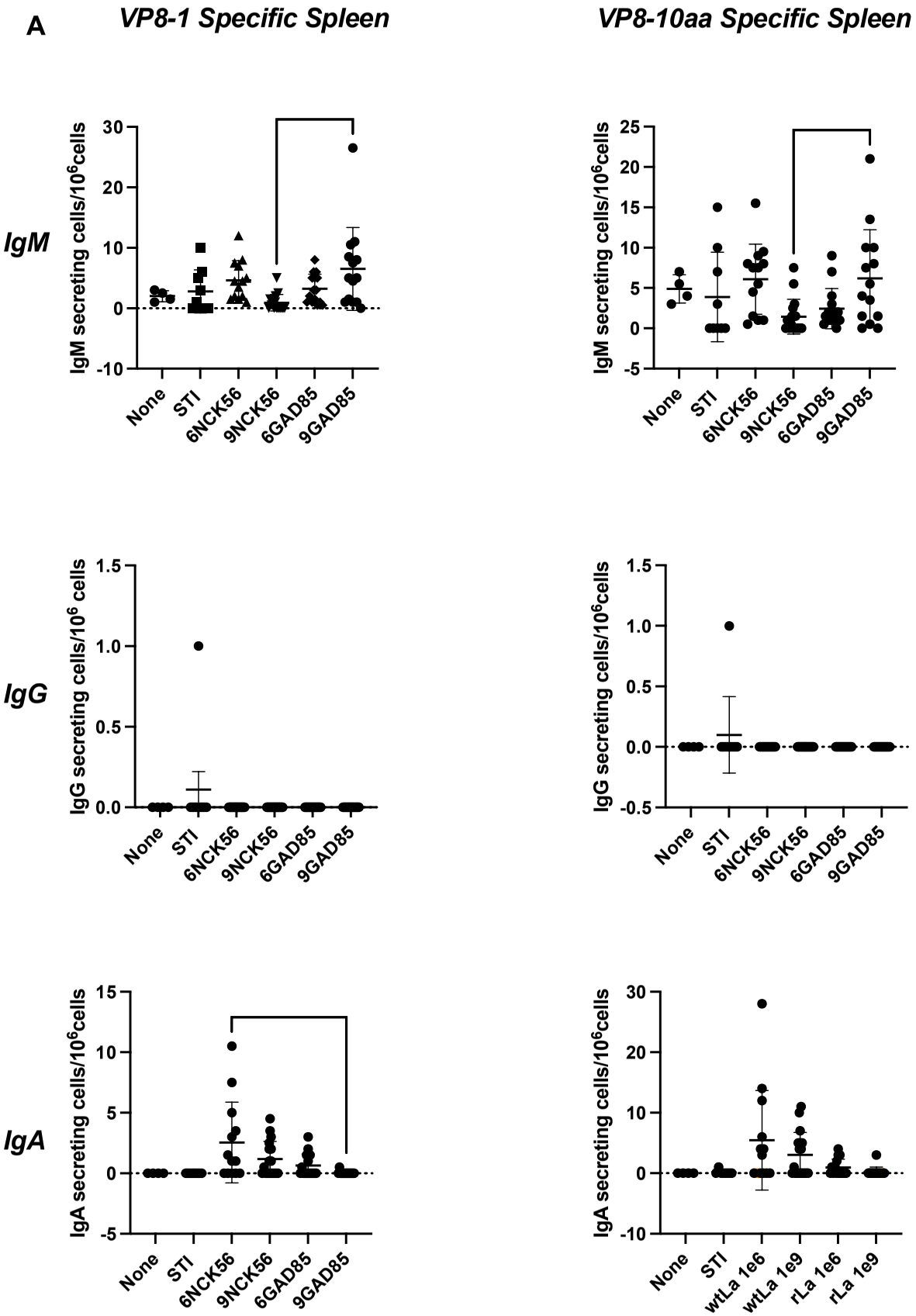
A
VP8-1 Specific Spleen
VP8-10aa Specific Spleen
IgM
IgG
IgA
IgM secreting cells/10^6cells
IgG secreting cells/10^6 cells
IgA secreting cells/10^6cells
None
STI
6NCK56
9NCK56
6GAD85
9GAD85
wtLa 1e6
wtLa 1e9
rLa 1e6
rLa 1e9

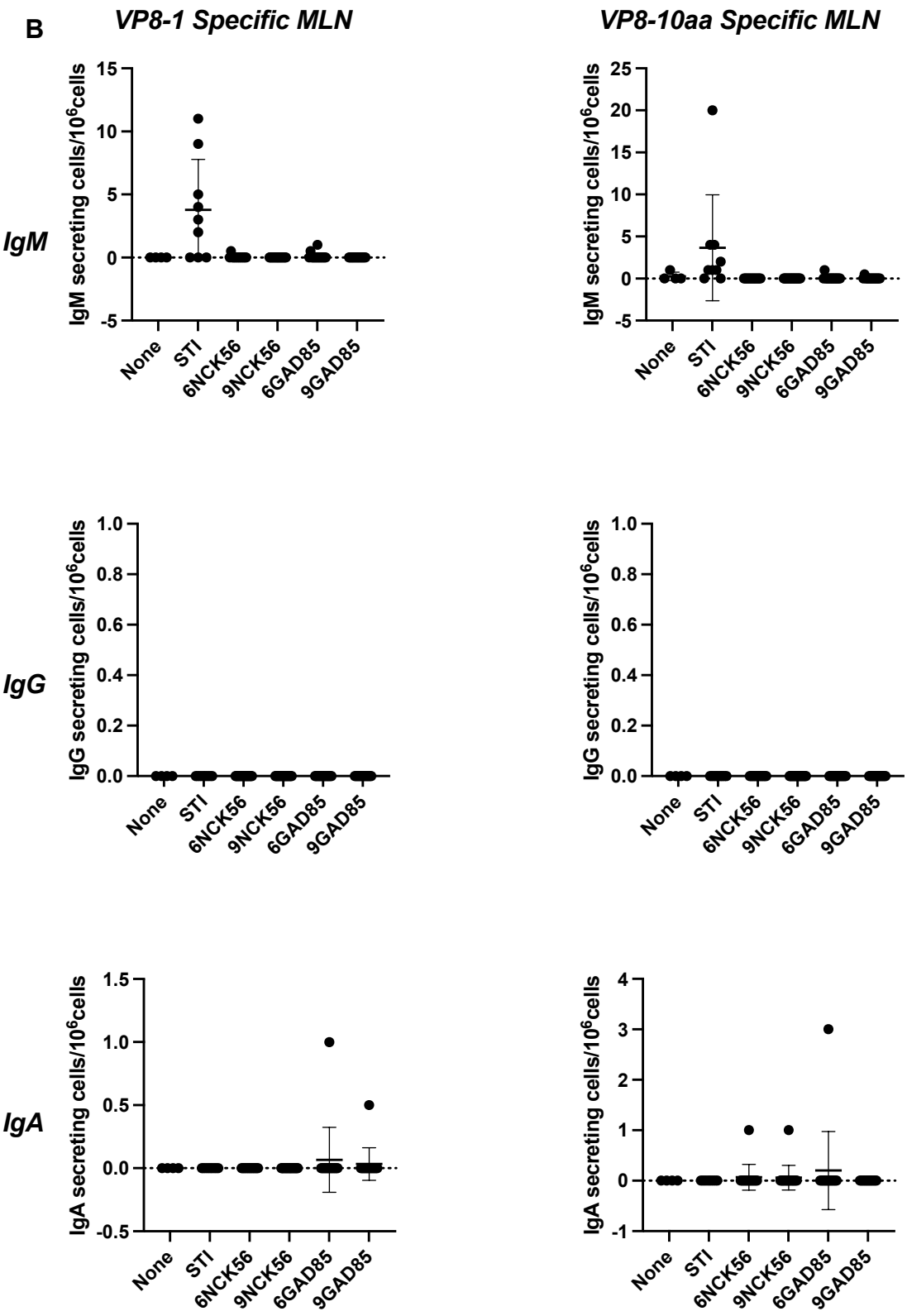
B
VP8-1 Specific MLN
VP8-10aa Specific MLN
IgM
IgG
IgA
IgM secreting cells/10^6cells
IgG secreting cells/10^6cells
IgA secreting cells/10^6cells
None
STI
6NCK56
9NCK56
6GAD85
9GAD85

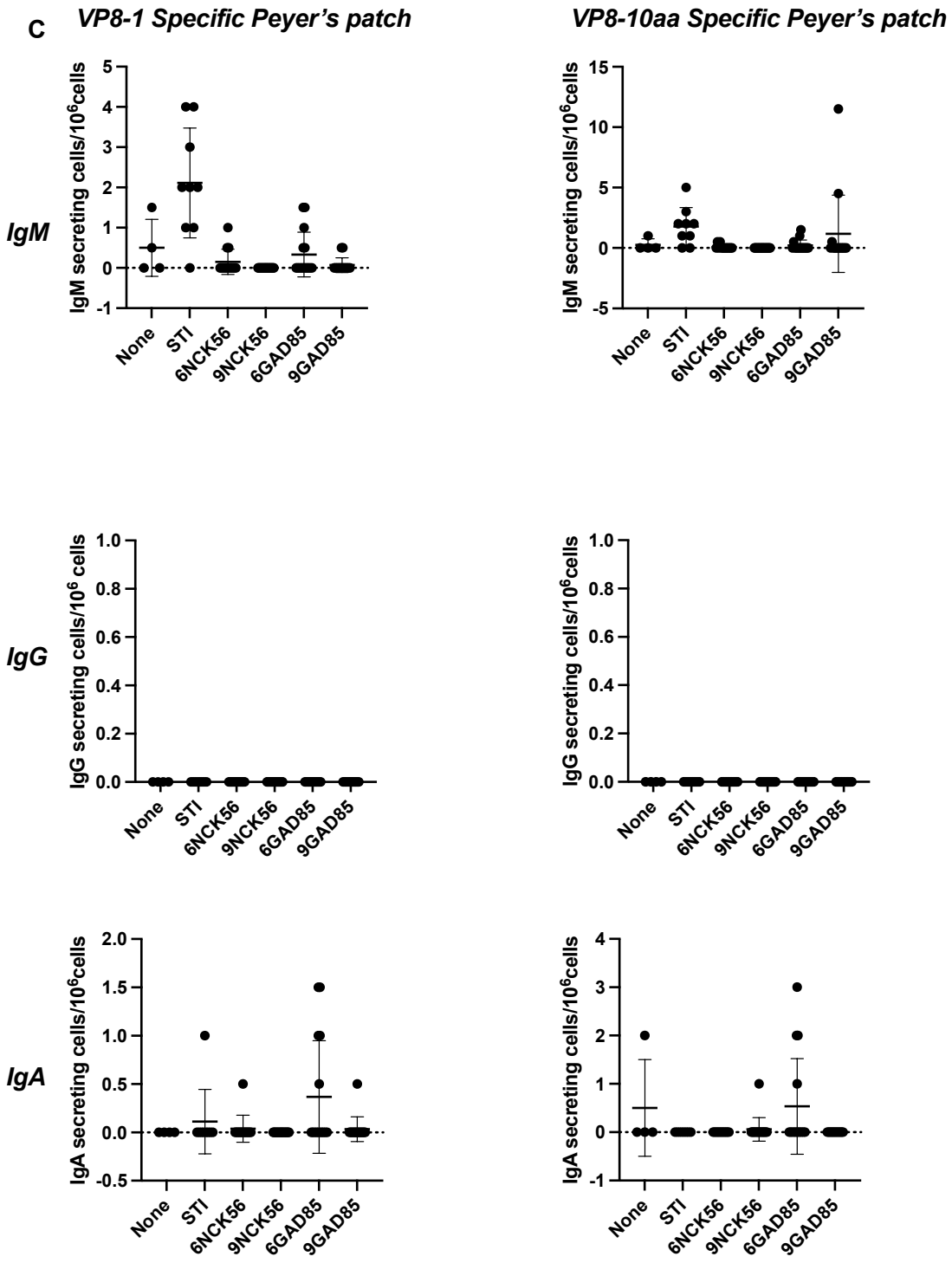

Supplemental Figure 0.9 A-C. VP8 specific IgM IgG, and IgA secreting cells in the spleen (A), MLN (B), and Peyer's patches (C) that were generated with the ELISpot assay and are represented as raw counts, not fluorescence intensity. We did not see significant differences in the VP8-1 specific responses MLN or Peyer's patches for any of the antibodies.

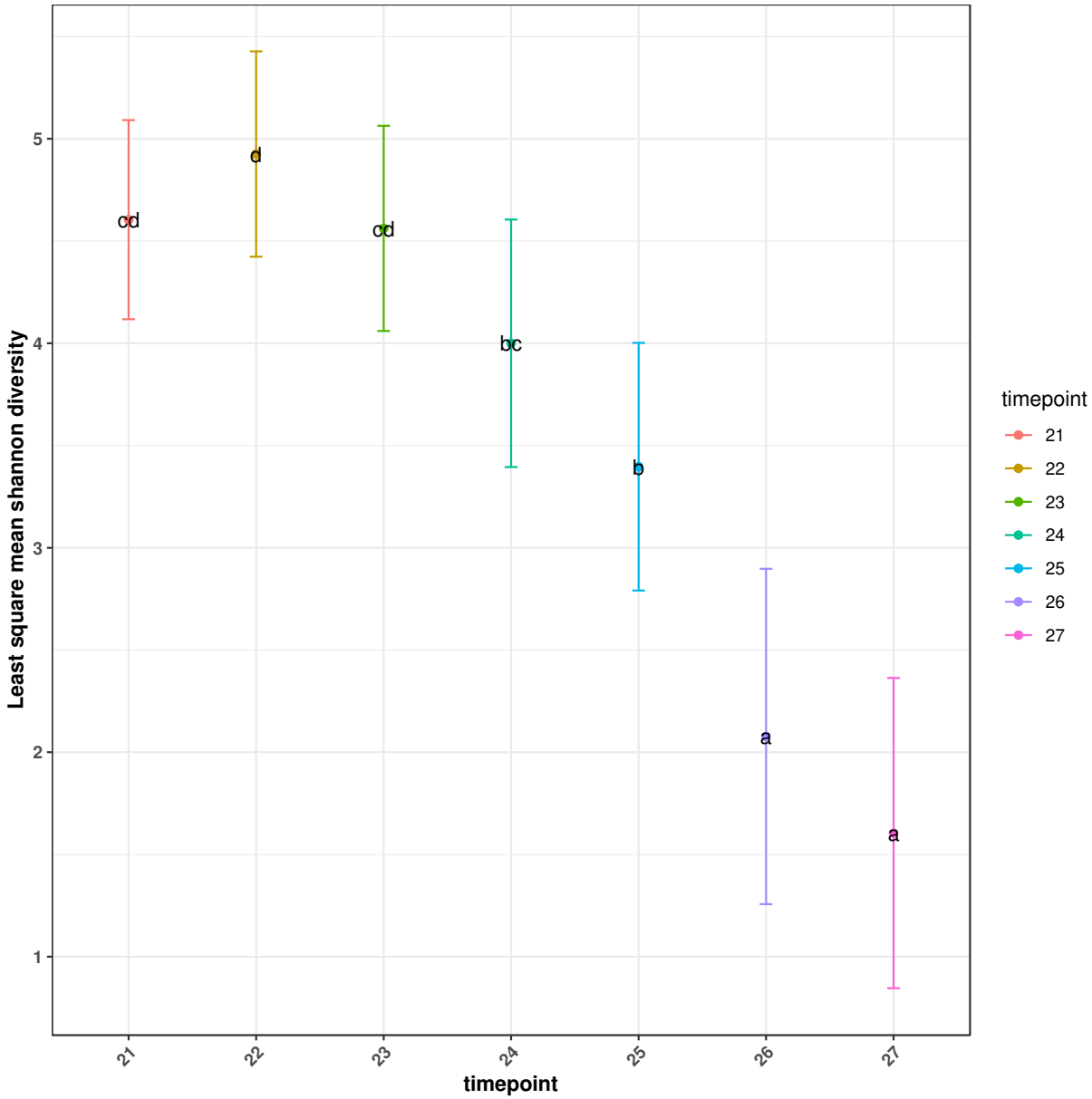

Supplemental Figure 0.10 Shannon diversity is significantly different one day post infection (22) compared to four, five, and six days (25, 26, 27) post challenge when treatment groups are combined. Overall, regardless of treatment group, shannon diversity decreased over time in neonates when given a rotavirus challenge.

Supplemental Table 0.19 ANOVA Table for the comparison between does within timepoint pre and post fecal microbiome transplant (FMT) levels for Pilot Neonate Vaccination Study (2.2.13.1), # represents significance at p<0.1, *represents significance at p<0.05 and ** represents significance at p<0.01 level of significance.

Response: Richness					
	Df	Sum Sq	Mean Sq	F value	Pr(>F)
Timepoint	1	465.14	465.14	12.245	0.008088**
Residuals	8	303.89	37.99		
Response: Shannon					
	Df	Sum Sq	Mean Sq	F value	Pr(>F)
Timepoint	1	1.2169	1.21687	5.243	0.05128#
Residuals	8	1.8567	0.23209		
Response: Inv Simpson					
	Df	Sum Sq	Mean Sq	F value	Pr(>F)
Timepoint	1	103.57	103.569	6.2247	0.03723*
Residuals	8	133.11	16.638		

Supplemental Table 0.20 ANOVA Table for the comparison between treatment (STI, 6NCK56, 9NCK56, 6GAD85, 9GAD85) for expanded dose neonatal vaccination study (2.2.13.2), * represents significance at p<0.05 level of significance.

Response: Richness					
	Df	Sum Sq	Mean Sq	F value	Pr(>F)
Treatment	5	626.71	125.34	1.906	0.112
Residuals	45	2958.89	65.75		
Response: Shannon					
	Df	Sum Sq	Mean Sq	F value	Pr(>F)
Treatment	5	3.032	0.606	1.055	0.398
Residuals	45	25.869	0.575		
Response: Inv Simpson					
	Df	Sum Sq	Mean Sq	F value	Pr(>F)
Treatment	5	224.87	44.973	1.691	0.156
Residuals	45	1196.56	26.59		

Supplemental Table 0.21 ANOVA table for the comparison between treatments (STI, NCK56, and GAD85) along the 7 timepoints of neonates' fecal antigen shedding. neonates within treatment levels for Pilot Neonate Vaccination & Challenge Study (2.2.13.3), * represents significance at p<0.05 level of significance, ** represents significance at p<0.01 level of significance, *** represents significance at p<0.001 level of significance.

	Df	Sum Sq	Mean Sq	F value	Pr(>F)
Treatment	2	1.442	0.721	44.522	1.61e-14***
Timepoint	6	0.367	0.061	3.775	0.002**
Treatment*Timepoint	12	2.872	0.239	14.773	1.2e-16***
Residuals	99	1.604	0.016		

Supplemental Table 0.22 ANOVA table for the comparison of neonates between treatments (STI, NCK56, and GAD85) along 7 timepoints after challenge in Pilot Neonate Vaccination & Challenge Study (2.2.13.3), # represents significance at p<0.1, * represents significance at p<0.05, ** represents significance at p < 0.01, and ***represents significance at p<0.001 level of significance.

Response: Richness					
	Df	Sum Sq	Mean Sq	F value	Pr(>F)
Treatment	2	38513	19257	3.038	0.0548#
Timepoint	5	273010	54602	8.615	2.64e-06***
*Treatment*Timepoint*	10	137154	13715	2.164	0.031 *
Residuals	65	411990	6338		
Response: Shannon					
	Df	Sum Sq	Mean Sq	F value	Pr(>F)
Treatment	2	2.383	1.192	1.897	0.158
Timepoint	5	53.894	10.779	17.161	8.65e-11***
*Treatment*Timepoint*	10	8.553	0.855	1.62	0.218
Residuals	65	40.826	0.628		
Response: Inv Simpson					
	Df	Sum Sq	Mean Sq	F value	Pr(>F)
Treatment	2	13035	6517.7	3.932	0.024#
Timepoint	5	75817	15163.4	9.149	1.26e-06***
*Treatment*Timepoint*	10	41521	4152.1	2.505	0.013#
Residuals	65	107736	1657.5		